Using Energy Storage to Maximize Wind and Solar Electricity Generators Effectiveness in Dispatchable Generation Replacement

by

David H. Kiefte

Submitted in partial fulfilment of the requirements
for the degree of Master of Applied Science

at

Dalhousie University
Halifax, Nova Scotia
August 2021

Table of Contents

List of Tables

List of Figures

Abstract

To aid in the replacement of fossil fuel-based electricity generation with renewable generation this thesis uses timestep wind and solar generation data with load data to determine the required storage demands for dispatchable generation retirement. The capacity value of wind and solar electricity generation is also calculated to determine the effectiveness of current wind and solar capacity at reducing dispatchable generation demand.

The capacity values for wind and solar generators were measured using the cumulative frequency analysis method, which determined the reliable generation at high load times. The data analysed covers three years at two-minute timesteps for wind, and five-minute timesteps for solar. The first analysis included all the data in the calculations. The next part of the analysis focused on each year individually to determine how much the results varied from year to year. The impact of data resolution was determined by averaging the data over wider timesteps to calculate the capacity value at a lower resolution. The data was sorted by temperature and analysed to determine how the capacity value changed at various temperatures. The next analysis sorted the data by hour-of-day and month-of-year to determine how solar compared to wind during daylight hours and summer months.

Then an energy storage model is used which determines the required capacities of solar, wind and storage to retire vast amounts of dispatchable generation. The energy storage requirements for various dispatchable generation retirement levels were used to calculate costs. The lowest cost combinations of wind, solar and, storage were plotted based on dispatchable generation retirement. For the first 200 MW of dispatchable generation retirement the most economic combination is storage alone; between 200 MW and 400 MW only storage and wind are needed for the lowest cost combination; between 400 MW and 750 MW solar, wind and storage are all needed for the lowest cost dispatchable generation storage; however after 750 MW, solar is no longer economical.

List of Abbreviations and Symbols Used

AC	Air Conditioning
CO_2	Carbon Dioxide
COMFIT	Community Feed-In Tariff
DG	Dispatchable Generation
ELCC	Effective Load Carrying Capacity
GHG	Greenhouse Gases
IG	Intermittent Generation
LOLE	Loss of Load Expectation
LOLP	Loss of Load Probability
NaN	Not a Number
NS	Nova Scotia
NSP	Nova Scotia Power
Pop	Population
P	Power
SOE	State of energy
T	Temperature
t	Time

Acknowledgements

I give thanks to my supervisor Dr. Lukas Swan for his guidance and encouragement during my MASc journey. Not just for the support provided when writing this thesis, but also for giving me the opportunity to work hands-on with batteries before shifting focus to this thesis. Additional thanks for pushing me to present my research when the limited opportunities arose, which allowed me to see strangers' perspective on my work.

Working with the group at RESL has been a huge aid to my research. I only wish I could have spent more time with them. Thanks to Nat for working so closely with me, thanks to Mark, Riley, and Chris for giving me the experienced guidance as veteran students, thanks to Byrne and Bryan for learning with me in our coursework and being there to share ideas with, and thanks to David T., and Mitch for giving fresh viewpoints and bringing new experiences to the lab.

I want to thank my parents and brother for supporting me and giving me advice when working on my degree, as well as my friends and roommates for providing emotional support. I'd also like to thank my girlfriend, Lyndsay, for the extensive support as the work reached its peak.

This work is made possible with funding from Nova Scotia's Department of Energy and Mines. This work was also made possible thanks to the data provided by Nova Scotia Power, and the Applied Energy Research Team at the Nova Scotia Community Collage.

Chapter 1. Introduction

Reliability of the electricity system is paramount for human comfort and health [1]. As it is used for many necessities such as lighting, cooking, heating, and refrigeration, many pieces of equipment and appliances involved in day-to-day life require electricity. This means losing power, even temporarily, can disrupt the lives of people. In extreme cases power outages result in injury or mortality through the misuse of non-electrical equipment such as using charcoal or gasoline-powered generators indoors, or loss of life-support equipment such as oxygen concentrators[1] [2]. Historically, using fossil-fuel based generation has been a very popular method to generate this electricity [3].

With the dangers of climate change becoming more clear [4], utilities are attempting to transition away from fossil-fuel based generators that emit high amounts of greenhouse gases (GHGs). In terms of GHG emissions, coal is the highest-emitting source of energy available. Coal releases 90.9 $g_{CO_2\text{-eq}}$/MJ, which is higher than other electricity sources such as natural gas (49.88 $g_{CO_2\text{-eq}}$/MJ) [5], and much higher than carbon-free sources such as solar, wind, hydro and nuclear [6]. In response to the growing danger of climate change and the impact coal has on it, the government of Canada has legislated that coal will be phased out by 2030 [7]. For Nova Scotia (NS), this means that 1250 MW of coal-power capacity needs to be either retired and replaced or converted [8].

Shifting away from fossil-fuel based generation towards renewable generation has drawbacks as the renewable generation usually varies independently from the demand. While renewable generators can produce sufficient energy, they do not always produce power at the right time. One way to measure the ability of a generator to meet demand is capacity value. This thesis presents a new evaluation of capacity of renewable generating sources in NS and also presents a new energy storage model to enhance the ability of renewables to meet the load in NS.

[1] https://www.fda.gov/consumers/consumer-updates/pulse-oximeters-and-oxygen-concentrators-what-know-about-home-oxygen-therapy

1.1. Research Objectives

The focus of this research is to create a model of the NS electricity system with known historical values of wind generation, solar generation, and electrical load. Using the historical wind and load data the capacity value of certain wind farms can be judged to determine the impact of various factors on the reliability of their production. Then a new model is developed which uses wind and solar generation, with storage, to improve the effect wind and solar generation have on reducing the load.

These two models provide new insight into future renewable energy builds, energy storage adoption, and dispatchable generation (DG) retirement. As the primary source of DG in NS is coal, this will help with coal retirement in NS as mandated by the federal government, without the need for conversion to natural gas, which, in turn, will reduce GHG emissions and the need for imported fossil fuels.

The objectives of this thesis are listed below. Objectives A through D focus on the generator capacity value analysis, while objectives E through G focus on the energy storage modelling and DG reduction analysis:

A. **Annual analysis:** The wind resource available in a single location may be predictable on an annual scale and imperfect forecasting is possible a few days in advance [9]; the long-term variability, the specific speed (power) of wind at a specific time, is not consistent at comparative years and cannot be predicted over a long timeframe [10]. With new data sources the value of each farm every year can be assessed numerically with statistical confidence. This part of the analysis will compare how the same wind farms perform in the winters of 2017/18, 2018/19, and 2019/20 with the expected outcome being that wind farms are more dependent on location placement than variations between years.

B. **Data Resolution:** Wind turbine generation is available at various resolutions. Different sources that supply data in 2-minute, 5-minute, and 1-hour timesteps are used in this thesis. Lower resolution data is less computationally intensive and results in smaller file sizes which can be shared more easily. However, it is important that the results of capacity value analyses are accurate as error could

result in failures to provide electricity. Therefore, this analysis aims to determine how the capacity value results vary depending on the resolution used. This part of the analysis compares 2-minute, 5-minute, 10-minute and hourly timesteps to determine whether the resolution has an impact on the calculated value of a wind farm. It is expected that there will be a significant difference in results across timesteps, as there thirty times the data points in the original 2-minute timestep data than for the hourly timestep.

C. **Ambient Conditions:** In NS, electrical demand is higher during the winter due to electric heating [11][12]. This means that electricity generated during cold days has greater value than during warmer days. This analysis determines how closely load is correlated to temperature and determines how well wind capacity value is correlated with temperature. It is expected that load is highly correlated with temperature and that as the wind increases during cold days, the heating load should increase as a result.

D. **Comparison of wind and solar generation:** Presently, there is a higher capacity of wind generation installed in NS than solar generation. These two technologies are being considered for further production. Therefore, this objective compares the capacity value of the two and looks at different factors that affect those results. It is expected that wind generation will have a greater capacity value than solar during the initial capacity value analysis because solar generation performs optimally during the summer and daylight hours, which is not when the load is the highest in NS. But when the analysis is adjusted to focus on the summer or daylight hours to account for potential summer load peaks, it is expected that solar generation will have a higher capacity value.

E. **Create Energy Storage Model:** This model will test various capacities of solar, wind and storage to achieve desired DG reduction. It will simulate an energy storage system using the inputs of IG, limited DG, and energy storage capacity to determine if there is a failure to provide electricity to meet the load, and will measure curtailment, total DG usage, and minimum state of energy (SOE) for the storage.

F. **Storage Requirement:** This will build on the energy storage model by simulating it using load, normalized IG inputs and DG maximum to output the required storage for multiple combinations of wind and solar generation. This part of the analysis will review the storage requirements in energy capacity (MWh), energy/power (hours), and costs ($). These values will be presented as a contour plot to show the varying results based on the different wind and solar levels at given DG retirement amounts.

G. **Technoeconomic Model:** To determine the lowest cost combination for achieving given DG reduction amounts, the optimum combination of wind, solar, and storage will be analyzed at various DG reduction levels. This will inform what trends occur as more DG is retired and can be used as a plan for future DG retirement.

Chapter 2. Background

This chapter provides information on the various types of electrical generation in use in NS, the methods by which renewable generation can be evaluated, and the types of storage being considered for NS.

2.1. Electrical Generation

2.1.1. Electrical Load

The majority of home appliances require electricity to operate, this includes anything plugged into an electrical outlet, as well as lighting and electric heating. When one of these is turned on, it draws power from the electrical grid and the combined draw of all these appliances is the load on the power grid. The total power from all the loads on the grid must be met at a given time otherwise a blackout or brownout occurs. The integral of the time-varying load is the electrical energy required by a system during a given time period. In 2019, NS used 10.82 TWh (38.95 PJ) of electricity, approximately 2% of Canada's total electricity demand that year [13]. While this accounts for the electrical energy demand, another necessary metric is the varying power demand of the province with time.

NS is described as a winter-peaking province, due to high space heating needs [11][12]. This means that more power is required during the winter than during warmer months because electricity is being used to operate electrical heating systems (electric-resistance heating or heat pumps), with comparatively lower air conditioning (AC) loads occurring in the summer [14]. This is observable in Figure 1, which shows a much higher average power demand during winter months than warmer months. This demand must be met using a resource that is capable of high production during those times of the year.

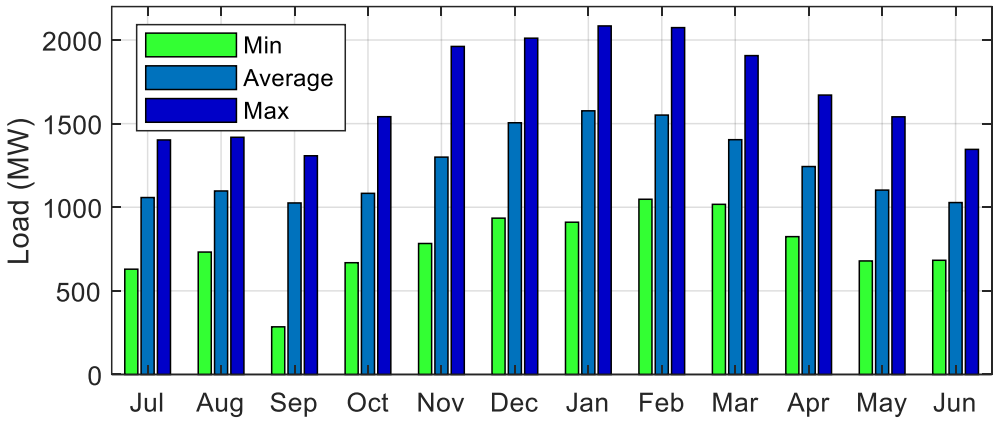

Figure 1 Minimum maximum and average electrical load each month

Figure 1 shows that the minimum, maximum, and average loads are all typically higher during the winter months than the summer months. Note the months in Figure 1 read July-June, rather than January-December, this is to focus on the higher loads in the winter. While there are seasonal changes to the load, there are also hourly changes. Typically, the peak loads occur in the mornings (07:00-12:00) and in the evenings (16:00-23:00), with lower usage when people are asleep or away at work. This trend can be seen in Figure 2.

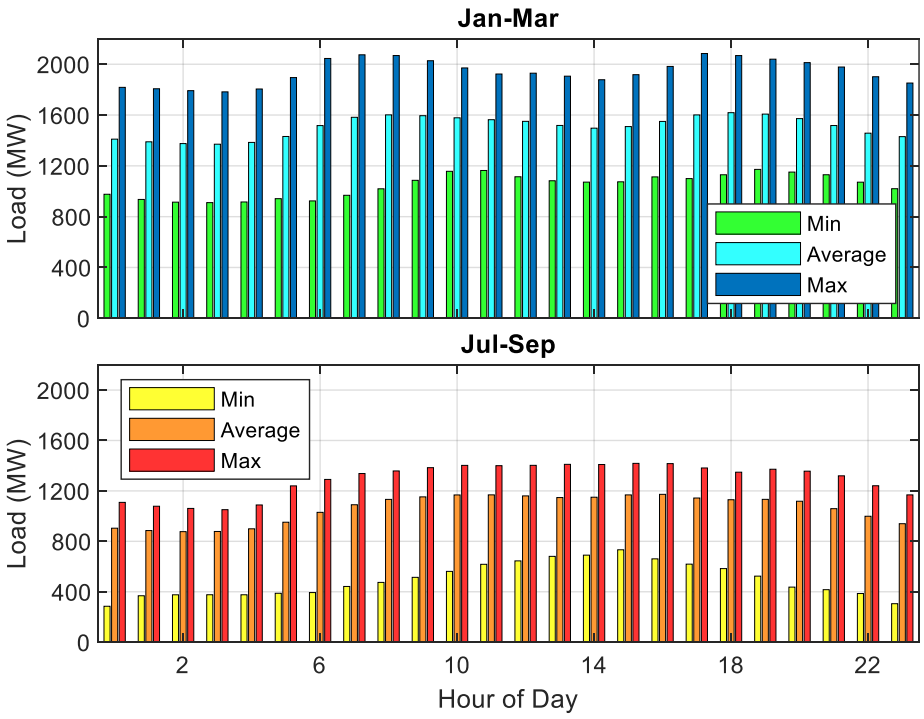

Figure 2 Minimum maximum and average electrical load for each hour during the winter and summer

Figure 2 shows that the load changes based on the hour-of-day, with the large difference in the average hourly loads between winter months (January to March) to summer months (July to September). Not only is the average load lower in the summer months, but the load for each hour is lower during the summer. *At no hour of the day during the summer is the average load higher than the average load of any hour of the day during the winter*. Due to these time-of-day peaks, Nova Scotia Power (NSP) is planning to offer time-of-use rates based on what time of the day power is used with the goal of shifting some of the power usage to the off-peak times [15][16] similar to other regions. In response to the load, NSP must either generate or import enough electricity to match the demand at any given time. This means generators that can either be controlled or tend to produce more during these timeframes are more valuable than ones that produce more power during the off-peak hours.

2.1.2. Fossil Fuels

Most of the electricity in NS is generated from fossil fuel generators. In 2019, 5344 GWh (70%) of electricity generation in NS was from fossil fuels. The makeup of fossil fuels

can be separated further: coal makes up 67% of fossil fuels used for generating electricity in NS, natural gas makes up 26%, and oil 7% [13]. NS has used coal for electricity generation since the 1970's, after transitioning away from imported oil during a time of high price volatility [17]. Recently NS has been reducing it coal generation in favour of renewables. However, there is still 1252 MW of installed capacity across four generating stations [8][17].

The disadvantage of coal is its very high GHG emissions as it is the absolute highest GHG emitter of any electrical power generator in use (90.9 $g_{CO_2\text{-}eq}$/MJ) [5]. Due to the shift away from GHG emitting resources to mitigate climate change, coal is now being replaced to comply with federal regulations [7]. Although there are multiple candidates with which to replace coal, the current plan is to convert the coal plants to the less-emitting natural gas, and to increase renewable production [17]. However, this still has the drawback of using the GHG-emitting source of natural gas.

Natural gas emits 49.88 $g_{CO_2\text{-}eq}$/MJ, which is 55% of the GHGs emitted by coal on a per unit energy basis. However, it is still greater than the emissions from non-carbon-based resources such as solar, wind, hydro, and nuclear [5]. Natural gas generates electricity by expanding during combustion to operate a gas turbine and, like coal, this can be controlled to generate electricity when needed.

Coal, natural gas, and oil all have the benefit of being sources of dispatchable generation (DG), which means they produce electricity when desired because the fuels can be stored [11][12]. DG also includes non-fossil fuel sources such as hydroelectric dams and nuclear. The benefits of a DG resource is that there is some flexibility to match the demand requested by the users, so that as there is electricity available when desired and excess electricity is not produced when unneeded [18].

2.1.3. Renewable Generation

In its current state, renewable electricity generation capacity in NS is not as plentiful as fossil fuel generation, however it is increasing. In 2019 2318 GWh of electricity was generated from renewable resources after achieving its goal of generating 30% of

electricity from renewable sources, compared to 1473 GWh in 2010 [13]. The main sources of renewable electricity generation in NS are wind and hydro.

Wind turbines produce electricity by converting kinetic energy from air particles in the wind to rotational energy in the rotor using turbine blades that spin a generator. Unlike a thermal generator which uses steam, or other gas expansion caused by combustion of fuel, wind turbines use wind which cannot be controlled. Without the need for carbon-based fuel, wind turbines have a much lower carbon footprint than fossil-fuel based generators, with the majority of GHG emissions occurring in the initial manufacture, transportation and installation [19].

NSP installed the province's first wind turbine in 1981, and now has 616 MW of wind generation across the province with more than 300 wind turbines either owned by NSP or operated independently [17][20]. Figure 3 shows the locations of the wind farms currently operating in NS.

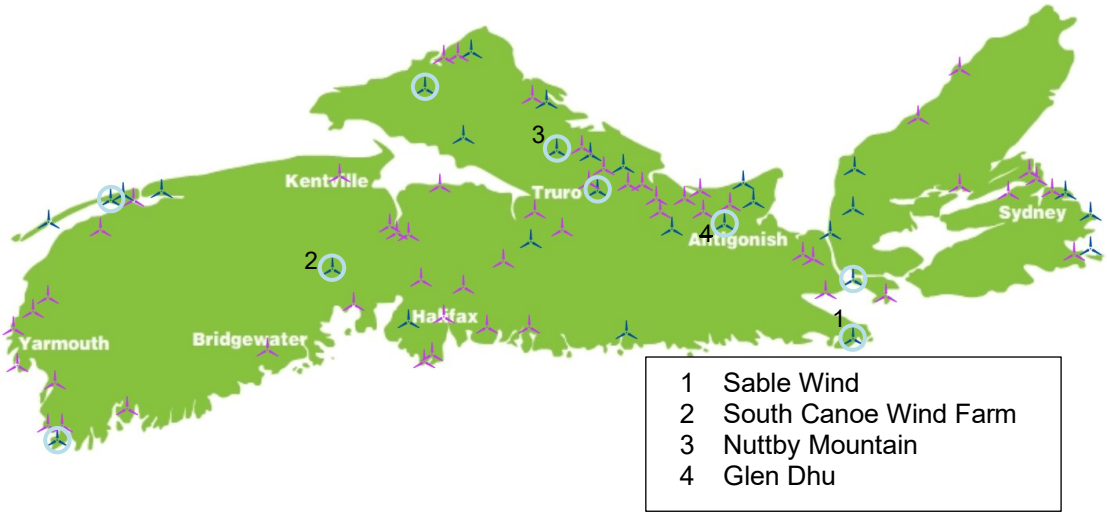

Figure 3 Wind farm locations in NS [21]

Figure 3 shows the placement of the 80 wind farms throughout the province. They cover all parts of the province allowing for a diversity of locations. The circled icons are major wind farms that collectively represent 64% of the installed capacity across the province. The data from the labelled wind farms is used in this thesis.

Hydroelectric power is the oldest source of electricity in the province, which was first installed in 1903. There is currently 400 MW of generating capacity in the province across 33 hydroelectric plants [22], shown in Figure 4.

Figure 4 Hydroelectric plants in NS [23]

A hydro plant can be operated using a store of water behind a dam, which is replenished by a river. Using this method hydro can be considered a DG resource. However, many hydro plants in NS use are run-of-river hydro, which do not store excess water and simply use the water as it is supplied by the river, which would not be considered a DG resource.

Another renewable resource option is solar generation, which like wind and hydro generation, does not require fuel and thus has no GHG emissions. Solar photovoltaic systems are used for generating electricity, and unlike wind turbines and most other generators, they do not use moving parts; instead, it converts energy from the sunlight to electricity using semiconductor materials. Solar in NS is mostly found on the roofs of residential or commercial buildings. Community buildings can generate up to 75 kW of solar electricity with residences being limited by their annual energy consumption [24].

While these types of renewable generation do not produce GHG emissions, they have a disadvantage in that they are dependent on intermittent phenomena to produce electricity. Wind turbines need wind to produce electricity, solar panels need sunlight. *Meaning the electricity produced cannot be increased by the operator if it is not windy or not sunny*

when the electricity is needed. When there is no wind or sun, the size of the wind farm or solar array does not aid the ability of the system to meet a load. Likewise, if it is an especially windy or sunny day and the load is low, the wind or sun cannot be saved it must either be used to produce electricity and stored afterwards, or it must be curtailed and wasted. Because they generate electricity intermittently, resources such as these are typically called intermittent generation (IG). Unlike dispatchable generation (DG), the IG resources cannot store their fuel if there is a lower generation demand. Instead, if the excess electricity cannot be stored, they must curtail their production, wasting potential electricity rather than saving it.

2.2. Capacity Value

In section 2.1, various types of generation were described as *dispatchable* (DG) or *intermittent* (IG) generation. The benefit of DG is that the fuel can be stored and used when the electricity is needed, whereas with IG, electricity is only generated when the intermittent phenomenon being exploited occurs. To prevent a blackout or brownout, the combined output of all the generators need to meet the electric load. This requirement results in DG resources, such as coal, being considered more valuable than IG resources like wind, for the same installed capacity; *600 MW of wind capacity does not matter if it is not windy when customers want to use electricity*. The parameter used to define the value of these resources is called capacity value, "defined as the amount of additional load that can be served due to the addition of a generator, while maintaining existing levels of reliability" [25]. A simplified explanation of this is if *a 100 MW wind farm is installed, but it only generates 12 MW of electricity during the peak load time, it actually only allows for 12 MW of additional load to be served, indicating it has a capacity value of 12 MW (or 12%)*.

There are two methodologies used to calculate the effective load carrying capacity (ELCC) and the cumulative frequency analysis.

2.2.1. Effective Load Carrying Capacity

The ELCC method uses data provided from each generator in a system and the electricity demand on the system to determine the hourly likelihood of a failure to provide electricity

which is called the *loss of load probability* (LOLP). LOLP is calculated using equation 1 [26]:

$$LOLP = \sum_{j} Prob(O_j) \frac{\sum t_{O_j}}{\sum t} \quad 1$$

Where $Prob(O_j)$ is the probability of a given capacity outage (*the probability that a coal plant is under maintenance or that wind at a wind farm is below a certain production level*). The sum $\sum t_{O_j}$ is the total time that the load is greater than the remaining capacity and $\sum t$ is the total time of the analysis.

The LOLP is used to calculate the loss of load expectation (LOLE) a value that represents the expected number of days during which the load will not be met [25]. This is done by multiplying the LOLP by the number of hours in a year. The load is adjusted iteratively so that the LOLE matches the reliability target for the system. This process can be seen in Figure 5: as the load increases so does the LOLE. Then the new generator is added to the system which results in an improvement in the overall reliability. The new maximum load achievable is found for the given reliability target. The difference between this load and the original maximum load is defined as the capacity value.

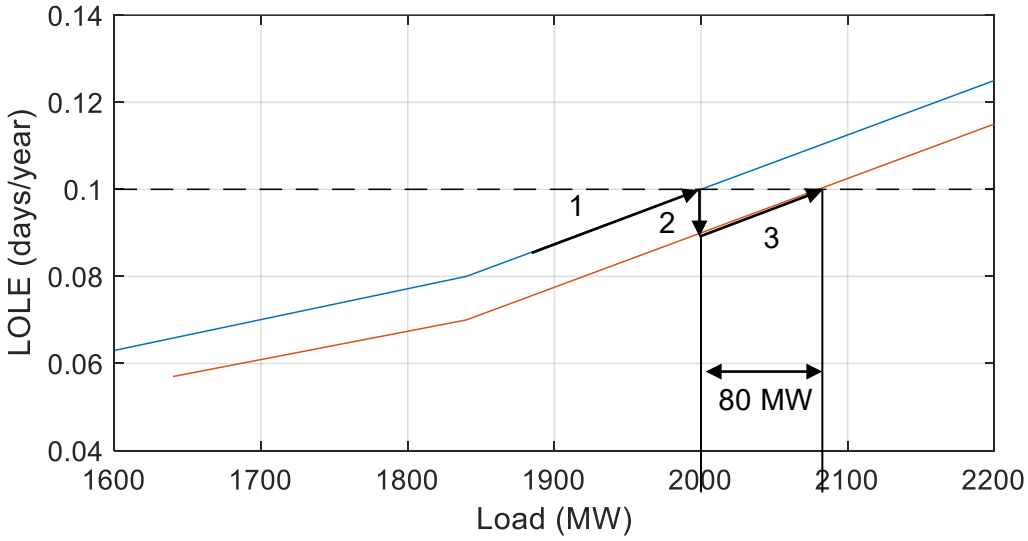

Figure 5 Effect of generator addition on LOLE during an ELCC calculation

In the example in Figure 5, the initial system LOLE is calculated for various loads to determine the load at which the LOLE is 0.1, in this case 2000 MW. Then the new generator is added which reduces the LOLE. Next the LOLE at various loads has to be determined again to find the LOLE of 0.1 which is now shifted to 2080 MW. In this example, the difference in serviceable load at the same reliability is 80 MW, so the ELCC capacity value for the added generator is 80 MW. If, in this example, the installed capacity is a 400 MW wind farm, it would have a 20% effective capacity.

Nova Scotia Power had a ELCC study performed in NS [27] for their Integrated Resource Plan [17]. The results from this determined that wind generation has a capacity value of 19%, compared to coal which has a capacity value of 92%. This disparity is typical when comparing a IG resource to a DG resource. Coal is not expected to have a 100% capacity, as there are occasions where a dispatchable generator fails when needed.

The ELCC method is limited because of the extensive data required to carry it out. The calculation requires information on the reliability of each of the generators in the system in order to know the probability of any of them failing, and, from this, the probability of a given amount of capacity failing. It also requires a long history of IG data to determine the probability it has of meeting a given load; a single year of data could be misleading since the timing of wind production could be completely different from one year to the next. It is also computationally intensive because the model needs to be run iteratively to determine the LOLE at different load levels, so calculating the ELCC capacity value for a single installation can be very time consuming.

2.2.2. Cumulative Frequency Analysis

The cumulative frequency analysis is a statistical analysis which uses historical data points of generation to determine how often a specific value is exceeded during a given load period [28]. This method has the benefit that the only data needed is production data from the new generator, as well as load data. The capacity value is then calculated as follows:

I. **The high-load time is determined:** the time at which the load is high is determined and logged. The definition of high load can vary, but one method is finding the 90th percentile load.

II. **Determine generation at high load times:** the generation at these high load times is then isolated and set aside for further analysis.

III. **Determine reliable production at high load times:** the reliable production from the dataset previously set aside is determined. This can be done by determining a low percentile value of the generation data.

An example of this method is illustrated in Figure 6:

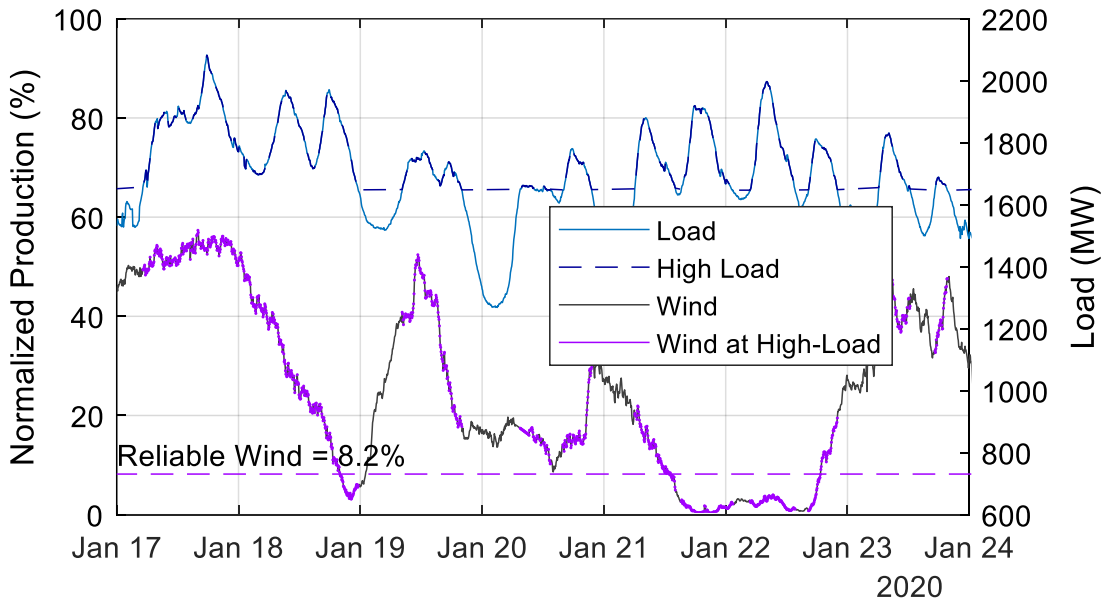

Figure 6 Cumulative frequency analysis demonstration

In Figure 6, the load and normalized generation data is shown. The steps described for performing the cumulative frequency analysis are carried out:

I. The high load times are determined by finding any time when the load is above the 90th percentile. This is shown in the dark-blue dashed line.

II. The wind generation is isolated for these high load times, shown in purple.

III. The reliable generation from these high load times is determined by calculating the 10^{th} percentile wind generation from this isolated dataset, shown in the dashed purple line.

The result is a capacity value of 8.2%, which means that if there were 100 MW of wind capacity installed, it will reliably provide 8.2 MW during peak load periods. The reliability level chosen can be adjusted depending on the confidence level desired, but there will never be 100% certainty that a generator will provide power when needed, as even a DG resource may not provide power at every time.

Castro and Ferreira [29] compared these two techniques for determining capacity value. They observed that cumulative frequency analysis was a representation of what has happened, whereas the ELCC method was a representation of what is expected to happen. The cumulative frequency analysis is a quick way to determine capacity value for a particular resource, whereas ELCC is more accurate but much more computationally intensive. In comparing results from the two analyses, they found that results were often similar between the two methods, depending on the penetration level of the resource.

Another benefit of the cumulative frequency analysis method is the ease of calculation as it does not require iteration like the ELCC method. It also requires less data, only needing information on the load and the actual generator being judged. However, the method is also limited because the capacity value calculated does not directly translate into a budget for increasing load or retiring capacity like the ELCC method does, it only works for comparing generators.

2.3. Energy Storage

Energy storage systems can be used to save excess electricity generated for when it would be more useful. This mitigates the intermittency of the generation and load by effectively shifting the load to times when it is lower or the generation is higher. This improves the ability of a system to reliably serve a higher peak load without adding more production. NSP expects to use batteries for energy storage as energy storage in NS [17][30].

2.3.1. Battery Storage

Batteries use chemical reactions to allow the flow of electrons through a connected load. Typically, a battery is made up of positive and negative electrodes. When power is required, the battery can discharge to supply a current. Alternatively the battery can be charged by flowing a current through it in the opposite direction to supply energy.

Batteries are highly useful as energy storage because of their flexibility. Their initial size can be low-voltage cells (3.2-3.6 V lithium-ion), but they can be combined into larger multi-cell modules (60 V), which in turn can be used together to form a larger pack or site-sized system for both higher power and more energy capacity. This means that rather than building one large utility-scale site, required by other forms of energy storage, smaller packs can be distributed among customers reducing the capital cost for the utility. Often household battery packs are the size of filing cabinets and can be used to reduce power usage during peak hours to reduce the owner's electricity usage during peak hours by discharging during these hours and then charging during off-peak hours, thereby helping the owner to save money on their power-bill and to help the utility reduce peak loads.

2.3.2. Energy Storage Facilities in Canada

In NS, there is an intelligent feeder project underway in Elmsdale, where battery technology is being tested to use renewable energy more efficiently and to reduce the frequency of power outages [31]. This is made up of a single grid-sized Tesla Powerpack[2] with 1.225 MW power output and 2.45 MWh storage, designed for peak shaving, load shifting, emergency backup, and demand response. The project also provided ten homes with residential Tesla Powerwalls each with 5 kW power and 13.5 kWh storage. The residential batteries can power these homes during power outages, or shift their load during off peak hours to reduce the time-of-use bill. The grid-sized battery can be used to store power from a nearby wind farm for use when it is needed more, and to power the town during power outages.

[2] https://www.tesla.com/en_CA/powerpack

In Alberta, TransAlta is operating a utility scale lithium-ion battery storage facility in Pincher Creek [32]. This uses Tesla battery technology with 10 MW of power and 20 MWh of capacity. This is located near a wind farm, to allow it to operate more effectively: by storing excess production for when it is needed more and by providing more reliability to the nearby community in case of failure somewhere else on the grid.

Saint John Energy in New Brunswick installed a 1.25 MW power, 2.5 MWh storage capacity Tesla Megapack in 2020 [33][34]. This has the objective of peak shaving, by discharging during times of the month when the electrical load is peaking, and then charging when the load is low. This prevents the need for more generation capacity to be installed as peak loads rise, or generation capacity is retired.

New Brunswick Power is developing a utility-scale solar farm paired with battery storage in Shediac [35]. It will have 1.63 MW solar capacity, with 1 MW power, 4 MWh capacity batteries. As the power provider advertises, the solar farm could produce enough energy to power 100 homes. However, these homes would still need power at night. So, the batteries will help the solar farm run more effectively by storing power for those times when generation is less available. This will also help power two net-zero community buildings nearby.

Ontario currently has 40.75 MW of power and approximately 162 MWh of energy storage contracted by the Independent Electricity System Operator [36]. This can be used for peak-demand reduction, grid reliability, and effectiveness of IG.

For the most part, energy storage systems tend to be combined with some form of intermittent generator or located near an intermittent generator. This helps control the effective output of the intermittent generator, by shifting the timing of the production to times when it is more necessary. This small-scale view may need to change in order to service an entire region rather than simply optimizing a single wind or solar farm.

2.4. Summary

This chapter reviewed the needs for electricity generation in NS, and some of the sources of generation used. Coal and other fossil-fuel based electricity generation has the benefit

that the fuel can be saved when the load is low, however the drawback is that fossil-fuel based generation releases greenhouse gases (GHG) into the atmosphere.

Wind and solar generation are two potential sources of GHG-free electricity generation. They are referred to as intermittent generation (IG) because the operator cannot freely increase or decrease generation. Capacity value is one metric for assessing IG, this measures the amount of additional load that can be served with the addition of a new generator. Cumulative frequency analysis is the method which will be used in this thesis, it is a statistical method which determines the reliable production of a generator at high load times. Energy storage can be used to store electricity generated at low load times and save it for times when the load is high, increasing the amount of load that can be served for a set amount of generation capacity.

Chapter 3. Literature Review

This chapter reviews and evaluates relevant literature studying capacity value analysis, and energy storage modeling with renewable generation.

3.1. Capacity Value of Renewables

Simoglou et al. studied capacity value of renewables extensively in Greece [37]. They evaluated the capacity value of four renewable energy sources: wind, PV, run-of-river hydro, and biomass. They also evaluated the capacity value of cogeneration plants. As biomass has a consistent output it had the highest capacity value, followed by hydro, solar, and wind, while the cogeneration plants had the lowest capacity value as they only run during the winter. They also looked closely at changes in capacity value after incremental additions to capacity for both solar and wind generation. As more wind or solar is added, subsequent additions have less impact on the load which means each addition has less capacity value then the previous. Simoglou et al. found that this drop was greater in solar generation than in wind generation in Greece. They did find that wind had a higher capacity value if there was already solar generation, and that solar had a higher capacity value if there was already wind generation, indicating that wind and solar generation are complementary and should both be used to provide power.

It is important to note that the complimentary nature of wind and solar generation is region specific. Mosadeghy, Yan, and Saha [38] found the opposite result in South Australia. Their study used wind-speed and solar-irradiance data to approximate wind and solar generation respectively, which they used to evaluate the capacity value of each. They found that when wind and solar generation were combined, they each resulted in a lower capacity value. They did confirm that incremental additions of wind or solar generation had depreciating capacity values.

Yáñez et al. [39] studied the depreciating impact of incremental additions of wind generation further. They compared three different regions with 31 potential sites in Mexico to evaluate the capacity value of potential wind generation in those regions. Because most wind generation in Mexico is concentrated in one region, they also used wind-speed data to simulate wind generation. They determined the capacity value as the

penetration of wind generation increased from 1 to 15% of the system capacity. They determined that the Nuevo Leon region of Mexico had the slowest decline in capacity value as more wind generation was added. They also found that the decline was lowest when they used generation coming from all three regions, rather than focusing the generation in one area.

Yáñez et al. are not the only researchers to compare potential locations. Jorgenson et al. [40] did this as well, using data estimated using meteorological data from 10,113 potential sites across the western United States. They also compared onshore and offshore wind. They found that offshore turbines had the highest capacity value, but that there were many potential land-based sites in Wyoming, Montana, Colorado, and New Mexico with high-capacity values. They did not account for the cost difference between land-based and off-shore wind. However, they also found that wind farms with higher average capacity factor had higher capacity values, indicating that performing better on average is a potential predictor of reliable instantaneous generation at high load times.

Some recent research has examined the impact energy storage can have on capacity value. Schram et al. [41] and Sodano et al. [42] investigate the capacity value of combining solar with storage using two different techniques for calculating capacity value. Both groups determined that introducing storage had a significant impact on the capacity value, as the storage allowed the electricity generated from solar to be used optimally. Schram et al. focused on a small-scale, residential neighbourhood from Utrecht in the Netherlands using electric vehicles charging and discharging to grid in addition to residential storage; while Sodano et al. study included a case study of two states in the United States using utility scale battery systems. Sodano et al. also looked at how incremental installations changed in capacity value when considering the impact each subsequent addition of solar capacity had on the system. The results indicated that the residual load is reduced when more solar is added causing the impact of subsequent additions to be lower.

Most of the literature reviewed focuses on determining the capacity value of a resource in a certain region, comparing two or more resources in a region, or on creating a new model for performing a capacity value analysis. There is also increasing interest in the capacity value when storage is used. There is a gap in the literature looking at other factors that

impact the capacity value, such as timeframe, resolution of data, or ambient conditions. Much of the literature has used predicted data based on models using meteorological data, rather than actual production data, meaning that there is some error caused in converting wind speed, or solar insolation to actual generation.

3.2. Renewables and Storage Modelling

Johlas, Witherby and Doyle [43] determined the storage requirements for high penetration of wind and solar in central USA. The goal of this research was to achieve a nearly 100% solar-wind portfolio by energy. The model used a control strategy that charged the battery when there was excess IG. The battery size was determined before the simulation was run, with the output being required power and energy from DG. This method has the drawback that it needs to be run iteratively to determine an unknown storage size but has the benefit that the parameters of the storage can be more finely adjusted with each simulation. They found that, with no DG, they required approximately 100 times the energy capacity than if they produced 5% of their energy from DG. This is an energy demand, not power demand, which is concentrated in a few short time-periods. For much of the year this DG would be inactive and would then need to ramp up considerably to help the storage when it is insufficient. This succeeds in reducing GHG emissions but does not allow for as much DG generator retirement.

The biggest differences between their research and the present thesis are the region, the focus on reducing DG energy, rather than power, and the fact that the cost of the system is ignored here. This minimization of energy from DG is repeated by Budischak et al. [44] who combine inland and offshore wind with solar and storage to power the grid in the eastern USA. In that study, they used simulated wind and solar data from the National Renewable Energy Laboratory to estimate production in this region and to optimize the best combination for reducing energy needed from DG. They then found the difference between IG and load, so that the storage was either used to supply the difference or charged if there was excess generation. As with the previous group, the storage energy capacity and power were input before the simulation was run, with the output being the amount of system coverage achieved. This does not focus on power from DG, but instead reducing energy, which will reduce GHG emissions, but requires dispatchable sources in

standby. This strategy has the benefit of limiting storage and IG to realistic combinations but has the downside that it requires iterative simulations to find the optimal combinations. In this case they had to evaluate 28 billion combinations of IG and storage.

Weitemeyer et al. [45] also considered cost, but focused on the storage cost. Their study assumed a high renewable penetration and considered the different forms of energy storage technologies and backup power to achieve electrical load. In this case, their model ran by charging the energy storage when the renewable generation exceeded the load, and discharging when the renewable generation was insufficient to meet the load. The energy storage capacity and initial stored energy were predetermined. They concluded that the lowest cost combinations were dependent on the main source of renewable generation. Solar generation results in daily storage demands, which requires battery storage, while wind often results in longer term storage, which led to hydrogen and pumped-hydro storage performing better.

Regional differences are most evident with Esteban, Zhang, and Utama [46]. Their research focused on Japan, which is a high summer-daytime peaking region in contrast to NS. They combined solar and wind with storage to provide load using a timestep model. They used biomass, pumped storage, and battery storage to supply power when the IG was insufficient to meet load. Their model set a limit on the biomass and pumped storage, prioritising their use first, then used the battery storage as needed. This has the benefit of maximizing the use of capacity that already exists in the system before installing new storage capacity. This assumes the system would use one source of DG or storage at a time rather than balancing all three. Due to the high summer-daytime loads the optimal combination involves a large solar to wind ratio. However, the need for wind is not zero as there is still load during the nighttime hours.

Much of the research reviewed used a model that charged energy storage when the IG exceeded the load. This works when the only form of generation is renewable, but many used some DG energy as backup, which means the DG had to ramp up to a large power output for a short amount of time. Many of the models also selected the storage capacity before simulating, which would mean they would have to iterate to find a combination that had sufficient capacity. The literature also shows different results depending on the

region, indicating that some of the results are not applicable to the NS system. The following section reviews some literature on storage modelling in the NS system.

3.2.1. Nova Scotia Analysis

Few researchers assessed combined renewables and storage in a NS context. One example of this is a focused study Manchester et al. [47] did on combining tidal, wind and storage for avoiding curtailment. This study focused on a potential in-stream tidal generator in NS that was limited by the energy demand of a nearby substation that already had a wind turbine nearby. The combined output of the turbine and the tidal generator had to remain below a 0.9 MW limit set by the substation. Manchester et al. modeled an energy storage system to determine the necessary power and energy capacity required to prevent curtailment. They used wind-speed and tide-velocity data as the production from the wind turbine and tidal generator was unavailable. The study used an iterative approach which simulated multiple combinations of power and energy capacity to see which ones would successfully prevent curtailment. This method would require excessive computation as it simulates slight differences until it finds the combinations that work.

Pearre and Swan [48] analysed this in 2013 for the purpose of introducing wind and storage to the province to retire coal-fired generation. The goal of this research is similar to that in this thesis; however, the methods differ. In their research, they use windspeed and load data from 2008 to 2010 to estimate the needs and production for 2015 and 2020, by converting windspeed to wind generation using a wind turbine generator power curve. At that time there was a required generation for these dates set by the provincial legislature, so rather than having a variable wind generation capacity, it was estimated based on this requirement. The timestep storage model uses set storage capacities that charge and discharge as needed, and records loss of load. In this way storage capacity and DG retirement are varied to output the number of hours per year with a failure to meet demand.

Pearre and Swan also did two more recent sets of research in this area. The first in 2020 [12] combines wind, solar, and in-stream tidal with storage to reduce load perturbations in NS. This study spanned two years from 2016 until 2018, using normalized wind and solar based on aggregate wind, and aggregate solar, as well as the actual load during this time

period; in-stream tidal is estimated based on the water velocity and tidal turbine power curve. The storage model sets the starting energy to 0 and depletes and recharges the storage as needed, using the minimum depletion amount to determine the needed capacity, with the resulting storage capacity varying depending on the wind, solar, and tidal capacities. This was done for different perturbation timescales.

Subsequent research done by Pearre and Swan in 2020 [11], uses the same data and time period to test a different model for ramp-rate control. As IG varies like load, it can result in a severe change in perceived load as the renewable generation falls as load rises. Therefore this research uses storage to flatten this change. The control strategy for this study set a limit on the ramp rate of the DG. Initially the load was met by the IG and DG resources, however if the variation of load or IG caused the ramp rate to exceed this limit it would either charge or discharge the storage to reduce the ramp rate. They then tried to return storage back to the neutral point when possible. The storage was initialized at 0 and charged and discharged as needed, determining the capacity by the difference between highest and lowest points, where the 0 point it began at was the approximate middle.

3.3. Summary

The literature regarding capacity value covered many techniques for calculating capacity value. Researchers make conclusions on the capacity value of different locations or on combining various locations, however there is a gap when it comes to the characteristics of the data used. This thesis will review how analysing data from a specific year and using data with different resolutions impact the capacity value results. This thesis will also take a closer look at how the capacity value is impacted by the ambient conditions.

Modelling storage used for DG reduction is lacking in the NS region. There are researchers who have done storage modelling in NS, however, the goal of their model was not DG reduction. This thesis will focus on the goal of reducing the need for DG. Research has been done outside of NS with the goal of DG reduction, however in many cases they do not use actual production data, instead they use data modelled from meteorological data. Additionally, storage modelling done regarding DG reduction often result in low DG energy usage, but do not limit DG power, meaning there is still a need

for a high DG capacity, that remains idle for long periods of the year. This thesis limits the DG power output rather than energy to allow for complete retirement of DG facilities.

Chapter 4. Data Sources

This chapter describes the types and sources of data used, and the ways the data was processed to be useable in the models. Wind and solar generation data, provincial load data, and environmental data were all used in the analysis, with various timesteps.

4.1. Wind

There are two sets of wind turbine data used in this project:

- Provincial aggregate wind power: the total wind generation across the whole province, available in 2-minute timesteps from 2016, and 5-minute timesteps from 2012-2016.

- Individual wind farm power from four NSP owned or partially owned wind farms in NS, available in 2-minute timesteps from 2015.

4.1.1. Provincial Aggregate Wind Generation

As of 2021, NS has 309 wind turbines across the province with 616 MW of installed capacity. While these wind turbines are spread out amongst dozens of wind farms the majority of the production comes from a small number of large farms. NSP uses the timestep data from nine wind farms and extrapolates the production to estimate the total production of the province. The wind farms used are listed in Table 1 and are circled in Figure 3.

Table 1 Major wind farms telemetered for extrapolating aggregate production

Wind Farm	Installation Year(s)	Number of Turbines	Installed Capacity (MW)
Amherst	2012	15	31.5
Nuttby Mountain	2010	22	50.6
Dalhousie Mountain	2009	34	51
Digby Neck (Gullivers Cove)	2010	20	30
South Canoe	2015	34	102
Pubnico Point	2004, 2005	17	30.6
Glen Dhu	2011	27	62.1
Point Tupper	2010	10	22
Sable Wind	2015	6	13.8
Total		**185**	**393.6**

The nine wind farms have a total capacity of 393.6 MW, which is 64% of the installed capacity across the province. The data was extrapolated by NSP to match the full capacity of NS and provided by them as an aggregate production, in a two-minute timestep. Each datapoint recorded the average power production by the province across the previous two minutes in megawatts (MW). This data was provided from January 2012 until the end of 2020, with only the period of July 2017 to July 2020 being used for the analysis. There were multiple wind projects in 2017, so it is expected the installed capacity is not as high in the beginning as it was at the end.

The data was pre-processed to account for gaps and errors in the data. The process for this is shown in Figure 7:

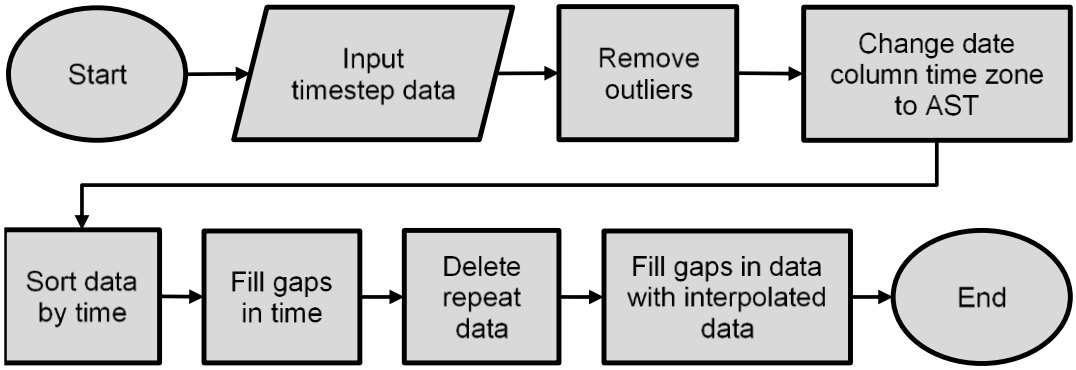

Figure 7 Timestep data processing flowchart

Figure 7 shows the generic way the data was processed for most sets of data used in this analysis. This was implemented for the aggregate wind data by:

- Defining outliers as any value above the known capacity of installed wind turbines (616 MW).
- Changing the time zone of the date column to Atlantic Standard Time (AST) to keep the time zone consistent across all datasets.
- Deleting repeated data (two or more datapoints at the same time).
- Filling gaps in time with non-number (NaN) values.
- Replacing NaN values by interpolating between nearby datapoints.

The resulting data during the used period is shown in Figure 8:

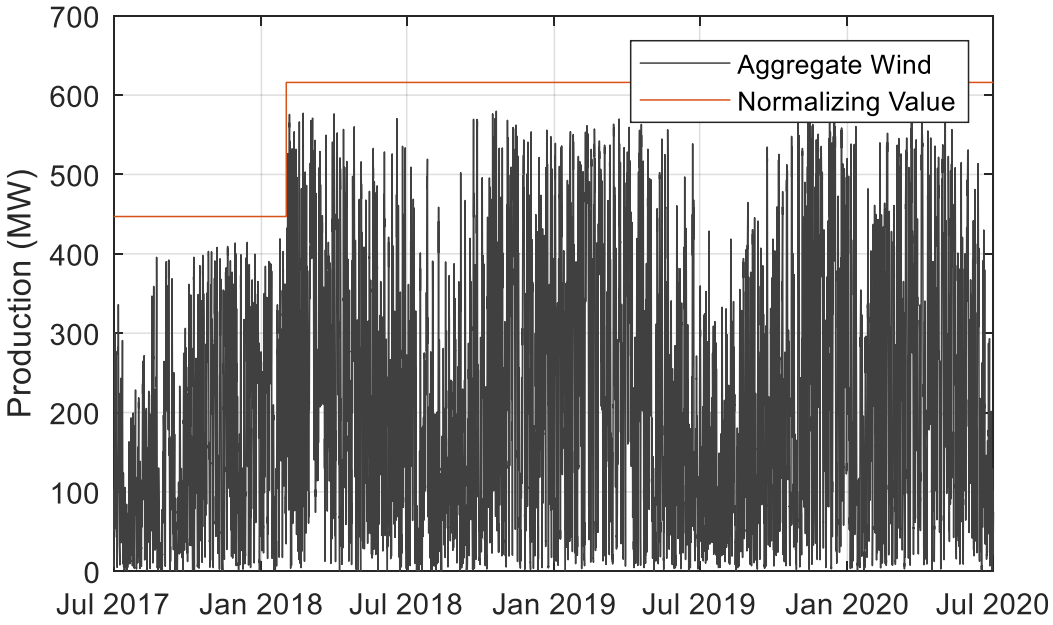

Figure 8 Aggregate wind as estimated by NSP using extrapolation of nine major wind farms

For most of the timeframe used, the production tends to peak close to the known installed capacity for the province, 616 MW, however, for the first few months the production is

significantly lower, most likely before the point in which a major wind farm was connected to the grid. The lower production during the summer than the winter is expected. Throughout this analysis, the normalized production, production as a percentage of capacity, is used rather than production in units of MW. This is so the capacity value can be compared between different sized farms, and so that the production can be scaled for the storage modelling. The equation used to normalize the power output is given below:

$$P_{\mathrm{norm},t} = \frac{P_t}{P_{\mathrm{rated},t}} \qquad 2$$

The normalized production, $P_{\mathrm{norm},t}$, is the percentage of rated power achieved at any given time, t; P_t is the power production at any given time, t; and $P_{\mathrm{rated,t}}$, is the rated capacity of the generator at that time, t. For an individual device or farm the rated capacity is often constant over its lifespan. But for the total aggregate production across the entire province, the rated capacity changes as new wind farms are commissioned, or old ones decommissioned. Farms can also change their rated capacity if new wind turbines are added to the farm, or are decommissioned during the farm's lifetime.

The normalized production value is displayed on Figure 8 as the orange line, at present NS has 616 MW of wind, so the more recent times are treated as having a rated capacity of 616 MW. This normalizing value is used from February 2018 until the end of the analysis, the power production is much lower in January 2018, so this is likely the point when a new farm was connected to the grid and NSP began scaling the aggregate production by a higher value. The rated capacity before this point is estimated by comparing the maximum production before and after February to be approximately 73% of the current capacity, or 447 MW. This results in the following time series:

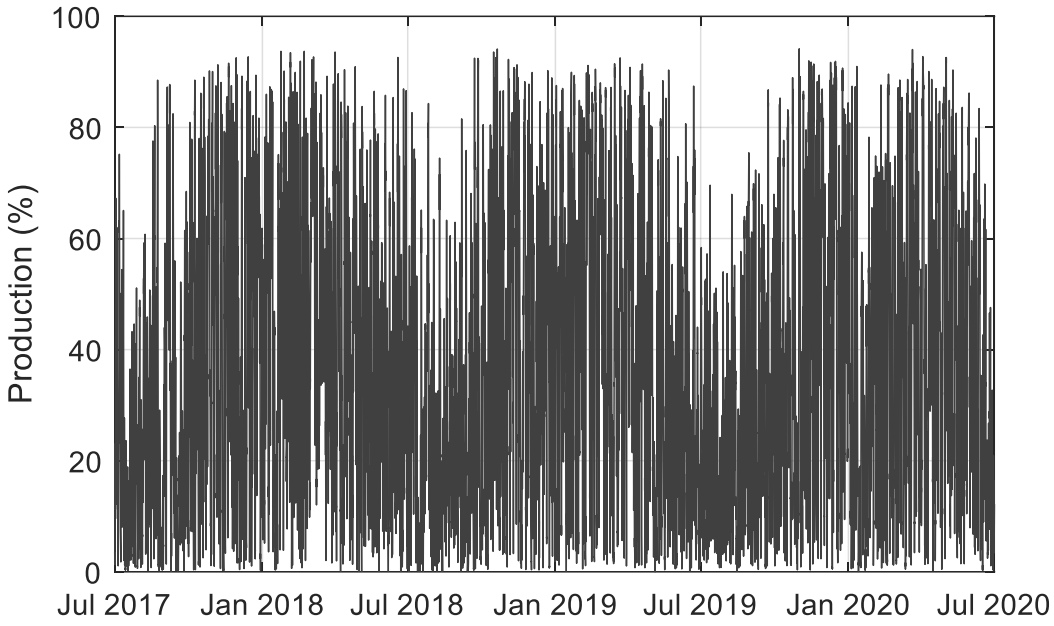

Figure 9 Aggregate wind as a percentage of total production using estimated rated capacity

After correction, the production occasionally reaches a maximum value of around 94% of its rated capacity. The failure to reach 100% capacity is expected; it is unlikely all 300 wind turbines in the province would ever be producing at their maximum capacity at the same time. There are various reasons some wind turbines could be producing less than others; at any given moment some may be undergoing maintenance, some may be down due to icing, some may be blocked because of the direction of the wind, or some may simply be in a less windy area, they may even have the potential to generate maximum power but be curtailed because there is already too much generation. The aggregate production also rarely hits 0% production, as it is rarely completely windless across the whole province. The summer shows lower production than the winter, as it is typically less windy during this time.

4.1.2. Individual Wind Farms

This analysis also used data from four of the wind farms from the nine major farms listed in Table 1. The farms used are:

- Sable Wind in Guysborough County

- South Canoe Wind Farm in Lunenburg County
- Nuttby Mountain in Colchester County
- Glen Dhu in Pictou County

The locations of these wind farms are labelled in Figure 3. The data is provided in two-minute timesteps, in the form of average power over the previous two minutes. This was provided from January 2015 to July 2020, however South Canoe Wind Farm was only operational in June 2015, so it has zero production until June 21, 2015. The analysis using these four wind farms only covered July 2017 until July 2020, so the availability of data was sufficient.

The data was processed using the same method as the aggregate wind data. Anytime power output was 20% higher than the rated capacity of the wind farm it was considered an error and deleted. Then the time zone was corrected to AST, and the data was sorted chronologically. Gaps in time were filled and interpolated between, note that since South Canoe was not operational until June 2015, the gap between January and June of that were was not filled in, it was left at zero production. The resulting data available for these wind farms is shown in Figure 10:

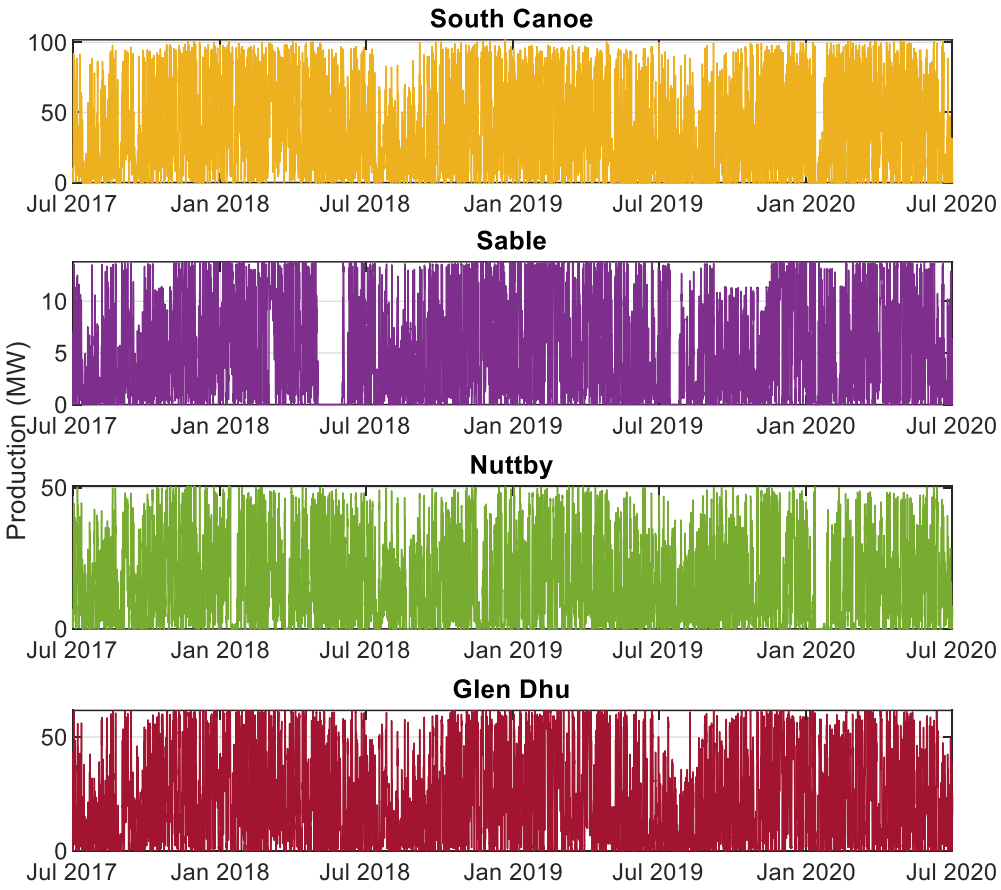

Figure 10 Individual wind farm production

This shows the total output of each from in terms of MW. The y-axis for each wind farm has a different scale, depending on the size of the wind farm, so they are incomparable in terms of MW output, as South Canoe far exceeds the capacity of the other farms. To make them more comparable they are converted to percentage of rated capacity. This is done using equation 2, using the rated capacity for each wind farm found in Table 1. The result is shown in the following Figure 11:

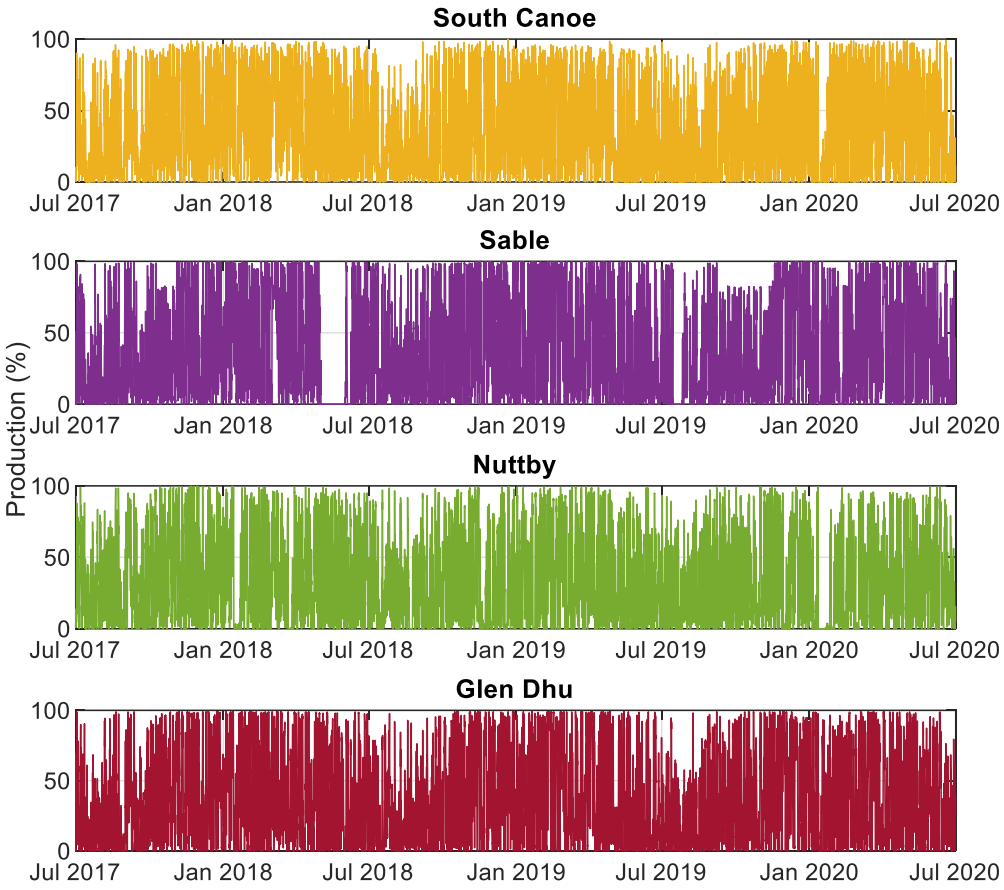

Figure 11 Individual wind farm production as a percentage of rated capacity

This shows the percent production for each individual wind farm. This data is used for analysis when comparing wind farms of different sizes. The data shown in Figure 11 is too broad to see instantaneous differences between the farms, but seasonal differences between the farms is observable. Sable is the most obvious, with a data gap in spring of 2018, indicating some loss of data collection, or farm shutdown. There is a similar gap in late summer 2019, and either curtailment or a single turbine failure in fall 2019. Nuttby also appears to have a gap in the data in early 2020, which could be from a farm shutdown or a data recording failure.

4.2. Solar

A solar array typically has multiple solar PV panels connected to an inverter or a set of micro-inverters that convert the DC output from the panels to air conditioning (AC) that can be used by the home or the electrical grid. The production output data from these

arrays is collected at the inverter and communicated to the Halifax Regional Municipality Solar City 2 program[3], which is databased on an open data portal. Nova Scotia Community College Applied Energy Research has built a database to make this data available to researchers[4]. In this case there are 200 arrays with data used in this analysis, the majority of which reside in Halifax County. The number of solar arrays is shown in Figure 12:

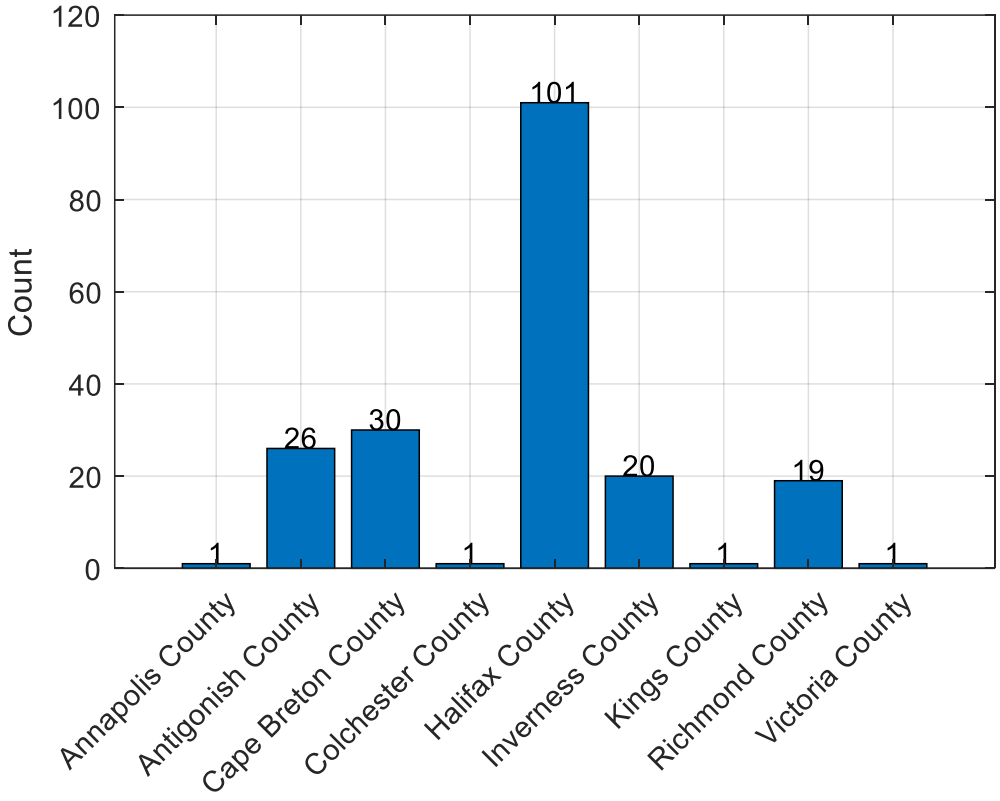

Figure 12 Solar array data availability by county

As with the wind data the solar production is shown by a power value, in watts (W), representing the average power produced during the previous timestep. For the case of the solar data, it is provided in 5-minute timesteps. The solar data did not have the benefit of as long a data history as the wind turbines, with many solar arrays being commissioned

com/tps://www.halifax.ca/home-property/solar-projects/about-solar-city
[4] https://data.solardatans.ca/communitysolar/signIn.php

during the span of the analysis. The following Figure 13 shows the data available across the range of solar arrays:

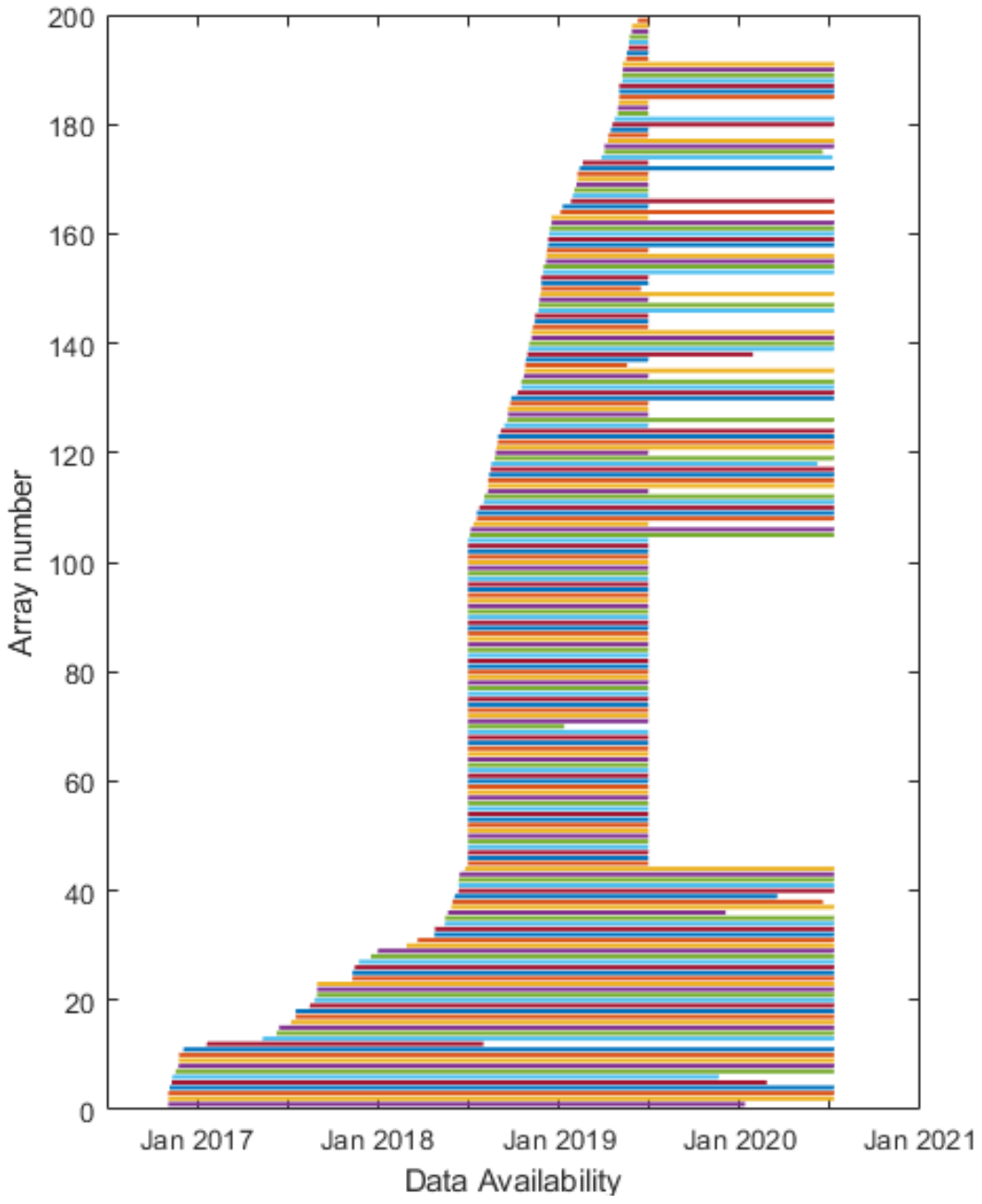

Figure 13 Solar array data availability by date

While many arrays only provide data for a limited time, after July 1, 2018 there are always at least 90 arrays outputting data. The arrays providing a limited timeframe were

used when available, but most of the data was used from the more available arrays. Because many of the arrays are only available during this limited timeframe, the analysis involving solar only covered July 2018 to July 2020.

The solar data was used to estimate a single set timestep normalized power data for the province. To do this the 200 arrays were combined in some way that would provide a realistic prediction of the solar resource in the province. The following flowchart and equations show the method in which the solar data is processed:

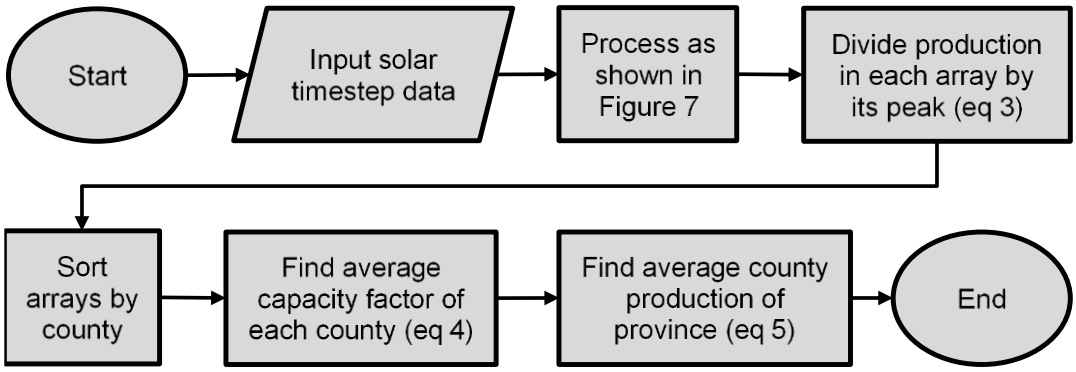

Figure 14 Solar data processing flowchart

The data from the arrays was first processed to remove errors using the same method shown in Figure 7. In this case the peak production was the 99.9th percentile production value, with anything significantly higher being removed as an outlier. Then the solar arrays were organized by county, so that each county had a set of arrays representing its production.

The first step is normalizing the arrays as a percentage of rated capacity, however, the rated capacity for each array is unknown, so instead of using equation 2, the rated capacity is replaced by the maximum production:

$$P_{\mathrm{norm},t} = \frac{P_t}{P_{\mathrm{max}}} \qquad 3$$

As with equation 2, $P_{\mathrm{norm},t}$ is the normalized generation, or the generation as a percentage of the rated capacity, P_t is the solar production at a given time, t. P_{max} is the

maximum power output of the solar array, used to estimate the rated capacity. This maximum power output is often limited by the inverter rather than the number of arrays, so this maximum is assumed to be the maximum MW_{AC} rather than MW_{DC}.

Next the capacity factor of the county is estimated by finding the average power of the arrays in that county:

$$P_{\text{norm},county,t} = \frac{\sum P_{\text{norm},i,t}}{n_{\text{arrays}}} \quad 4$$

In equation 4 $P_{\text{norm},county,t}$ is the average normalized production across the whole county, $P_{\text{norm},i,t}$ is the capacity factor of each array in the county, and n_{arrays} is the number of arrays in the county. Once this is done, the average capacity factor for the whole province is found, by calculating the mean capacity across all of the counties:

$$P_{\text{norm,NS},t} = \frac{\sum P_{\text{norm,county},t}}{n_{\text{counties}}} \quad 5$$

Using this method each county is weighted equally as long as it has at least one operational solar array providing data. If the average capacity factor of all solar arrays was found, then the resulting data would be heavily weighted by Halifax County's 101 solar arrays rather than the entire province's solar resource. This simulates a series of utility-scale solar arrays, if the only solar in the province continues to be on residential buildings than simply finding the average of all the data would be a better estimation.

Figure 15 shows the resulting data from the described processing.

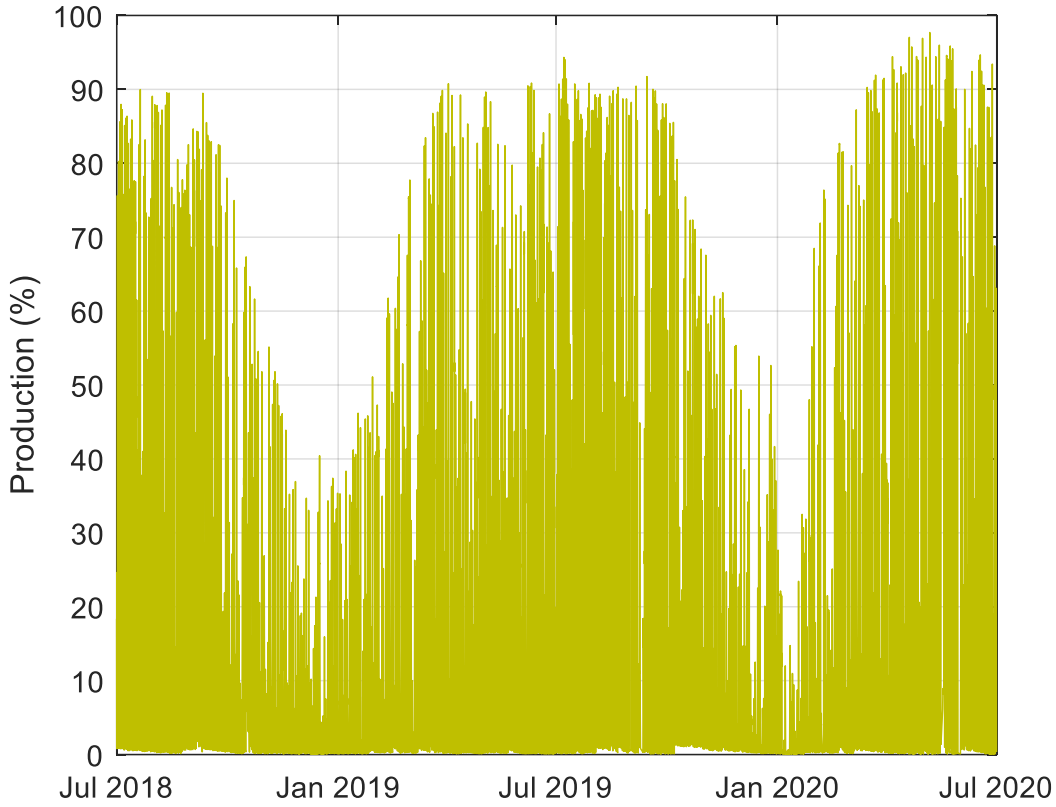

Figure 15 Resulting solar resource data

As expected, the solar production is highest during the summer, and lower during the winter. It typically peaks around noon each day, shifted depending on when solar noon occurs. Notably it never reaches 100% production, because there is never a point when all solar arrays are producing at their peak production. The peak production is also stretched, rather than the peaks following a sine curve, this is likely a result of the various orientations across all solar arrays in the province, so each array peaks at a slightly different time of year.

4.3. Load

The provincial load represents the total power demand of the province that the electric utility, in this case NSP, sees. This would ignore any load that is met by consumer owned generators, such as solar panels, that would provide power to appliances before they pull electricity from the grid; this is considered to be insignificant to the load. This value is

provided in the same format as the aggregate wind by NSP, provided in 2-minute timesteps and available from 2012 until the end of 2020.

The load is processed using the same method shown in the flowchart in Figure 7. Any value that was significantly larger than the 99.9th percentile value was considered an outlier in this process. The resulting data is shown in Figure 16:

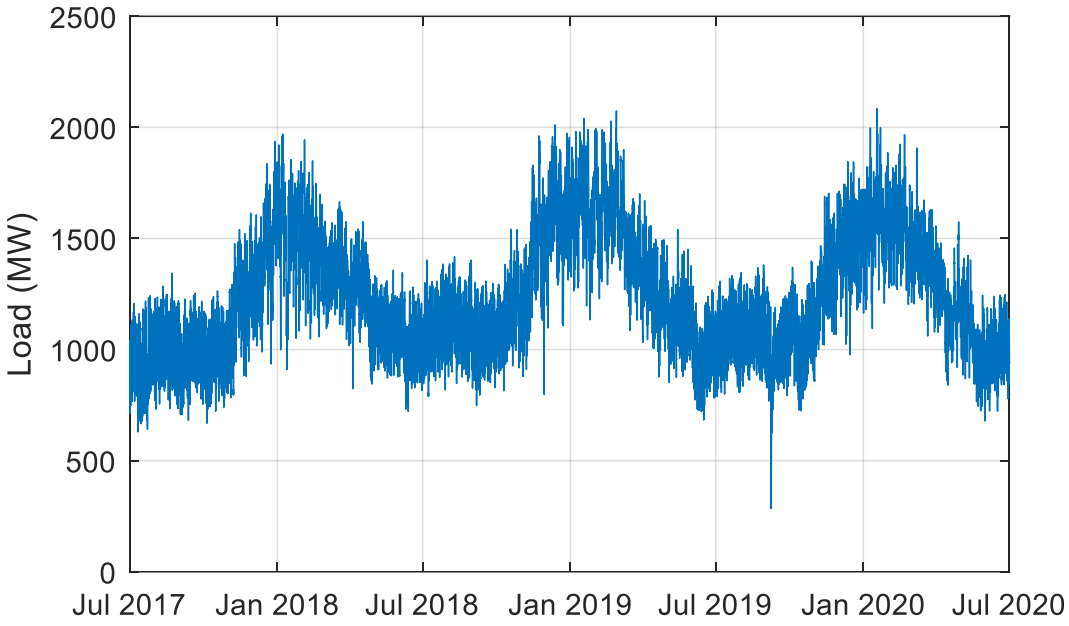

Figure 16 Provincial load data

For the most part the data follows the typical seasonal and hourly pattern expected for NS. The load is highest in the winter due to space heating requirements. The load is lowest in the late spring and early fall. There is a slight bump in the summer as there may be some cooling, but not nearly the magnitude of the heating load in the winter. In September 2019 there was a hurricane which caused a blackout across the province which explains the drop in demand near the end of the 2019 data.

4.4. Ambient Conditions

The ambient climate conditions data was downloaded directly from the environment Canada website using the historical weather reports[5]. A script was running using

[5] https://climate.weather.gc.ca/climate_data/daily_data_e.html?StationID=50620

MATLAB to download from this website for every day. The data was downloaded from stations near the largest population centres of NS. These stations and the cities they reside near are listed in Table 2:

Table 2 Weather stations used for city temperatures

Station	City
Halifax Dockyard	Halifax
Sydney	Sydney
Debert	Truro
Caribou Point	New Glasgow
Yarmouth A	Yarmouth
Kentville CDA CS	Kentville
Nappan Auto	Amherst
Lunenburg	Bridgewater

The data from each weather station listed in Table 2 was used to determine the average temperature experienced by Nova Scotians, by calculating a weighted average temperature across all the stations based on the population of the city they were close to.

$$T_t = \frac{\sum T_{i,t} \times Pop_i}{\sum Pop_i} \qquad 6$$

Equation 6 shows the calculation used for provincial temperature, where $T_{i,t}$ is the temperature at each city at a given time, and Pop_i is the population of that city.

Chapter 5. Capacity Value of Wind and Solar Generators

Historically in NS, expansion of wind generation has been prioritized over solar. The scale of wind projects in NS is typically larger than that of solar projects in the province. Most of the solar power output is generated from installations found on customers' roofs. Section 4.2 described a new way to estimate a potential aggregated large-scale production of solar electricity in NS using the data from the small installations across the province. The resulting data from this will now be used for a capacity value comparison between wind and solar.

Comparisons between wind and solar generation have been done before, even NS. The unique focus of this analysis is on various factors that impact capacity values for the two generation technologies. First analysing how timeframe or resolution of data affects the capacity value results for wind, then determining how the capacity value of wind changes with ambient conditions. After this, the capacity value of solar is compared to wind using all the data available, then analysing based on month of year or hour of day.

5.1. Methods

The calculation of capacity value is done using the cumulative frequency analysis. The general technique for this is described in section 2.2.2, but this section provides specific details of how it was calculated using the data available. In addition, this section describes the steps made to isolate the specific factors that impact capacity value. Cumulative frequency analysis was chosen over the ELCC method because it allows better isolation of different timeframes of data, which enables the comparison of different factors. Additionally, the cumulative frequency analysis method is less computationally intensive, so multiple studies can be run in a shorter timespan which allows for easier comparison. The flowchart in Figure 17 shows the steps used for calculating the capacity value using the cumulative frequency analysis method:

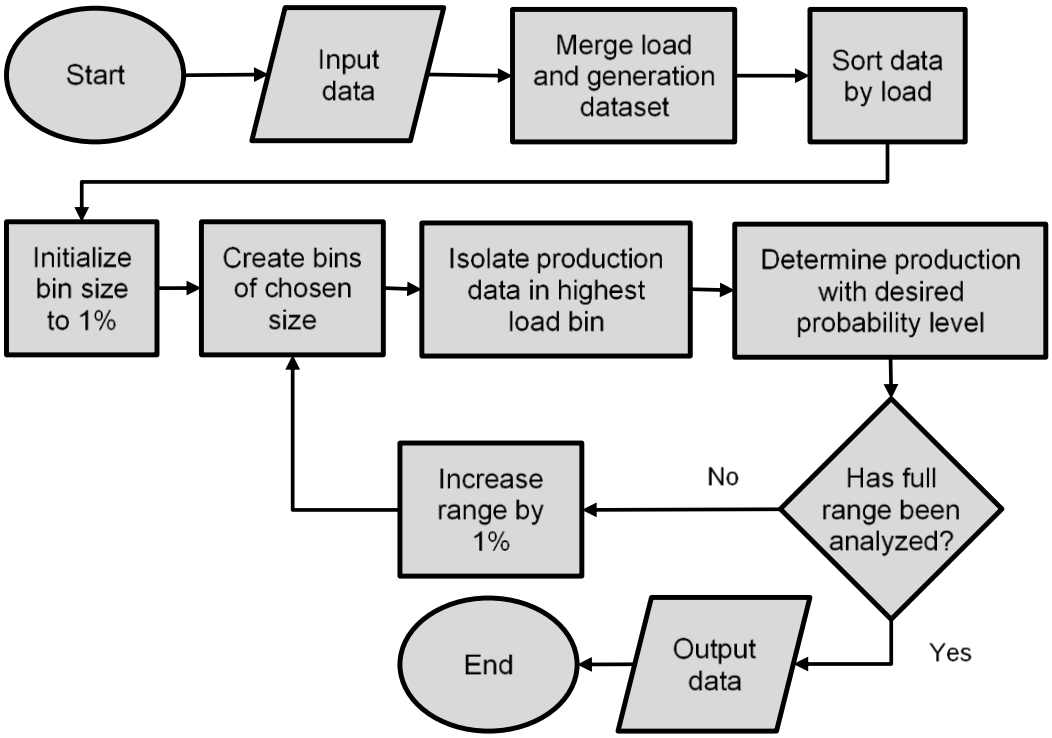

Figure 17 Cumulative frequency analysis flowchart

The data required for this analysis is:

- Provincial load data
- Normalized wind or solar generation data

The load and generation data are synchronized so that any given time has both a known load and IG production. This production data should have already been normalized, so it is a percentage of the rated capacity. The data is sorted by load to examine the high load times.

After this initial preparation, a loop begins that continuously increases the amount of data analyzed to graph the changes in reliable production as the load increases. After each iteration the range of data increases. The production data within this new range of loads is then reviewed to find at what percentage of its total capacity it will produce at a given confidence level. This is done by determining the 20^{th}, 10^{th} and 5^{th} percentile production during these times of peak demand. The 5^{th} percentile represents the value which is lower

than 95% of the datapoints, indicating there is a 95% confidence that the generator will produce more power than that value; likewise the 20th percentile corresponds to a 80% confidence, and 10th percentile corresponds to a 90% confidence. Once the loop is completed the output shows how the reliable generation of each farm changes as the load threshold decreases.

The way these factors were isolated is described in the following sections.

5.1.1. Annual Capacity Value Analysis

The annual capacity value analysis compares how each farm changes the capacity value from one year to another. This analysis simply bins the data by year before sorting it by load. However, since all high load times in NS occur during the winter, each year centres around the winter. So each year of analysis begins in July and ends in June, to keep a continuity of each winter. For example, *the 2018/19 analysis included the data from July 1, 2018 to June 30, 2019*. The process for this analysis is shown in the flowchart shown in Figure 18:

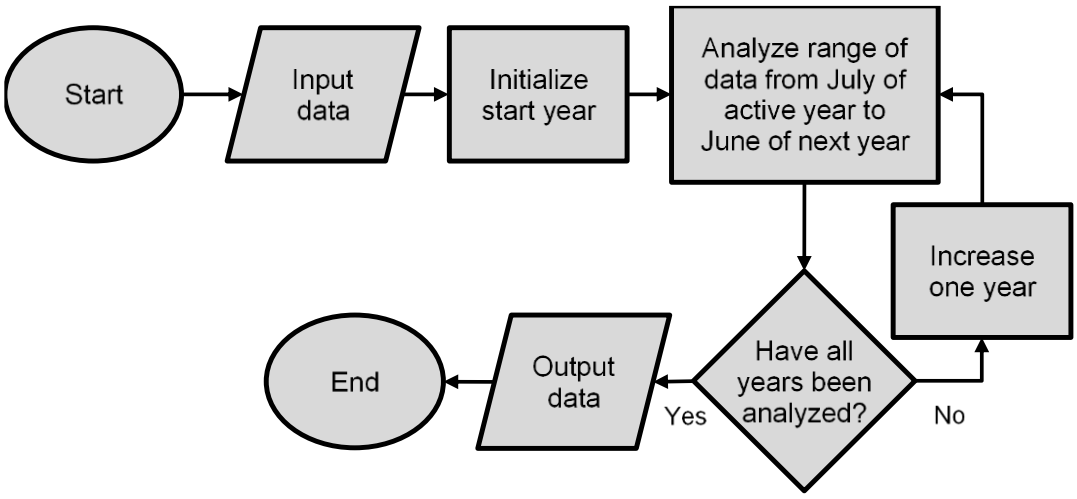

Figure 18 Annual capacity value analysis flowchart

This analysis uses a single loop to repeat the cumulative frequency analysis described in Figure 17, after isolating one year of data at a time. The output is three sets of capacity value data, one for each winter analysed.

5.1.2. Data Resolution

This analysis reviewed the change in capacity value as the dataset resolution decreases. To evaluate this, the timestep was averaged across multiple datapoints to create a more coarse analysis. The process is shown in the following flowchart:

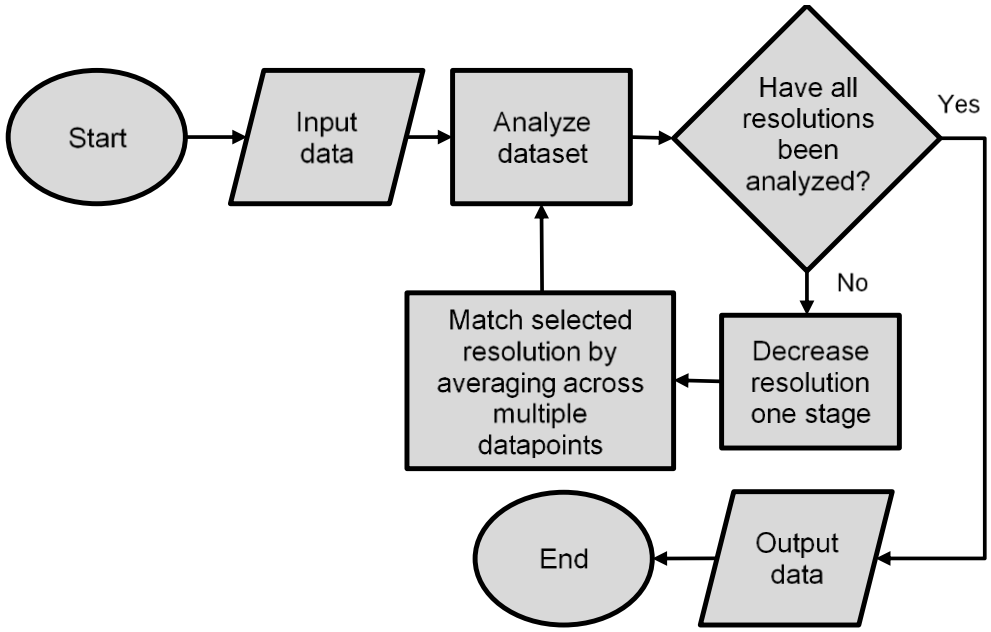

Figure 19 Data resolution analysis flowchart

In this case the loop changes the resolution every iteration. The initial timestep was two minutes, so it was increased to match timesteps typically available for data. These values were 5 minutes, 10 minutes and hourly. To best simulate the data being naturally recorded at these longer timesteps the values measured that occurred during these timesteps are averaged and recorded at the following interval. For example, *the 01:20 value in a 10-minute timestep would use the average windspeed using all datapoints from 01:12 to 01:20*. Then the capacity value of this new dataset was calculated normally.

5.1.3. Ambient Conditions

The ambient condition data was analyzed using a different method than the other two sets of analysis. To start off the correlation between load and ambient temperature, and windspeed and temperature was analyzed. For the load and temperature correlation a scatterplot was made showing temperature on the x-axis and load on the y-axis. To compare windspeed and temperature, the windspeed was categorized into high, medium

and low windspeeds, where the high windspeeds were in the top 67th percentile, medium were between 33rd and 67th percentile, and low were below the 33rd percentile. This was used to examine any correlation between windspeed and temperature or load.

Then an analysis of capacity value depending on temperature was performed, as described in the following flowchart:

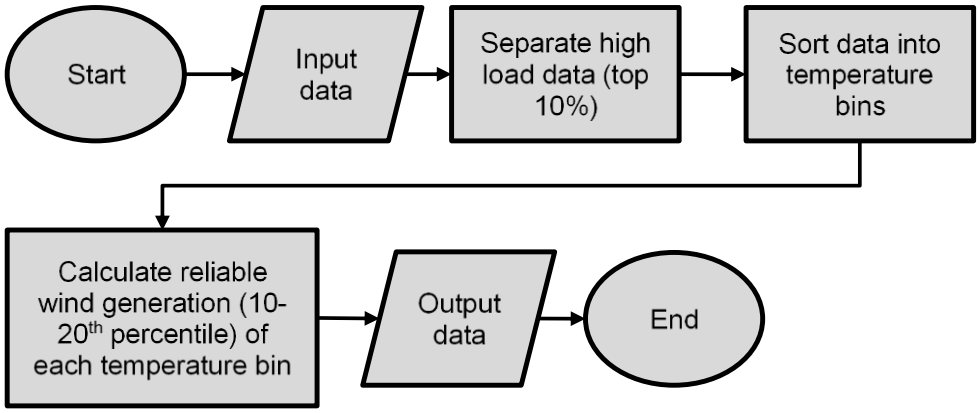

Figure 20 Ambient temperature analysis flowchart

This uses a different method than the previous analysis, rather than performing iterative capacity value analysis after manipulating the data. In this analysis the high load data above the 10th percentile load is separated, then sorted by temperature. These temperature bins, each have the reliable wind generation determined by calculating the 10th and 20th percentile wind generation based on the data inside the bin.

5.1.4. Comparison to Solar

To compare the solar to wind, first the cumulative frequency analysis, described in Figure 17, was performed on the solar data. Then a annual capacity value comparison was performed, by separating the solar data by year and applying the same technique used for wind. Due to the high penetration of wind in NS, an analysis on the incremental value of each intermittent resource was performed, to see if adding new solar would perform better than new wind. This was done using the same cumulative frequency analysis described in Figure 17, except instead of the total load for the province, first the current production of intermittent resources was subtracted from the load to calculate the net load. This calculation is shown in equation 7:

$$P_{\text{Load,net},t} = P_{\text{Load},t} - \left(P_{\text{wind},t} + P_{\text{solar},t}\right)_{\text{IG}} \quad (7)$$

Where $P_{\text{wind},t}$ and $P_{\text{solar},t}$ are the power output from wind and solar generation at a given time t, respectively. $P_{\text{Load},t}$ is the electrical load at time t, and $P_{\text{Load,net},t}$ is the net load. This net load determined the residual load experienced by DG in the province. The purpose of looking at the net load is because that is what needs to be targeted by subsequent IG installations to reduce the need for DG.

Next an analysis comparing the hourly capacity value was done, to separate data based on the hour of day investigate the times at which solar generation is producing during the day. The steps taken for this analysis is shown in the following flowchart:

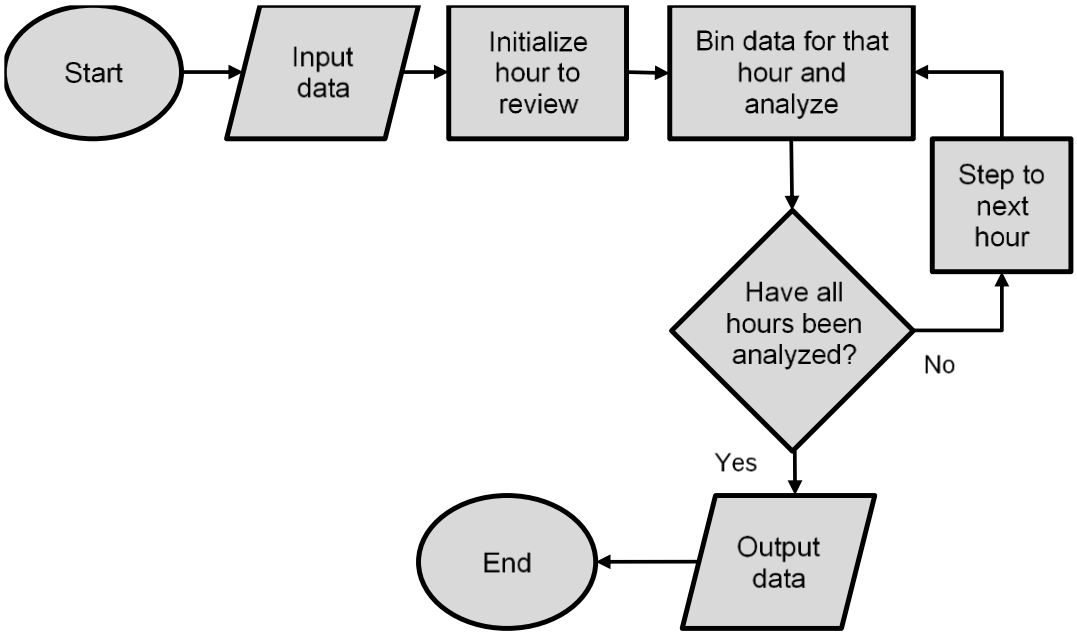

Figure 21 Hour of the day analysis flowchart

In this analysis, the data is separated by hour of the day (in AST), and the cumulative frequency analysis was performed on each hourly dataset. In this case the results were plotted against time, so a single load level was selected to display, 90th percentile loads was used, as the top 10% load level was often used in literature. Finally, an analysis on each month of the year was done. This examines the capacity value of each during the summer to see if solar generation is the best option for matching AC loads or accounting

for lower production from run of river hydro. The only difference in method between the month of year analysis and hour of day analysis, was that the month of year analysis initially binned the data by month rather than hour.

5.2. Results

An initial analysis is done to determine the baseline production and capacity value. The relative demand and production is determined, Figure 22 shows the energy demand per month, and the monthly energy production for wind and solar generation. It is important to note that since there is not sufficient utility scale solar to be comparable the solar data has been scaled up to match the installed capacity of wind in MW.

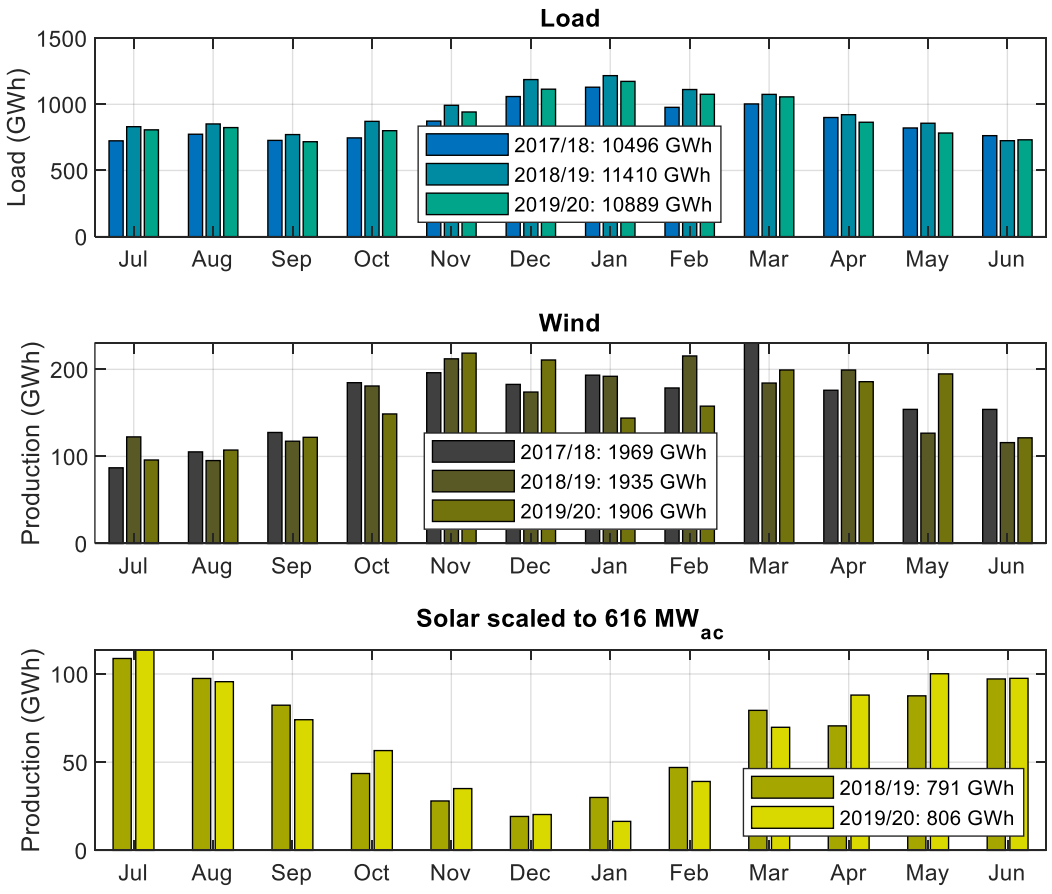

Figure 22 Energy demand per month, and energy production per month for wind and solar in NS

Figure 22 shows that the average electrical load is higher in the winter, which is the same for wind, however, this is the time of lowest average power output for solar. This high winter load is typical for NS, as it requires more space heating in the winter, than cooling in the summer. The low production of solar is expected, due to the shorter days and the lower solar radiation in the winter. Using this, a higher capacity value for wind is theorized, as solar has a lower average production, it is less likely to be producing a high yield during the high load times.

Due to the high average load in the winter months, it is theorized that instantaneous load will be higher during these months than in the summer months. Since the winter season is more relevant to the analysis, the year has been split halfway, rather than on January 1. Each 'year' analyses the data from July-June. This way, high load events that occur in the same winter, but two different calendar years are not separated.

Next, to set a baseline for the analysis, the capacity value of wind generation alone is determined, that can be used for comparison. This was done for the aggregate wind production, as well as the individual farms and is shown in the Figure 23:

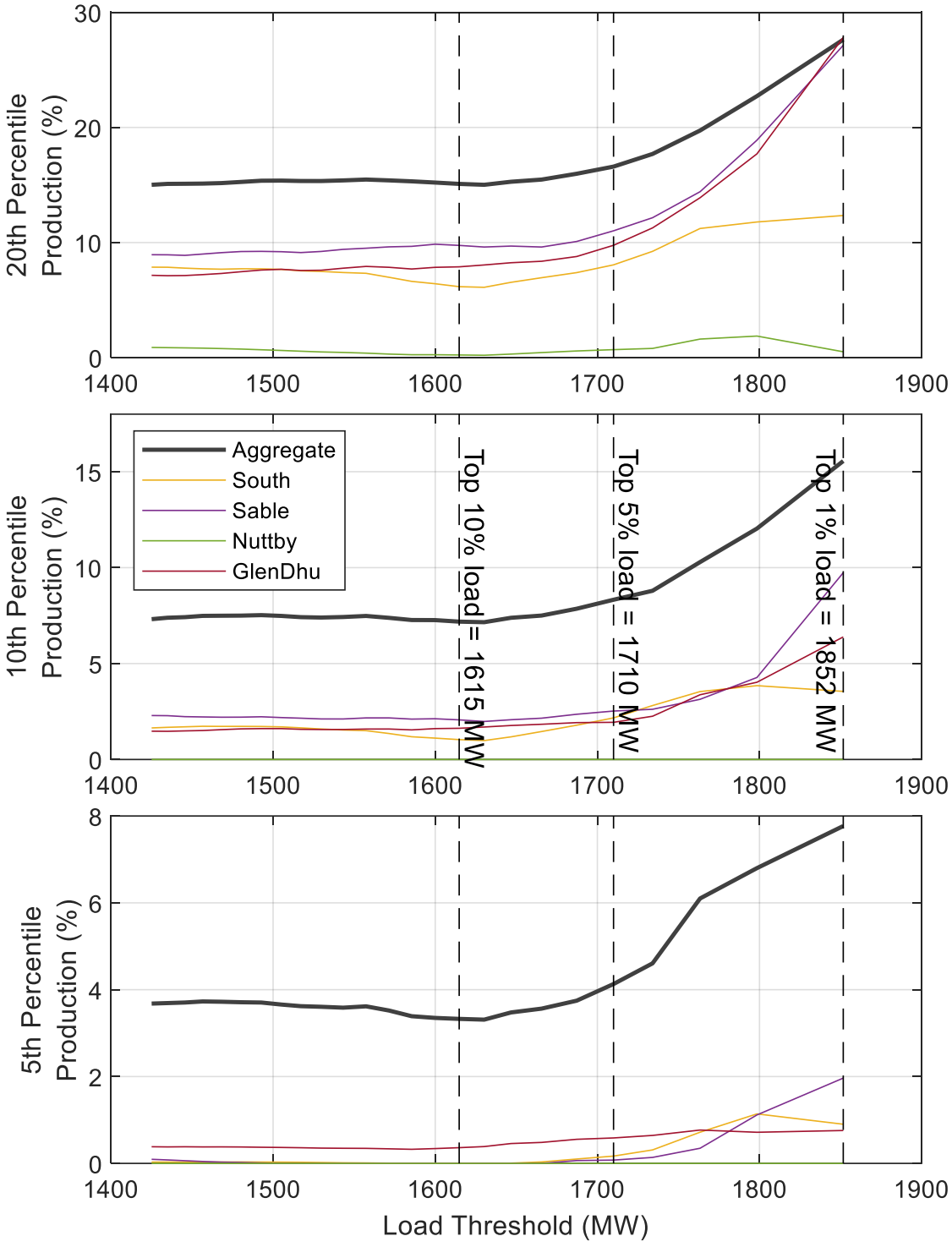

Figure 23 Capacity value with 80%, 90% and 95% confidence level

The capacity value reflects the reliable production of each wind farm at high loads. The x-value on the graph shows the load threshold considered 'high-load', while the y-value shows the reliable production when the province is at or above that load. In the top graph

of Figure 23, the production is considered reliable if it is producing above the plotted level 80% of the time; in the middle graph it requires a production over that level 90% of the time; and for the bottom graph the wind farm or aggregate needs to be above the displayed level 95% of the time.

There is a clear upwards trend in most of the wind farms, and aggregate, as the load increases the reliable wind production increases. This means that a farm will reliably produce more electricity as load increases. The three vertical lines on the figure indicate different specific load levels. They are top 10%, 5% and 1% loads, which are equivalent to 90th, 95th, and 99th percentile load, the capacity value at these levels is listed in the following table:

Table 3 Load and aggregate production at various load levels

Parameter	90^{th} percentile load	95^{th} percentile load	99^{th} percentile load
Load (MW)	1615	1710	1852
20^{th} percentile production (%)	15	17	28
10^{th} percentile production (%)	7.2	8.3	16
5^{th} percentile production (%)	3.3	4.1	7.8

The 20^{th} percentile production at the top 90^{th} percentile load results in a wind capacity value of 15% which is comparable to the 19% ELCC capacity value found for NS Power's integrated resource plan [27]. The difference between the two results is due to the difference in methods used. Cumulative frequency analysis determines the statistical reliable production of historical generation, while ELCC uses probabilities to forecast the future load carrying capability of a generator. While the results are different, the change is not drastic, indicating there is some agreement on the magnitude of capacity value using each method.

The trend of reliable production increasing as load increases is evident in the table as well. At each confidence level, the production approximately doubles from the 90^{th} and 99^{th} percentile load, indicating that wind generation becomes more reliably higher as the load increases.

Another noticeable feature in these results in the distinct difference between the aggregate wind capacity value, and each individual farm capacity value. In the top graph, the individual wind farms begin at approximately 50-60% the value of the aggregate but rise to match the aggregate at the peak load. In the middle graph the individual wind farms begin at only 25-35% of the aggregate and rise to no more than 70% of the aggregate, while the final graph they begin at approximately 10-15% of the aggregate and end at 30% of the aggregate. This indicates that they perform much worse, proportionally, than the aggregate as the reliability demanded increases.

As described in section 4.1.1, the aggregate wind is an estimate of the total wind production of the province, generated using the top nine wind farms in the province. These nine wind farms are located across the province, while each individual wind farm is comprised of wind turbines concentrated in one location. This means that there may be times that the wind resource is low in one area at a given time, which would result in all the wind turbines in a single farm having low production. It is less common that the entire province will experience a low wind resource at the same time, resulting in the entire province having low production.

Due to the dispersed wind production the aggregate sees fewer minimums, which results in greater reliable production. This has an inverse effect too, it is unlikely that the wind speed will be high across the whole province, so NS would experience its maximum wind production less frequently than any individual farm. This drawback is not seen in this analysis because the capacity value when using the cumulative frequency analysis is only impacted by the worst-case scenarios, and rewards more reliable, but potentially lower, generation over more intermittent farms that see 100% and 0% production equally. This shows that adding new wind farms in new locations will improve diversity, resulting in more reliable production, and thus greater capacity value.

The farm that is most penalized by being concentrated in one location is Nuttby Mountain. It has no reliable production at the high load thresholds at any of the displayed confidence levels. Figure 24 shows the production of the wind farm, as well as a comparison wind farm and load for reference:

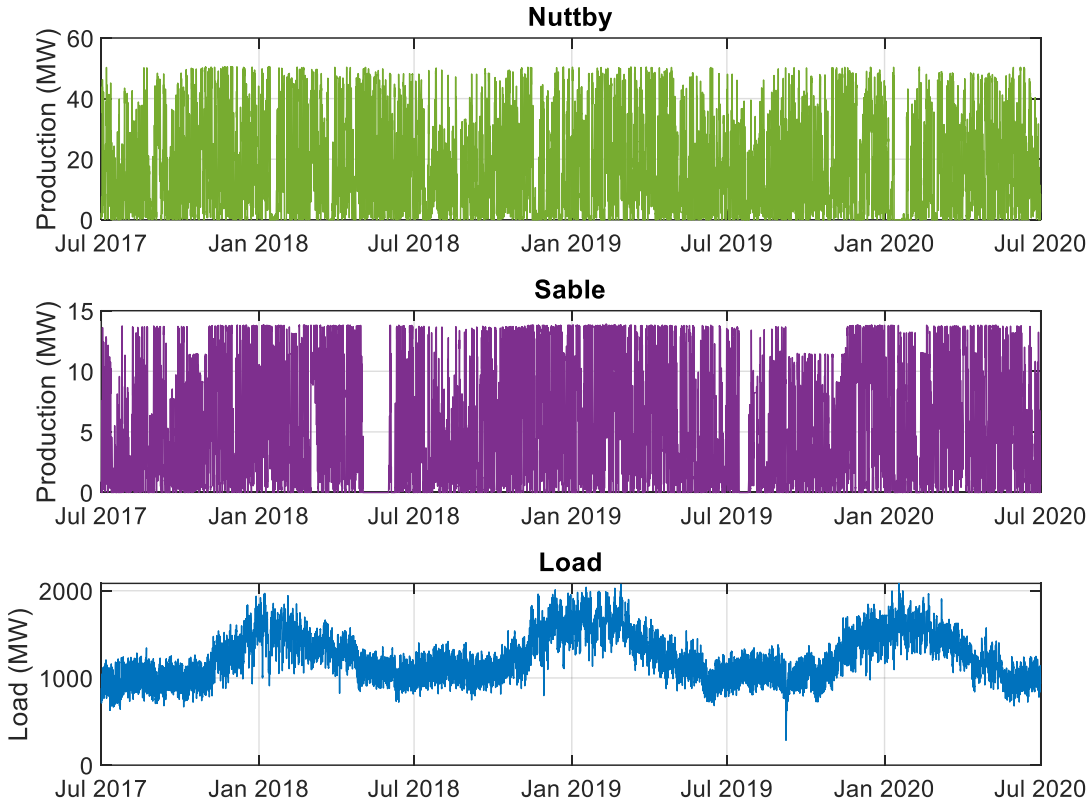

Figure 24 Nuttby Mountain and Sable wind farm production and NS demand time series

In the top graph from Figure 24 Nuttby Mountain has a zero-production period during January 2020. This could have been caused by icing, a failure at the inverter, a data collector failure, or transmission failure. The reason does not matter when considering the effect it has on the analysis. The zero-production period takes two weeks, out of three years or 1.3% of the data. However, this occurs during the load peak of the 2019/20 winter, which means that most of this zero-production time happens during the peak loads. While it may produce greater than zero most of the time, when the analysis focuses on the high load times, it will appear to have a much lower reliability, if a substantial period of high load times is made up of a continuous zero-production period.

By contrast, Sable, had much larger zero-production periods in summer 2018 and summer 2019, despite this Sable has a much greater capacity value in Figure 23. This is due to the load being much lower when Sable had zero-production than when the zero-production

period occurred at the Nuttby Mountain wind farm. Indicating the clear importance of reliability when the load is high to the capacity value analysis.

In this analysis, three years of data was used. With two minutes timesteps this resulted in a significant amount of data, as described in the Table 4:

Table 4 Data significance of each confidence level at various load levels

Load Threshold	**All Data**	80% confidence	90% confidence	95% confidence
All Data	**789120**	157824	78912	39456
Top 25% loads	**197280**	39456	19728	9864
Top 10% loads	**78912**	15782	7891	3945
Top 5% loads	**39456**	7891	3945	1972
Top 1% loads	**7891**	1578	789	394

At two-minute timesteps, there are 789120 datapoints over the three years worth of analysis. The leftmost datapoint in Figure 23 is the top 25% loads threshold, which accounts for 197280 datapoints, which means at the 80% confidence level there are still 39456 datapoints that occur under the marked production level. By contrast, the top 1% loads accounts for 7891 datapoints, with the 95% confidence level only having 394 datapoints falling under.

Out of 789,120 total datapoints 394 seems insignificant, however, this accounts for 13 hours worth of low power production at high loads. Indicating that even at the strictest measurements, there are still 13 hours at which the turbines produce less than the marked amount when peak loads are occurring. Looking at each year individually will break this down further, reducing each value to a third of what is shown .

5.2.1. Annual Capacity Value Analysis

This analysis determines how the capacity value changes each year. To begin, the data was split up by year, from July of the first year to June of the next. Then the data was sorted by load, rather than chronologically. The results are shown in Figure 25, the production shows the median value across 1% of the data points, rather than showing all the data points, as there are two many to plot individually.

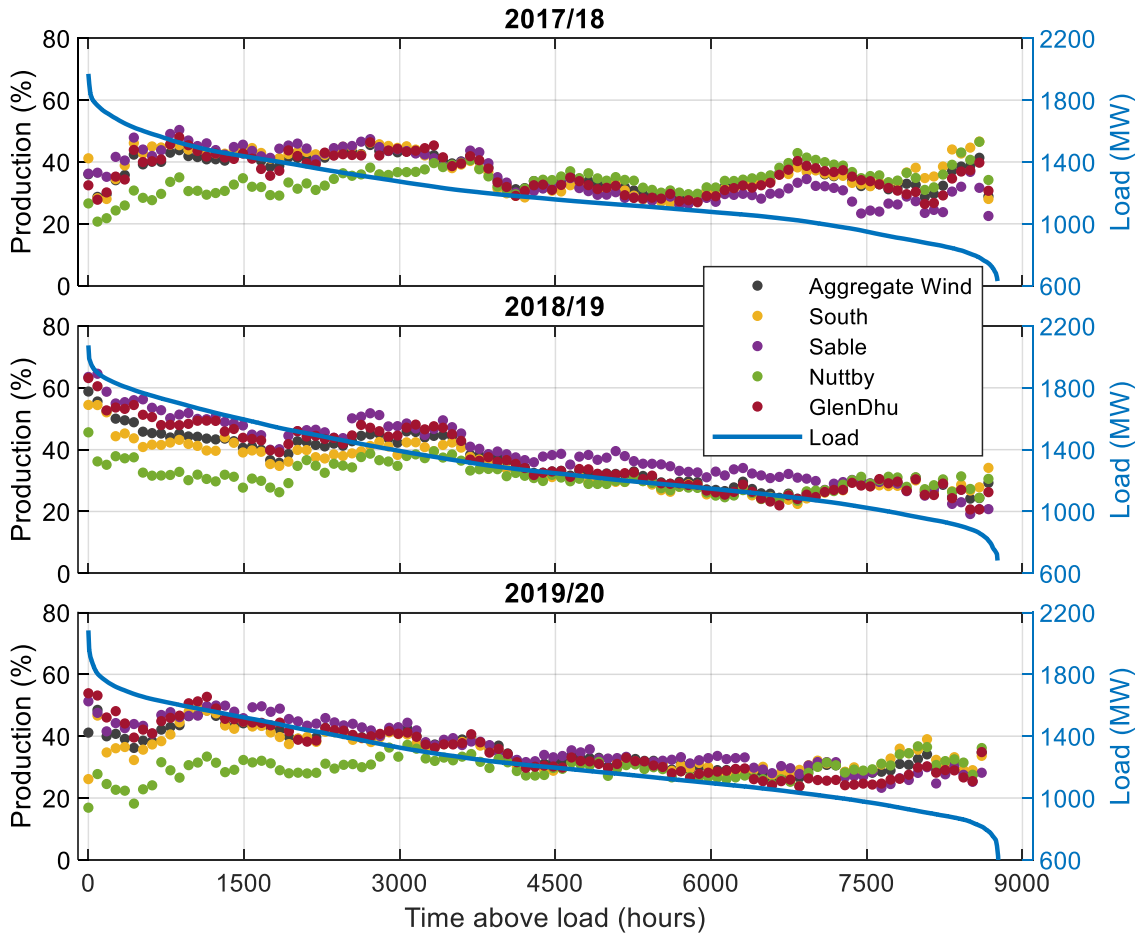

Figure 25 Median wind production and load data sorted by load

Figure 25 shows the variation in the trends occurring during each year. In 2017/18, production is relatively flat as load decreases, rising and falling slightly but ending approximately the same as it began. This is very different for 2018/19, where the production is highest at the peak loads then decreases as the load decreases. The trend in 2019/20 is a between these two years, with a slight peak at the highest loads, but then decreasing right after this very highest load, before leveling out and slowly decreasing as the load falls.

Most of the farms are grouped close together, and some are actually greater than the aggregate at times. This is different than in Figure 23 because this is displaying the median power production, not the 20th, 10th or 5th percentile production. Nuttby Mountain is the exception which stands out with poor performance each year, especially in 2019/20

which is likely due to the gap in production shown in Figure 24. Even in previous years Nuttby did not perform well, so it is expected to have the lowest capacity value for each year.

This variation between the years shows the importance of investigating multiple years. If a single-year worth of data were picked the results could be drastically different depending on which year was analysed. This will be greater emphasised by the capacity value analysis performed for each year, which is shown in the following figures:

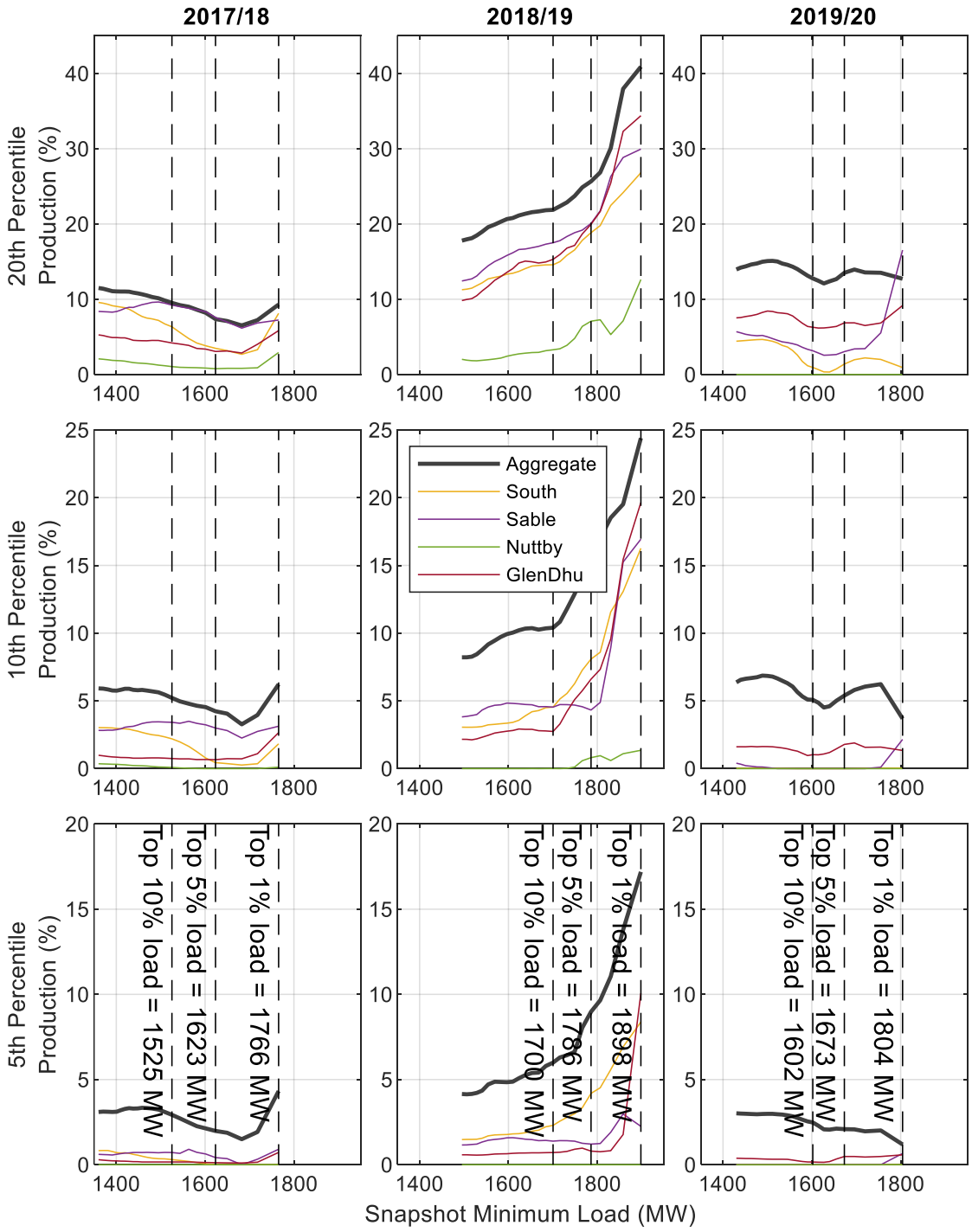

Figure 26 Capacity value of wind farms per year for 80%, 90% and 95% confidence levels

In Figure 26 the capacity value for each farm is plotted as in Figure 23, however the data was first separated by year. The nine graphs are made up of different combinations of year, and confidence level: all of the leftmost graphs use data from July 2017-June 2018, the middle column is 2018/2019, and the right column is 2019/2020; the top row is 80% confidence, the middle row is 90% confidence, and the bottom row is 95% confidence.

The y-axis remains constant between each column for comparison between years, however the y-axis changes maximum between rows as the reliable production is expected to decrease as the confidence level increases. Due to the different load profile each year, the x-axis of each figure has the same range, showing how the actual data shifts depending on the year, this is related to the load experienced during that year. The distribution of loads between years is explored in Table 5. Also included in Table 5 is the difference between the 99th - 95th percentile load, and 99th – 90th percentile loads, to show how these change depending on the year.

Table 5 Comparative loads between years and differences between high load levels

Year	99th percentile load (MW)	95th percentile load (MW)	**Delta 99th – 95th (MW)**	90th percentile load (MW)	**Delta 99th – 90th (MW)**
2017/18	1766	1623	**143**	1525	**241**
2018/19	1898	1786	**112**	1700	**198**
2019/20	1803	1673	**130**	1602	**201**
Three year analysis	1852	1710	**142**	1615	**237**

The 95th and 90th percentile loads are higher for the 2018/19 dataset, than the other two years. Additionally the difference between the 99th and 95th or 90th percentile load levels is lower for 2018/19 than in the other two years, indicating not only are the top loads higher, but that there is a greater concentration of these higher loads. As a result the 2018/19 must dominate total analysis of three years as it would have the most high load times. This explains why the magnitude of the three year analysis shown in Figure 23 is closer to the 2018/19 result, and the upwards trend occurs in the three year analysis matching 2018/19.

The trend of capacity value increasing as load increases, observed in the full analysis, only occurs in the 2018/19 analysis when the years are separated. In the 2017/18 dataset the capacity value does eventually spike after a decrease, resulting in a shape like a hockey stick or backwards check mark. In the 2019/2020 dataset the capacity value consistently decreases as the load threshold increases. This shows that on a long scale analysis this trend of increasing capacity value as load threshold increases may occur, but on a single year analysis the trend is not guaranteed. As the multi-year analysis was driven by the high loads in 2018/19, it cannot be concluded that this trend would occur consistently, it may be unique to that year.

Not only is the shape of the trend different, the scale is noticeably different between the three years and the total analysis. In the multi-year analysis the peak capacity value was 27.4%, while in in 2017/18 it was 11%, in 2018/19 it was 41%, and in 2019/20 it was 15%. This wide variation shows the difference between each year, indicating that in 2018/19 wind production matched load much more closely, while in 2017/18 wind production often failed to produce electricity at high loads. The dramatic difference in both shape and magnitude between years could be the result in mechanical failure due to weather conditions, such as icing. If the 2019/20 winter has significantly more freezing conditions this would explain it. Another cause could be that the wind events are out of sync with the load and are occurring at lower load times as opposed to the 2018/19 year.

To compare *like load to like load*, the capacity value at a single load threshold can be compared. Rather than comparing peak load capacity value, where the 2018/19 peak is 132 MW higher than 2017/18, this can compare the capacity value at the same load threshold by selecting 1610 MW. 1610 MW is chosen because it is the 90^{th} percentile load for the full three-year analysis shown in Figure 23. The capacity value when using this load threshold is shown in Table 6:

Table 6 Capacity value of wind farms per year for 80%, 90% and 95% confidence levels at the 1610 MW load threshold

	2017/18	2018/19	2019/20
20^{th} percentile production (%)	7.88	20.8	12.6
10^{th} percentile production (%)	4.44	10.0	4.96
5^{th} percentile production (%)	2.07	4.86	2.38

While 2017/18 and 2019/20 are closer at the 90% and 95% confidence levels, 2018/19 still exceeds them. This indicates that there is not an issue related to the range of loads being observed. Lower average production cannot be blamed for the low reliable production at peak load times, either, as Figure 22 showed the energy produced by wind was consistent for each year. This confirms that capacity value is not consistent each year, even when looking at the same load threshold and confidence level. It is not clear from this data if 2018/19 was an especially good year for the correlation of wind generation to high load, or if the other two winters were especially bad. As such a single year cannot be selected to be representative of the behaviour of wind generation in the province.

The conclusion of these results is that a single year is not representative of the performance of wind in terms of capacity value. If only a single one of these years were chosen it would provide wildly different results then any other year, or the aggregate of three years. Figure 26 showed the difference in trend between each year, different conclusions about winds relation to load could be made if only a single year were reviewed. Table 6 shows the difference in capacity value at the same load threshold between three years, if only a single year were reviewed it would have dramatically different results.

5.2.2. Data Resolution

Many sources vary in the resolution of data. The literature reviewed in section Chapter 3 often used data in hourly timesteps, this thesis has data in 2-minute and 5-minute timesteps, often data also comes in 10-minute timesteps. The following figure shows a calculation using each of these timesteps to show the variation of results caused by the variation of resolutions:

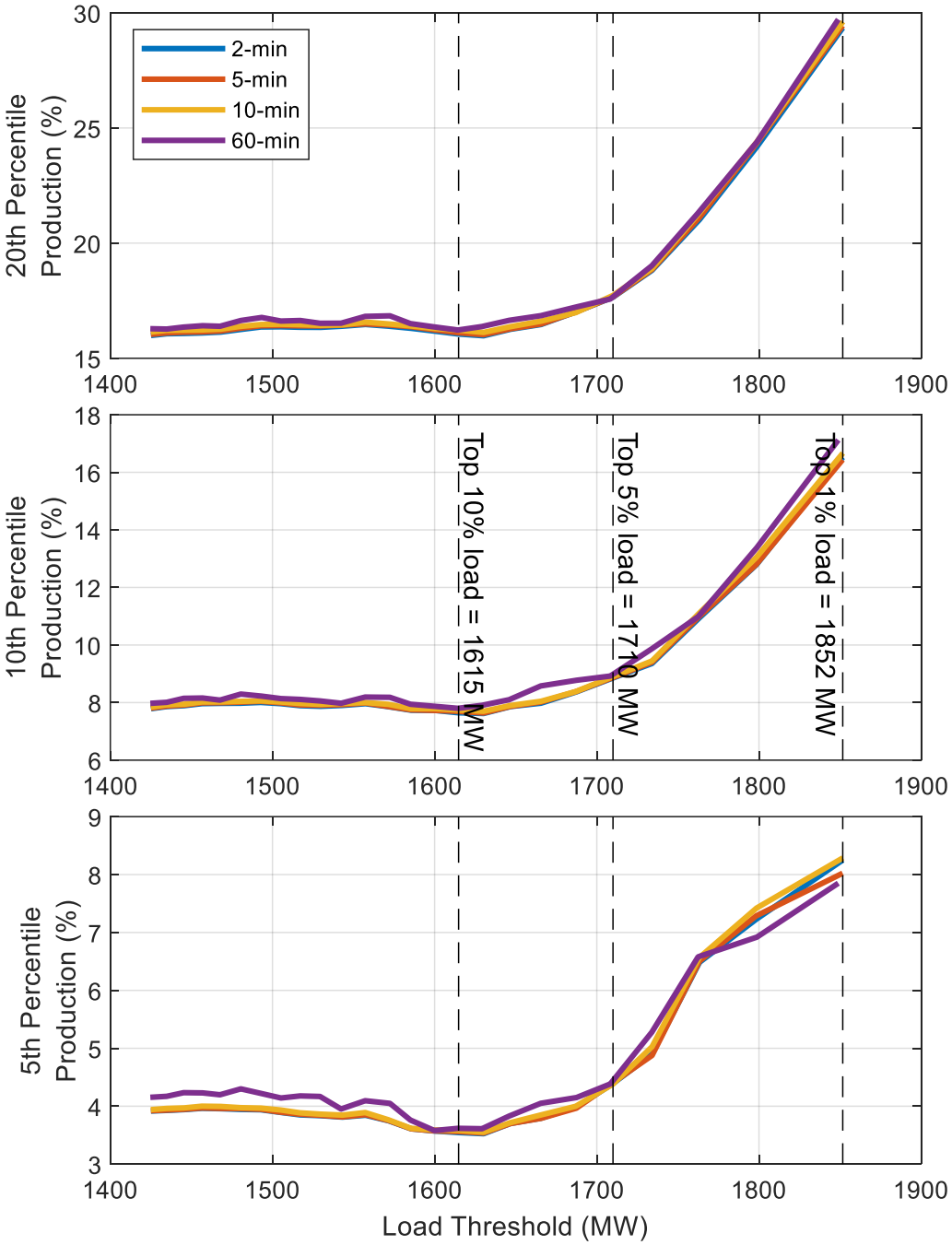

Figure 27 Resolution variations in capacity value of wind with 80%, 90% and 95% confidence

In Figure 27 there is little observable differences between capacity value in the 2-minute, 5-minutes, and 10-minute timesteps, however there is a slight difference between the first three timesteps and the 60-minute timestep. For easier reading, the values at various points are displayed below:

Table 7 Capacity values with 80%, 90% and 95% confidence for each timestep at notable points

	Capacity Value for each timestep (%) 80% confidence level			
Load (MW)	2-minutes	5-minutes	10-minutes	60-minutes
1852	29.4	29.4	29.6	29.7
1710	17.6	17.7	17.7	17.7
1615	16.1	16.1	16.2	16.2
1571	16.4	16.4	16.5	16.8
Load (MW)	Capacity Value for each timestep (%) 90% confidence level			
	2-minutes	5-minutes	10-minutes	60-minutes
1852	16.5	16.4	16.7	17.1
1710	8.9	8.9	8.9	9.0
1665	8.0	8.0	8.0	8.6
1615	7.6	7.7	7.7	7.8
1571	7.9	7.9	7.9	8.2
Load (MW)	Capacity Value for each timestep (%) 95% confidence level			
	2-minutes	5-minutes	10-minutes	60-minutes
1852	8.3	8.0	8.3	7.9
1800	7.3	7.3	7.4	6.9
1710	4.4	4.4	4.4	4.4
1615	3.5	3.6	3.6	3.6
1571	3.8	3.8	3.8	4.0

At the 80% confidence level all the values are close to each other, but they are ordered based on their resolution, the larger timesteps result in larger capacity values. This is also the case at the 90% confidence level. Even at the 95% confidence level the 60-minute timestep is higher than the other values for most of the figure, indicating that there is a minor perceived improvements in capacity value as the resolution decreases. However, there is a drop at the end, at which point the hourly timestep has the lowest capacity value. This indicates that the capacity value is always better at the higher timestep.

The expected result was that at finer resolution, the intermittency of wind would have a greater impact, resulting in more frequent low production amounts causing a lower reliability. Whereas at a lower resolution, the wind generation is smoothed, causing the peaks to drop and the valleys to rise, resulting in greater reliability. This did not result; while there was a change in capacity value as the timestep changed, the difference was insignificant.

5.2.3. Ambient Conditions

As NS is a winter peaking province, it is expected that the electrical load in the province has a negative correlation to the temperature. Figure 22 previewed that wind tended to be higher in the winter months which supports the theory that load in NS is higher when it is colder. This section examines the correlation between ambient temperature and load, and investigates the relationship between wind resource, wind energy production, and wind capacity value, with ambient temperature.

The relationship between ambient temperature, windspeed and load is shown in Figure 28:

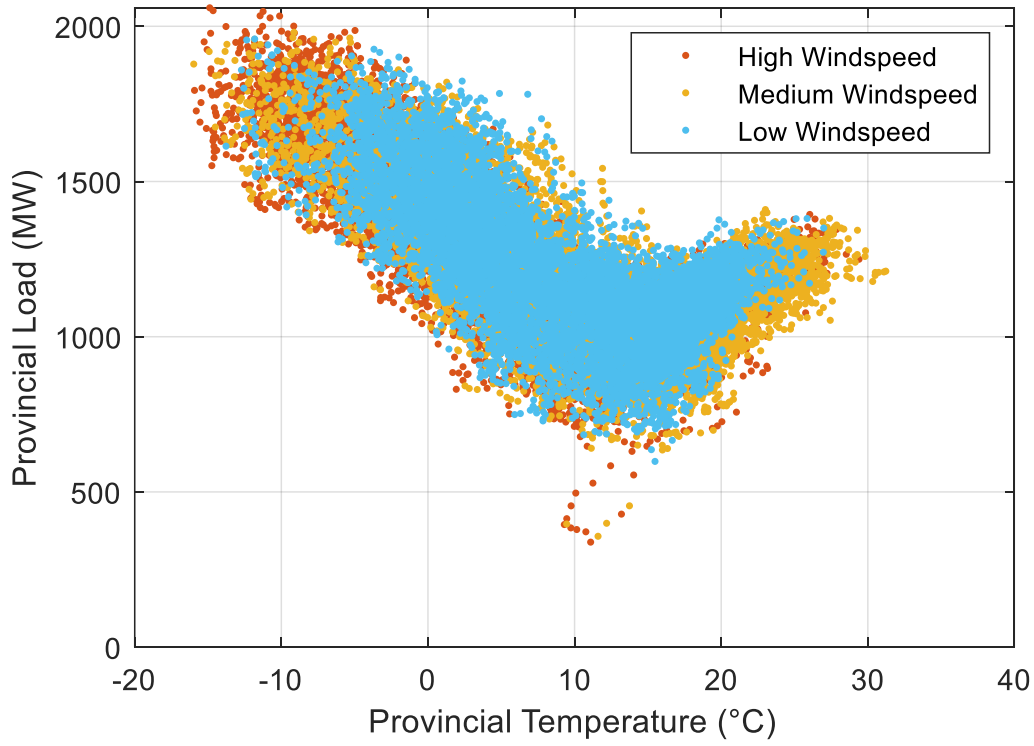

Figure 28 Load distribution with temperature in NS

Figure 28 indicates there is a negative correlation with temperature until approximately 10°C or 15°C. After this point the correlation reverses to a slight increase in load as temperature increases. This indicates the load rises as space heating is needed, with a small amount of cooling from AC at the warmer times. The datapoints below the 600

MW line are all from the mass power outage that occurred across NS after a hurricane in 2019, predictably there are no low windspeed times that occurred during this period.

The low windspeeds appear to be remain closer to the median temperatures, rather than approaching either extreme. This is relevant at the colder side as it shows a strong potential for greater wind production at the colder temperatures. This is shown more clearly in Figure 29 which provides a histogram detailing the windspeeds at various temperatures:

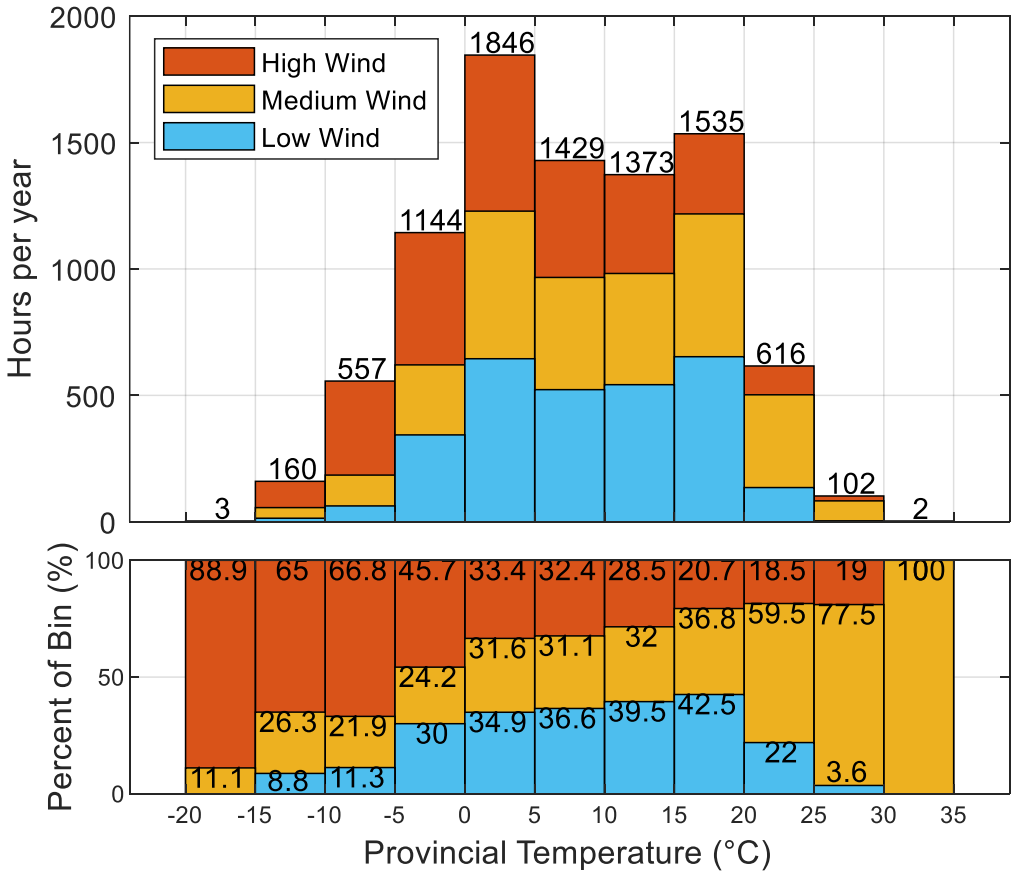

Figure 29 Distribution of windspeeds across temperature in NS

The top part of Figure 29 shows the amount of time per year that NS experiences each windspeed and each given temperature range in the analysis. The bottom figure shows the makeup of each bin in terms of percentage. Since it is a stacked bar graph, the top figure

also shows the number of occurrences of each set of temperatures. While more cases of high wind speed occur during above zero temperatures, that is a result of there simply being more occurrences of that temperature during the timeframe.

The bottom chart in Figure 29 shows a clear bias of high wind speed at the lower temperatures. The three hours per year at the coldest temperature do not experience any of the lowest wind speed, and only 8.8% of the 160 hours at the next temperature range experiences the lowest windspeed. At that temperature range 65% the wind is at the high windspeed. As the temperature gets warmer the percentage of high windspeed decreases, which indicates wind energy production is more likely to produce higher at these colder temperatures.

The next figure shows the capacity value across various temperatures, in this case the data is first filtered by load, to only include the 90th percentile loads, then it is sorted into equally sized bins based on temperature before performing the cumulative frequency analysis.

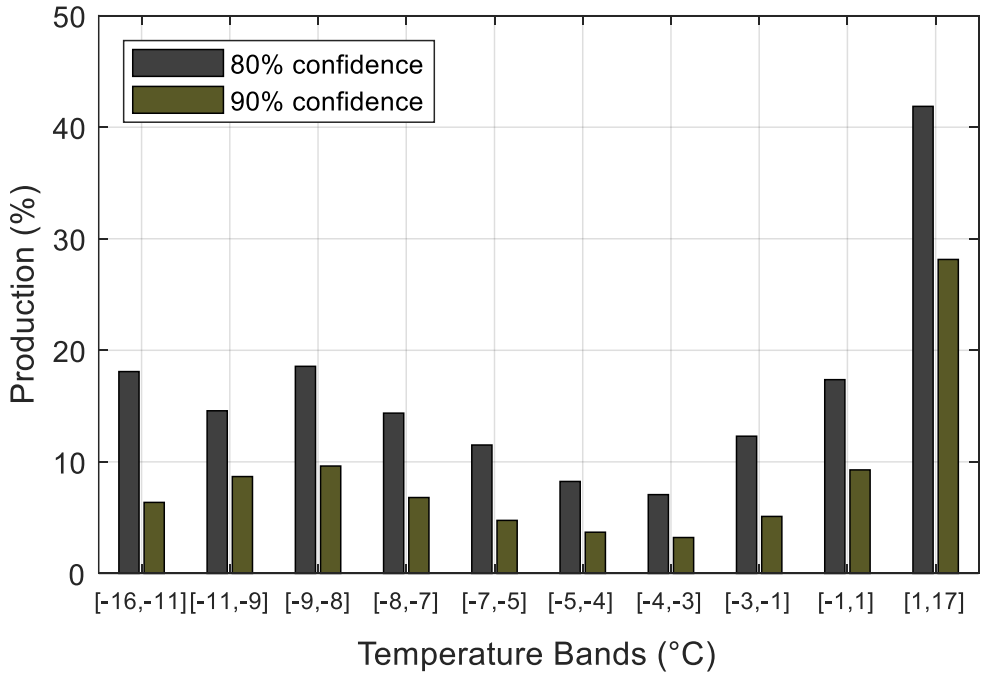

Figure 30 Capacity value of wind depending on temperature

It is important to note the inconsistent temperature difference in the bins used in Figure 30, this is a result of the bins being sized so that there was an equal number of datapoints in each bin. Each bin is equally sized in terms of datapoints so that no bin has too few datapoints to perform the analysis.

The 80% confidence analysis shows a high capacity value at the lowest temperatures, with a decrease as the temperature increase, before a sudden jump in capacity value as the temperature goes above 0°C. This higher capacity value at the very coldest temperatures is consistent with the windspeed findings in Figure 29. The trend is not the same for the 90% confidence level, at this level the capacity value increases as temperature increases to the -9°C to -8°C band, then decreases again, before jumping back up at the above 0°C band. There are much fewer datapoints in each of these temperature bands than in previous analysis, as the resolution is lower for temperature, and then the data is split up. This difference in result is likely due to the low data count at these points, causing the results to be less significant than other analyses. So, no conclusion can be made from the change in capacity value across the two coldest temperature ranges.

The large increase in capacity value at the warmest temperature range is much more significant than the differences between the other temperature bins and is consistent between the two confidence levels. This is significant enough to warrant analysis. One explanation is icing of the turbine blades causing them to be less reliable below 0°C, as this could not happen above 0°C. Icing of the blades could result in a substantial difference in reliability if this were happening frequently. If mass icing were happening that would warrant introducing more anti-icing technology to thaw turbine blades.

Another explanation that the load below 0°C is always high, independent of the windspeed, so the wind farms need to always produce and any drop in production will show up in the capacity value analysis. But at the warmer temperatures the only time load is high, is when the windspeed is high resulting in a greater loss in heat and more space heating requirements. These high windspeeds would result in more generation from turbines, which would make them appear more reliable at these temperatures, while in reality they are only being measured when the wind is high.

5.2.4. Comparison of Wind to Solar

Solar is expected to have a much lower capacity value than wind. Since the load is typically higher in the winter and the evenings, both of which are times of poor power output from solar. Even if there are high load times occurring during the day, capacity value focuses on the worst 20% or 10% of production at the high load times, which means the occasional high production time from solar will be an outlier. The initial results for solar capacity value are shown in Figure 31:

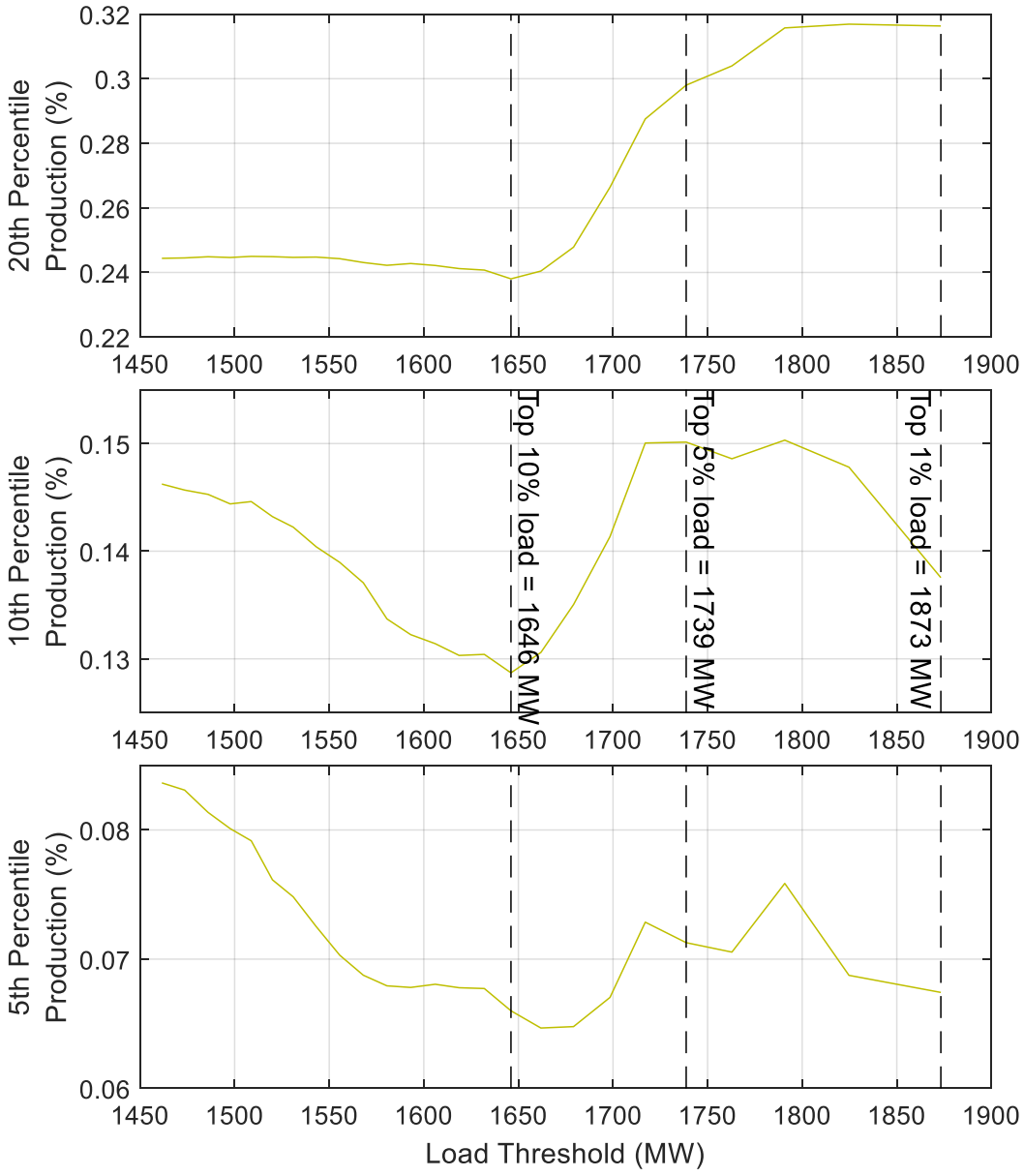

Figure 31 Capacity value of solar with 80%, 90% and 95% confidence

As expected, Figure 31 shows a near zero capacity value for solar in NS. Even at the 80% confidence level the solar capacity value is far less than 1% across the high loads. Using the same method wind generation resulted in a capacity value of 18-25% shown previously in Figure 23. The appearance of an increase in capacity value as load increases in the top graph is negligible as the magnitude of the change is only 0.07% of installed capacity. Additionally, this trend does not continue for the 90% or 95% confidence levels so no conclusion can be made from it. Looking strictly at the capacity value, solar provides an insignificant amount of reliable production at high load times, and is much worse, in terms of capacity value, than wind in NS.

The low capacity value of solar in NS is not surprising based on what was already known about the high load times in NS. The goal is not to just look at the pure capacity value. To look further into the data, an annual comparison between wind and solar can be made. Like Figure 25, in this case the data for wind and solar is displayed in an order sorted by load. Since there is too much production data, the results are the median of the nearby datapoints, so for each dot there are 500 datapoints above, and 500 datapoints below the production.

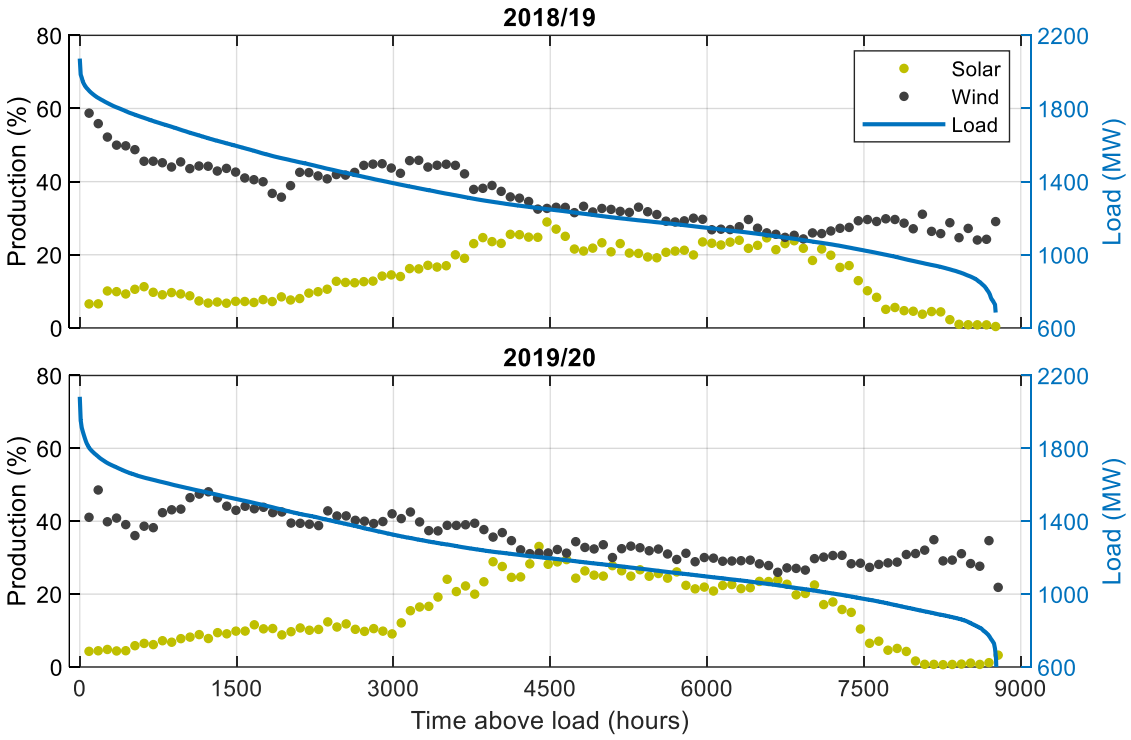

Figure 32 Median solar, wind and load data sorted by load

As expected, Figure 32 shows a substantially lower solar production than wind during high load times. While Figure 31 graphed reliable production, in this case median production is plotted, if only the previous figures were reviewed, solar effectively contributes no power during high load times. Figure 32 shows there is some production occurring at these high load times, however it is unreliable. Most of the solar generation occurs at lower loads during the summer. This is emphasised by Figure 22, which showed a that solar is contributing the energy demand of the province over time, it just does not help meet the power demand at high load times.

NS has a high penetration of wind in the province already, so while wind may contribute more reliably to the electrical load of the province, there is a question of whether subsequent additions of wind will help much, or if the wind production that exists currently has already shifted the residual load away from any times that have a high wind resource in NS. To determine this, the net load is used instead of the total load. By subtracting the existing IG from the load, this estimates the benefit new additions would contribute:

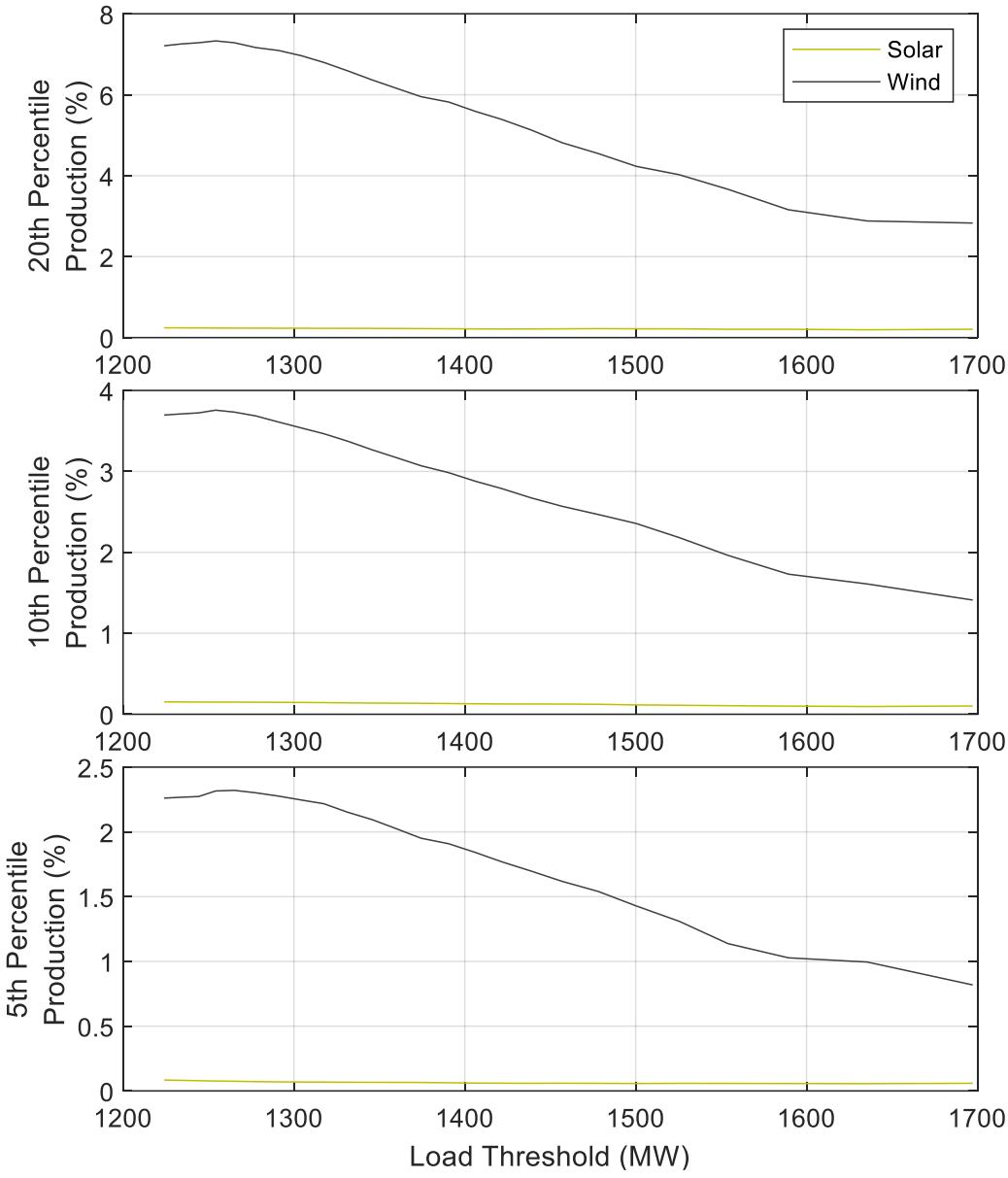

Figure 33 Capacity value comparison between wind and solar using net load with 80%, 90% and 95% confidence

While the wind capacity value has decreased using when using the net load as compared to the results in Figure 23, the solar is still significantly lower than wind, at effectively 0% capacity value. This indicates that even when considering the high wind penetration currently in NS, it does not reduce the capacity value of wind enough to make solar preferable.

One notable aspect of Figure 33 is comparing the wind results to those seen in Figure 23 using the gross load. In Figure 33, the wind capacity value decreases as net load decreases. This behaviour is predictable as the times of high wind the net load would be reduced enough to no longer be the high load times. Consequently, by the definition of 'net load' there can only be high net load times when wind is low enough to not impact the load significantly. Solar does not have this problem because of the low solar penetration; however, it still has a low capacity value because these high load times still occur during the winter, when solar has less performance. As before, the data can be sorted and displayed to see how the median production changes depending on load:

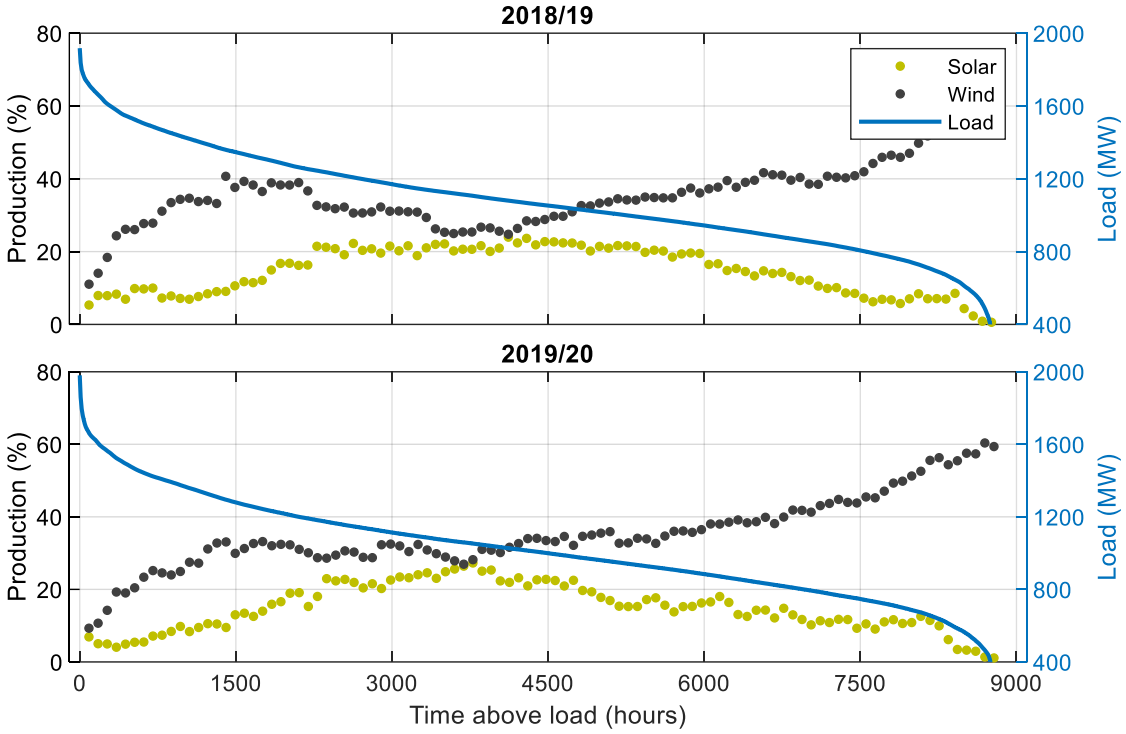

Figure 34 Solar, wind and net load data sorted by net load

Solar has slight improvement between Figure 32 and Figure 34, the performance of solar is slightly flatter with the middle peak lower and the high load side slightly greater than in the total load example. Wind has a drastic reduction in generation at high net loads. As with the capacity value charts, the trend seen in Figure 32 is reversed, now wind increases as net load decreases. This is most likely because the times of high wind production reduce the net load, so the higher the net load the lower the wind definitionally. With 616

MW of installed wind, a high wind time could result in a peak load dropping from 2000 MW to 1400 MW pushing its position below the high load times.

Solar performing worse than wind at high load times is unsurprising. The next capacity value analysis will be done to focus on the times when solar should be high, to see if it at least performs well when its expected to output. This is done by categorizing the data by time before performing a capacity value analysis on each hourly bin of data:

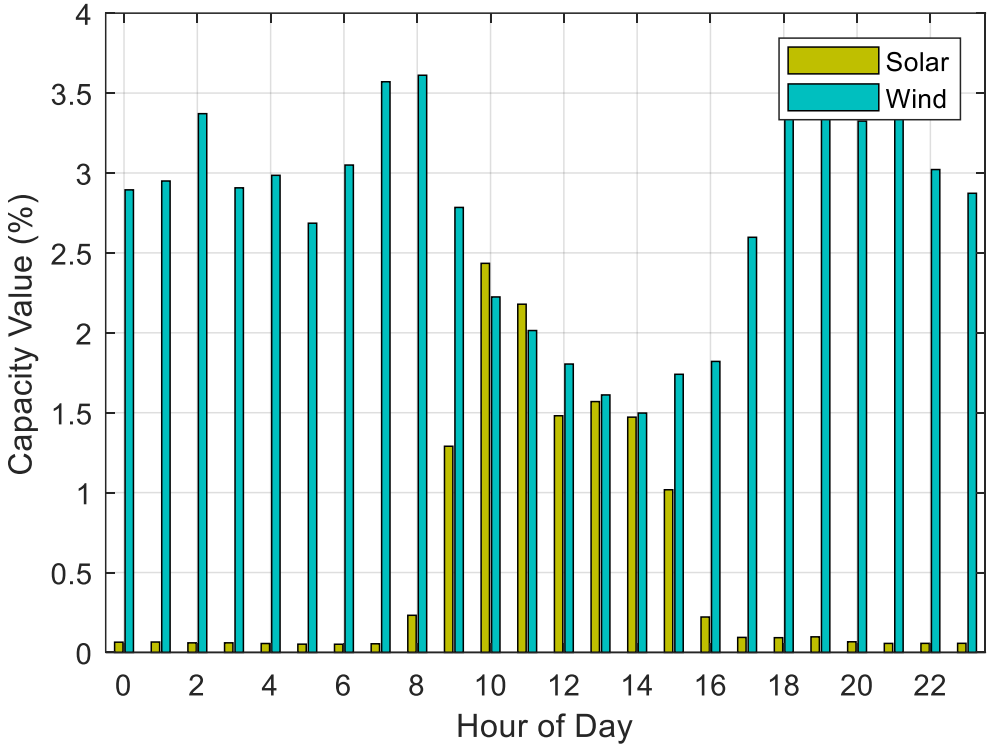

Figure 35 Hourly capacity value comparison of wind and solar using peak net load with 90% confidence

As expected, solar provides no value during nighttime hours when there is no sun, so wind outperforms during these hours. The solar production outperforms wind during the hours of 10:00 and 11:00, it is also very close to wind during the hours of 13:00 and 14:00. Interestingly solar does not have peak performance during the 12:00 hour, when the sun is typically at its peak. This may not be a result of the timing of the loads, rather than the output of solar. There may be a greater proportion of high load between 10:00-12:00 occurring during the summer, than for the time between 12:00-13:00.

While solar may perform better during a few hours of the day, overall wind helps reduce the load more effectively per MW installed. Solar having a greater capacity value between 10:00-12:00 may mean that if a load shift occurred, pushing peak loads from morning and evening towards noon, solar may be needed. This may not happen as the time of use rates reward shifting the load further to the night, which this may result in an even worse value for solar.

One aspect that may cause solar to become more valuable is the adoption of AC across the province, as space cooling loads increase the peak loads may begin to occur during the summer. Figure 36 shows the capacity value of wind and solar based on the month:

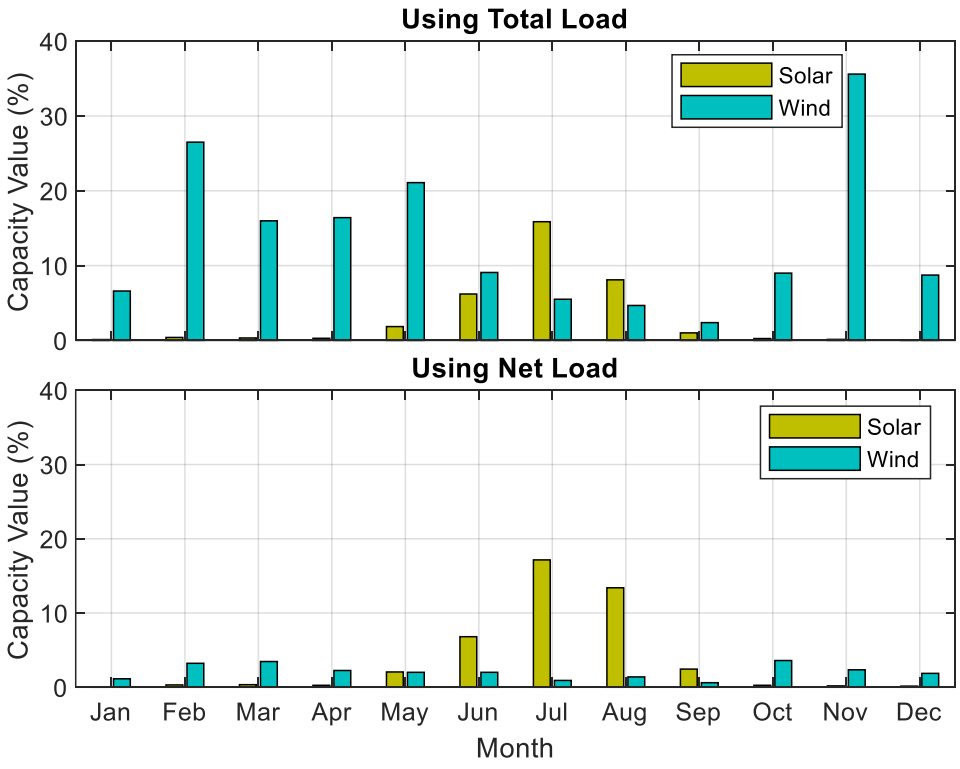

Figure 36 Monthly capacity value comparison of wind and solar for peak net load and total load with 90% confidence

In Figure 36 both total load (top) and net load (bottom) are presented for comparison, the colours of each are shown in the legend. Solar has a clear advantage over wind for the summer months when using both net load and total load. The capacity value using net load is always higher for solar than when using total load, with the opposite being true for

wind. The month of May has approximately equal capacity value when using net load, although is much lower when using total load. While June is much higher when using net load and slightly lower when using total load. July and August are much higher for both the net load and total load analysis. September, like June, has a significantly higher capacity value when using net load, but lower when using total load. At the current state of energy usage, NS experiences peak loads during the winter, due to the demand of space heating. But if more people begin using heat pumps or AC units to cool their homes, then a summer peak may occur, at which point Figure 36 shows solar has a clear advantage. Alternatively, as the penetration of wind increases, the additional installations of wind may become less and less valuable, until eventually solar begins to provide more value as the net load has shifted away from when wind is producing.

5.3. Summary

The capacity value of wind generation varies from year to year, indicating that a single year of data is not adequate for determining the capacity value. The data resolution on the other hand had little impact on the capacity value while the timestep remained less than 60 minutes, which means the hourly timestep can be used to analyse the capacity value. The capacity value raised significantly when the temperature was above 0°C compared to the capacity value at lower temperatures, this could indicate icing of turbine blades at below freezing temperatures.

In NS solar generation has a much lower capacity value than wind generation, even when considering the high penetration of wind generation that is already installed in the region. Even when isolating for the hour of day, even at its peak solar generation barely outperforms wind. The only case in which solar has a greater capacity value than wind is when the data focuses on the summer months, which indicates that if the load were to shift to a summer peak, then solar generation would have a greater capacity value than wind.

The preceding analysis was of the resource and converters alone, by adding energy storage the value of solar or wind generation would be improved by providing a reliable backup of energy when they fail. The following chapters study combining wind, solar and storage to reduce the need for DG, to show the effect increasing storage has.

Chapter 6. Modelling of Wind and Solar Generation with Energy Storage

The previous chapter assessed the capacity value of two forms of IG. It assessed their individual reliable contribution to the load during high load periods. Using a single energy source simply because it is perceived to be the best based on its capacity value, may not be the best way to reliably supply the load. Having two independent resources producing IG improves the likelihood of one producing when the other is not and providing power during a peak load event. Especially if the load profile is altered because of the existing IG, resulting in a net load peaking at different times than the load.

To improve this further, storage can be used to capture excess electricity at times of low net load. The excess electricity can be stored until the net load is high, during a combination of high load and low IG, then used to reduce the net load. Reducing the peak demand on the utility and requiring less installed capacity of DG. This can improve the energy production of IG if it reduces the curtailment, by storing excess generation rather than wasting it. It can also provide more energy security, by having a reliable source of electricity saved as a backup.

This chapter develops a model used for determining the storage requirements set for a given DG peak, wind capacity, and solar capacity. The model is tested using data from NS, however, can be adapted for any load, and generation inputs.

6.1. Method

The model is designed to take timestep data for normalized solar and wind generation, and electrical load; along with user-selected maximum DG and solar and wind capacities. The model outputs the required energy storage power and capacity to limit the DG to the selected amount. Normalized wind and solar generation data is used so the model can have adjustable capacity for each. This way the model can be used to simulate the system using various proposed installed capacity amounts, to predict what would be needed if more IG were installed.

Since the storage amount is undetermined in the beginning the model operates in a deficit. This means that the storage is initially fully charged and has unlimited capacity. As the

model executes, the depth of the capacity utilized is noted, and gives the necessary energy storage capacity to achieve this performance level.

To do this, the energy storage capacity is set to 0 MWh. As energy is needed the battery discharges, which makes its state of energy (SOE) a negative value. As it charges it is limited to the maximum of 0 MWh. When the analysis is done the absolute value of the lowest SOE is equal to the necessary storage capacity of the energy system. The flowchart used to describe the model is shown in Figure 37:

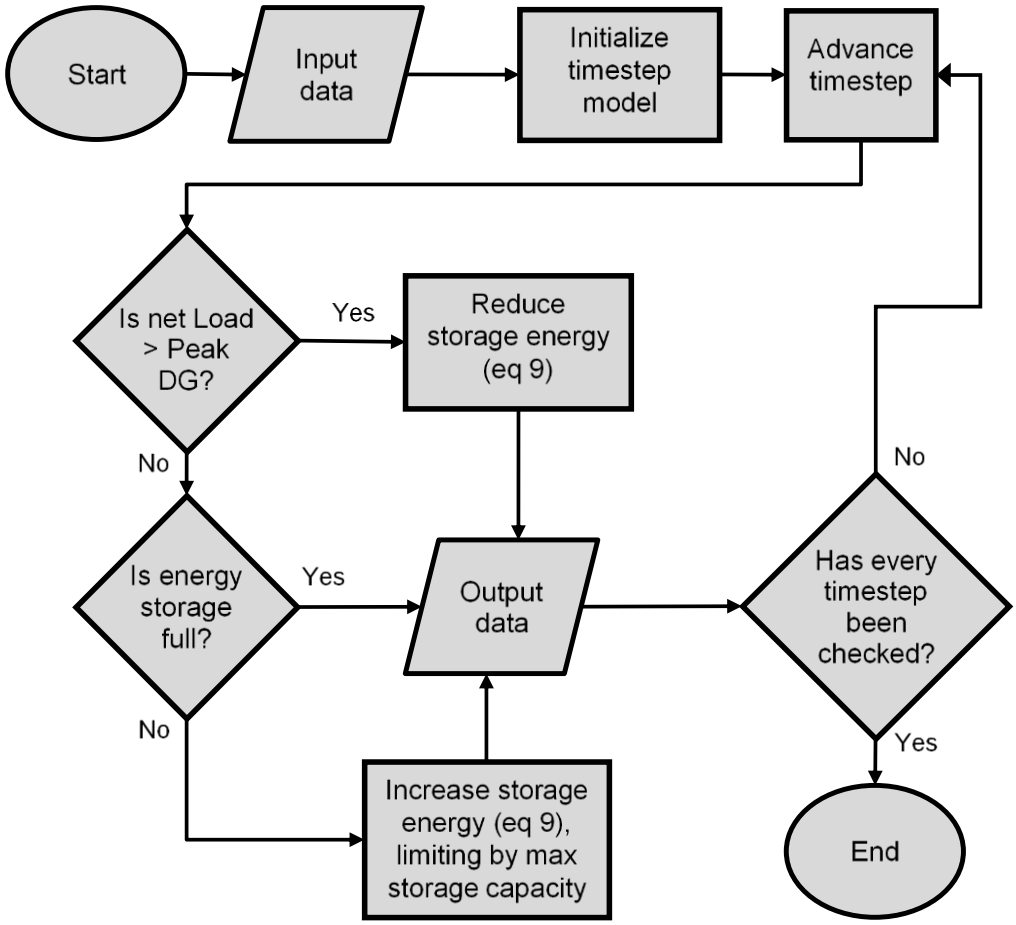

Figure 37 Wind, solar and storage model flowchart

The input data and parameters needed by this model are:

- Provincial load data
- Normalized solar and wind generation data

- Maximum DG allowed or DG capacity reduction
- Desired solar and wind generation capacities

The power output from the two forms of IG is determined by multiplying the normalized generation at any given time by the desired capacity. This is done using a rearranged version of equation 2:

$$P_{\text{gen},t} = P_{\text{norm,gen},t} \times P_{\text{rated}} \tag{8}$$

Where $P_{gen,t}$ is the resulting generation from either form of IG at any time t. $P_{\text{norm,gen},t}$, is the normalized generation or generation as a percentage of rated capacity for that type of IG any time t. P_{rated} is the user-selected rated capacity of that type of generator in the province. This equation works for both wind and solar if used separately with each of their timestep capacity factors. This model assumes the capacity does not change for either type of IG, this is a conservative approximation as there is likely to be increasing amounts of both as time goes on.

The timestep production data is then combined to determine the total IG production, which is then subtracted from the load to determine the net load. This is calculated using equation 7, described in section 5.1.4.

The state of energy is calculated using equation 9, there are three options depending on whether or not the storage is discharging, charging or if it hits the maximum charge (0 MWh), as shown:

$$SOE_t = \begin{cases} SOE_{t-1} - \Delta t \dfrac{P_{\text{Load,net},t} - P_{\text{DG,max}}}{n_{\text{discharge}}}, \text{discharge} \\ SOE_{t-1} + n_{\text{charge}} \Delta t \left(P_{\text{DG,max}} - P_{\text{Load,net},t}\right), \text{charge} \\ SOE_{\text{max}}, \text{overcharge} \end{cases} \tag{9}$$

In these equation SOC_t and SOC_{t-1} are the current and previous state of energy in MWh respectively. Δt is the time difference between the current time, t, and the previous step's time, $t-1$. $P_{\text{Load,net},t}$ is the electrical load of the province in MW after accounting for

IG, while $P_{\mathrm{DG,max}}$ is the peak dispatchable generation allowed, set by the user. The difference between $P_{\mathrm{Load,net},t}$ and $P_{\mathrm{DG,max}}$ represents the load exceeding the DG limit needed to be met by the storage, or the excess generation that could be used to charge the battery. $n_{\mathrm{discharge}}$ and n_{charge} are the energy efficiency of the storage for discharge and charge respectively, both set to 93% to simulate lithium-ion batteries, resulting in an 86% round trip energy efficiency. With this round-trip energy efficiency, for every 1 MWh put into storage, only 0.86 MWh can be retrieved, however it requires 0.93 MWh of capacity to store.

The charge is limited to not exceed the maximum capacity, which in the case of a depletion model is zero, as it should always be operating at a deficit. Once the energy storage is at maximum capacity, it may be required to curtail excess generation, however the storage will reduce this need as it will first store the excess before curtailing it.

6.2. Demonstration

To test the effectiveness of the depletion model, it was run using the following input parameters:

Table 8 Depletion model validation run parameters

Parameter	Value
Wind Capacity	616 MW
Solar Capacity	300 MW
DG reduction	300 MW
Charge energy efficiency	0.93
Discharge energy efficiency	0.93

The wind capacity was set to 616 MW to simulate the capacity of already installed wind, with solar capacity being set to 300 MW to simulate a new installation of utility-scale solar in NS. A 300 MW DG reduction represents a retirement of multiple fossil fuel burning units. The charge and discharge energy efficiency were both kept at 0.93 to represent the installation of lithium-ion batteries across the province at large scale. The output data results in the following time series:

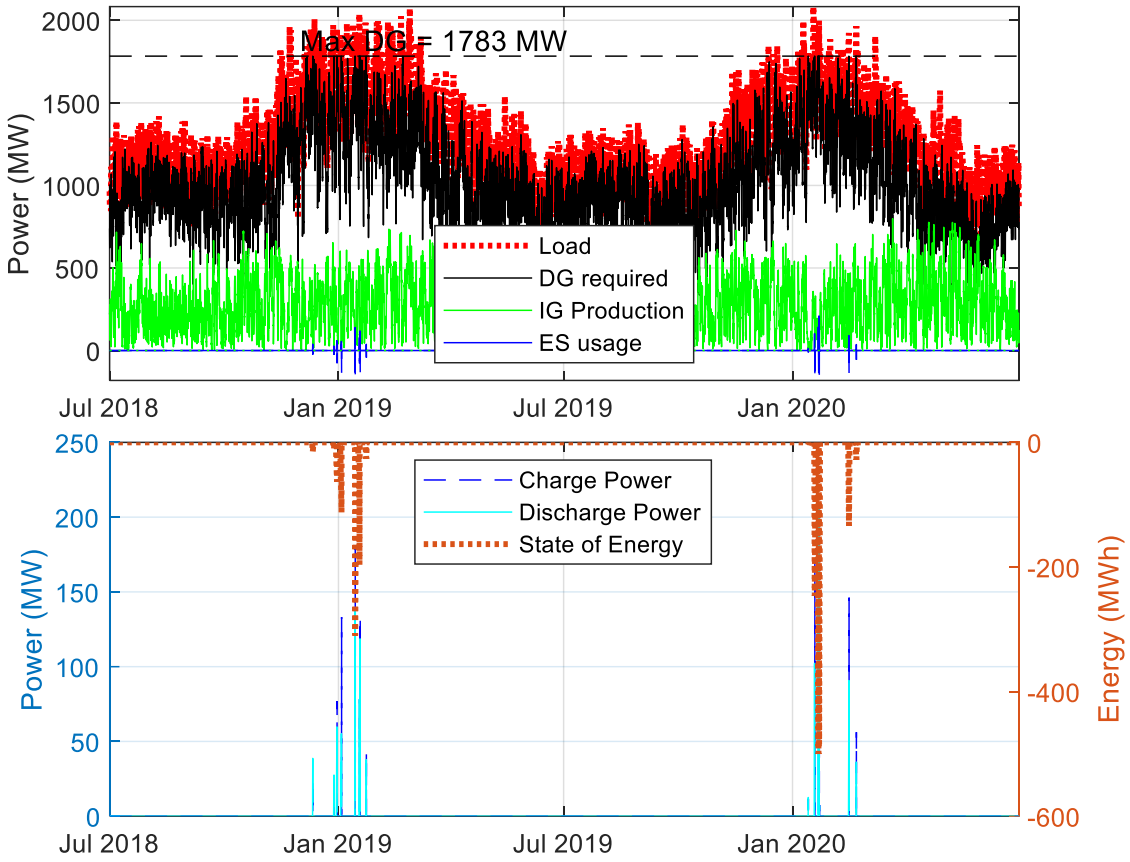

Figure 38 Power flow and energy storage time series for demonstration

The top graph in Figure 38 shows power flow time series, which displays the system power sources and draws. The red line shows the total electrical load of the province; the green line shows the combined IG production; the black line is the DG response that picks up the remaining demand within the limit set; the blue line shows the energy storage usage, this discharges when the load cannot be met by IG or DG, and charges when there is sufficient production to do so. This graph is from the perspective of the system, so when the energy storage power is negative it is pulling from the system (charging), when it is positive it is outputting to the system (discharging)

As expected, during the summer months the load falls well below the DG limit, which means the focus of the analysis should be on the winter. This also means that the storage is not used at all in the summer months, so it could be programmed to perform some other service during these months when they are not needed to reduce the peak loads. Due to the minimum power turn down on thermal generators, the availability of storage may be

used to turn off thermal generators during the summer, rather than forcing them to operate at minimum power as a backup.

The bottom graph in Figure 38 shows the input and output power and state of energy for the storage device. There are two y-axes, the left axis indicates power, the dark blue line and light blue line are read from this axis; the right axis indicates energy, which uses the orange dotted line. The dark blue dashed line shows the charge power, or the instantaneous power being taken by the battery from the system; the light blue line shows the discharge power output of the battery, or the instantaneous power output from the battery contributed to the load. The orange dotted line indicates the state of energy of the energy storage device, it is always at or below zero, as the zero point maximum is a placeholder for the maximum energy. The delta from maximum to minimum SOE is read to determine the necessary capacity to perform its role.

As with the power flow time series, the activity for the battery is focused on the winter months, when the load is highest. The following Figure 39 isolates the event the battery requires the most energy:

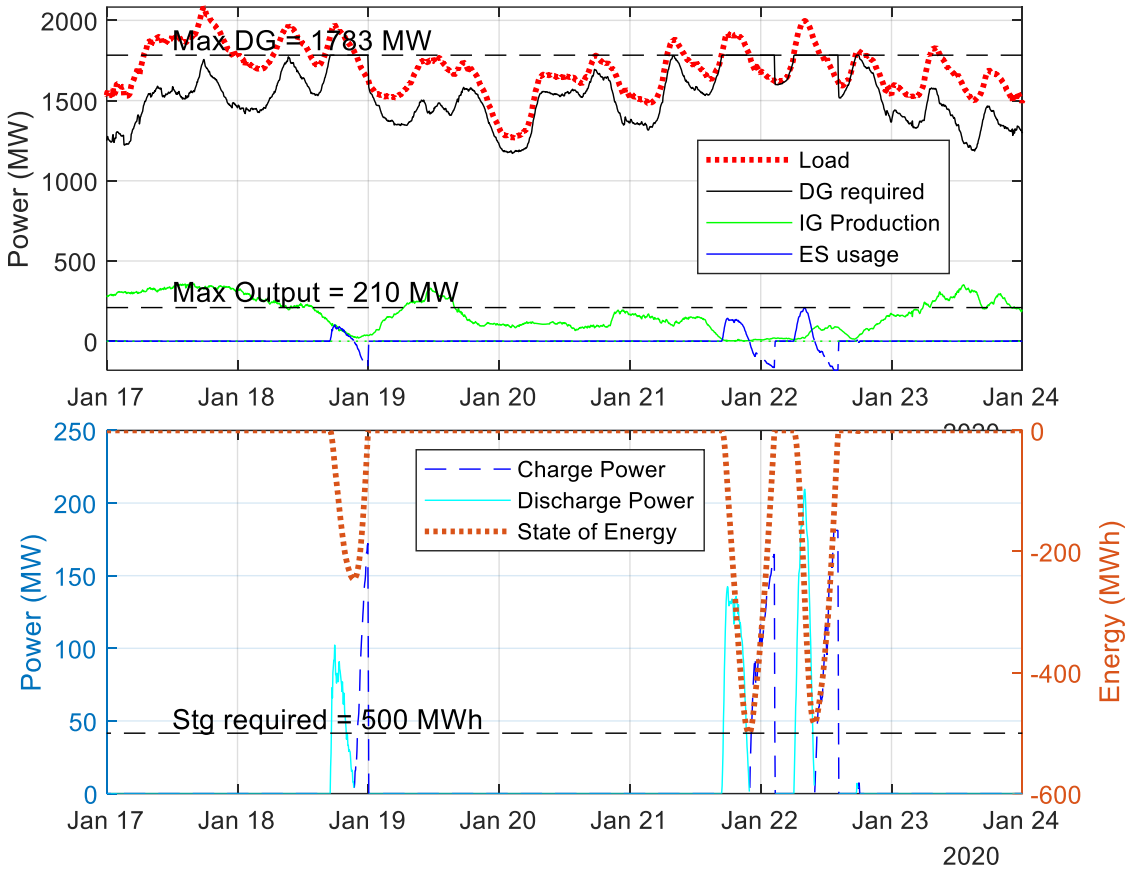

Figure 39 Power flow and energy storage time series demonstration focused on period of peak storage usage

When focused on a weeklong period, the data is easier to interpret. Figure 39 is organized the same way as Figure 38, with the top graph showing the power flow for the system and the bottom graph focusing on the energy storage system. From the top graph the peak power needed from the storage is 209 MW. As expected, this occurs during a period of high load and low IG. Despite a total reduction of 300 MW in DG output, the energy storage only needs to supply 209 MW of power because the remainder is reduced by the IG. The fact there is no IG at the point of peak power indicates that originally the peak load occurred at a different time, but the IG was enough to shift the peak to this point.

The instantaneous difference between load and DG output is more observable when focusing on a single week. For the most part the difference between load and DG is a result of the IG reducing the load before DG is needed; in some cases, the energy storage

reduces the DG to below the maximum DG line, then once the load drops the DG is then increased to charge the energy storage system.

From the bottom graph in Figure 39 the minimum energy state reached by the battery is -500 MWh, meaning that the system needs 500 MWh storage capacity to prevent failure to provide electricity when needed. With a power requirement of 209 MW and capacity of 500 MWh the energy/power ratio is 2.39 hours.

Even though this is the week of highest usage, there are only three events requiring electricity from the energy storage during this period. Using the sum of the energy flowing into the energy storage, the whole two years covered in the analysis the energy storage had 2311 MWh flow through it, equal to 4.6 full charge-discharges or an average of 2.3 discharges per year. Clearly at this level of DG and IG, storage is only needed occasionally to fulfill the electrical load. During times when the load is not high enough to warrant energy storage use for peak shaving it can be used for other services.

6.3. Summary

In this chapter the model used for simulating an energy storage system working with IG to reduce the need for DG. The model works by inputting the wind and solar generation, load, and peak DG allowable. The model uses a depletion technique which does not set the capacity before the simulation. Instead, the model allows the storage to operate at a deficit and determines the required capacity at the end of the simulation by finding the minimum SOE. The energy storage is only used when the difference between load and IG is greater than the DG capacity limit, which means there is a potential for other services to be performed at times when the load is low.

The model was demonstrated using a wind capacity of 616 MW, solar capacity of 300 MW, and a DG reduction of 300 MW. The resulting storage capacity was 500 MWh, with a power of 210 MW. This test shows that the model can be used to determine the energy storage requirements to meet a given dispatchable amount or reduction. In this case the solar and wind were input; when this is run iteratively it can determine how the storage varies as the combinations of wind and solar capacity change. This is explored in the following chapter.

Chapter 7. Dispatchable Generation Reduction

The previous chapter used known values of wind and solar production, a known provincial load, and a peak DG to determine a required storage energy capacity. In this chapter, a parameter index controller is designed that runs the model iteratively to determine the optimal combination of wind, solar and storage for given DG reductions. In this case 'optimal' means the lowest cost combination of wind, solar and storage for a set amount of DG reduction.

7.1. Method

The purpose of this strategy is to simulate wind, solar and storage in NS, using the model described in Chapter 6 to iteratively simulate the system on a wide range of solar and wind capacities, for multiple levels of DG reduction. This parameter index controller is shown in Figure 40:

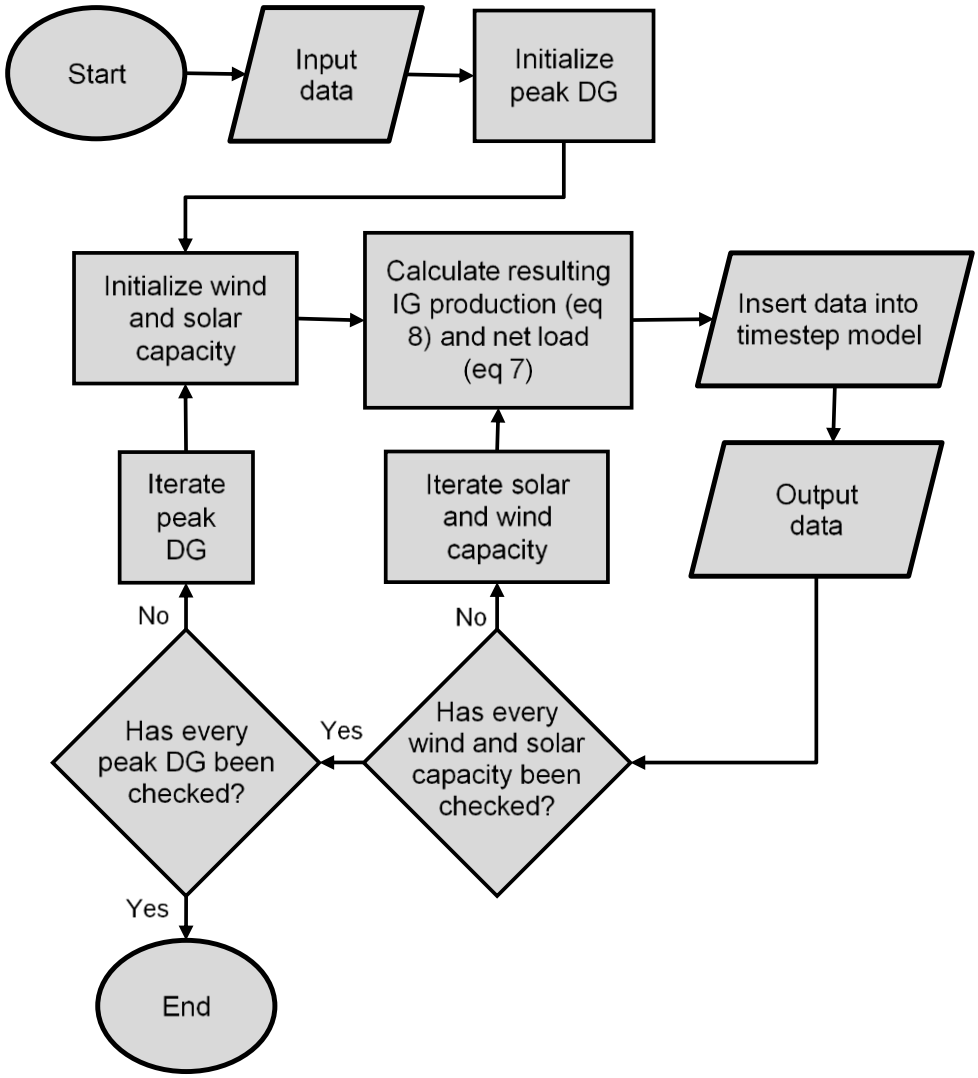

Figure 40 DG reduction parameter index controller flowchart

The model begins by loading certain input data and parameters:

- Provincial load data
- Normalized wind and solar generation data
- Set ranges and increments for wind and solar capacity
- Set range of DG reduction levels

The parameter index controller has three adjustments: the capacity of solar, the capacity of wind, and the DG reduction level. The initial range of parameter inputs was set to 0 to

1000 MW for each solar and wind, with 5 MW increments, with the range increasing for high levels of DG reduction. Within each iteration a combination of wind, solar and DG reduction is selected by the index controller, then it is run through the storage model described in Figure 37.

This method outputs a series of arrays describing the following for each combination of wind and solar:

- Storage energy capacity requirements
- Storage power requirements
- Total amount of charge and discharge used in the storage
- Resulting curtailment from excess IG

At the range and precision selected there are 40401 parameter combinations, so results output as 201x201 arrays. These arrays can be used to calculate the energy/power ratio by dividing the energy by the power to get units of hours. The number of discharge equivalents is similarly calculated by dividing the total energy discharged from the storage by the capacity of the storage.

The cost, obtained by using matrix addition and scalar multiplication, is shown below.

$$[C]_{\text{total}} = C_B[B]_{\text{w,pv}} + C_{\text{w}}[W]_{\text{w}} + C_{\text{pv}}[PV]_{\text{pv}} \quad 10$$

Each array has identical dimensions depending on the range and precision of wind and solar. The total cost array is calculated using the cost per unit of each technology, C_{B} for battery (\$/kWh), C_{W} for wind (\$/kW) and C_{PV} for solar (\$/kW$_{\text{AC}}$), multiplied by the capacity array of each respective technology. This model simulates large scale installations of each technology, so the costs used are based on utility-scale installations. Due to the large scale of the expected installations (>10 MW) a cost factor scaled solely on the size alone (per MW for generation, per MWh for storage) is used, this is summarized for each technology in Table 9. The cost for the energy storage is based on

the cost of large-scale lithium-ion battery system to match the same technology chosen for the energy efficiencies.

Table 9 Capital cost of each technology

Technology	Symbol used	Capital cost from literature (USD)[6,7]	Converted capital cost (millions CAD)
Utility Scale Solar	C_{PV}	$900/kW	$1.197/MW
Land Based Wind	C_W	$1250/kW	$1.663 /MW
Energy Storage	C_B	$393/kWh	$0.523/MWh

The costs shown in Table 9 are used to calculate the cost of every combination of wind, solar and storage from each DG capacity reduction result. The lowest cost combination for each can be determined and plotted, to identify what trends persist as the DG capacity is reduced.

7.2. Results

As the simulation runs it outputs the series of arrays described in section 7.1. Each dependent datapoint is based on three independent variables, wind capacity, solar capacity, and DG reduction; as such they are displayed as a contour plot in Figure 41. The graphs displayed in Figure 41 (as a demonstration) are the 300 MW DG reduction plots, which can be compared to the demonstration in section 6.2:

[6] Lazard, "Levelized Cost of Energy and Levelized Cost of Storage," 2020. https://www.lazard.com/perspective/levelized-cost-of-energy-and-levelized-cost-of-storage-2020/
[7] W. Cole, A. W. Frazier, W. Cole, and A. W. Frazier, "Cost Projections for Utility-Scale Battery Storage : 2020 Update Cost Projections for Utility-Scale Battery Storage : 2020 Update," 2020. https://www.nrel.gov/docs/fy20osti/75385.pdf

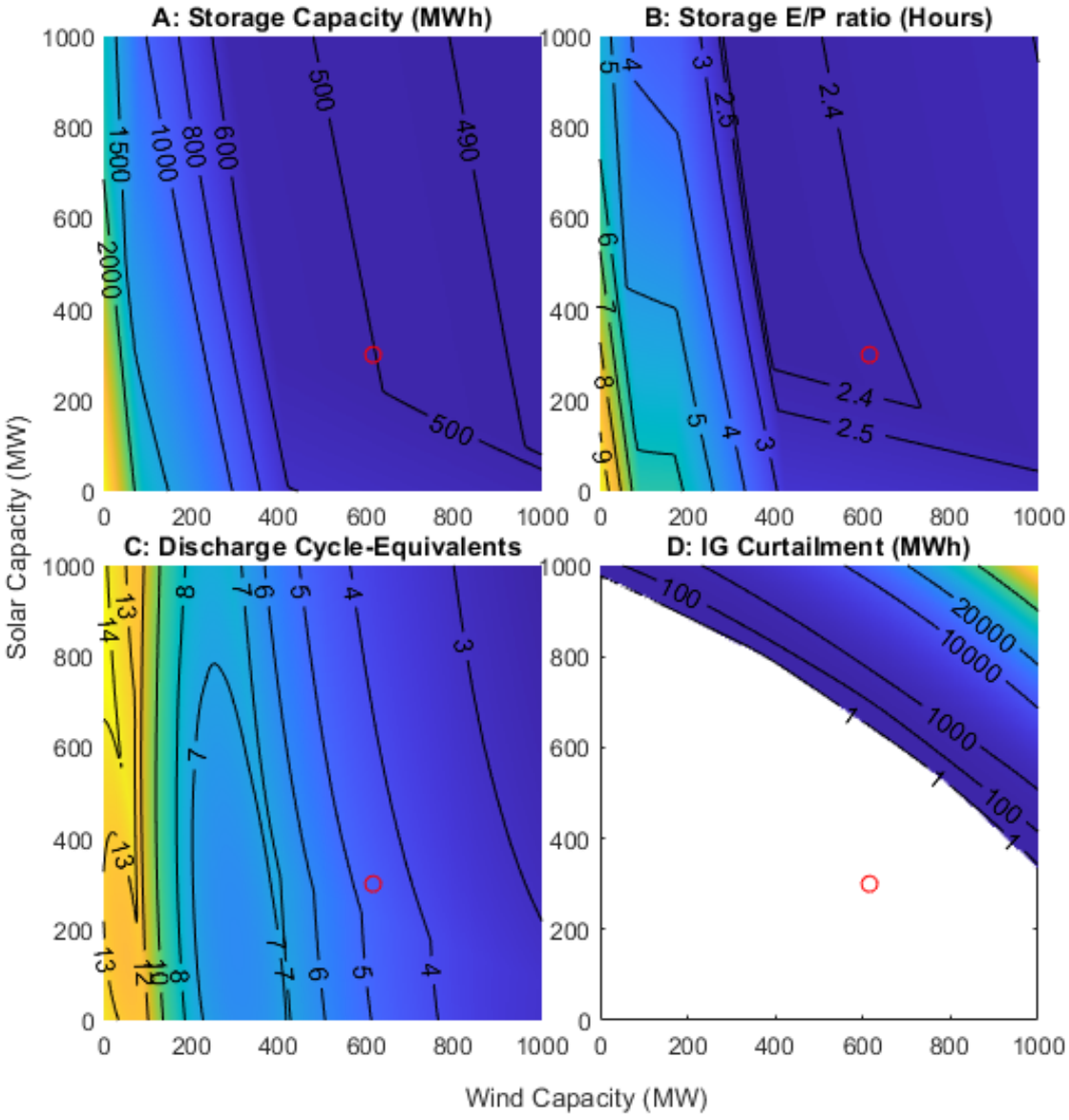

Figure 41 300 MW DG reduction results

The four graphs shown in Figure 41 show some of the technical results generated based on the simulation run; the economic results are shown further in Figure 42.

Figure 41A shows the storage capacity requirements in for each capacity of wind and solar at 300 MW DG reduction. The contour lines and colours on Figure 41 show the increase in storage requirements as IG decreases. When the lines are vertical that indicates the storage requirement is more sensitive to the wind capacity, when the lines are horizontal the storage requirement is more sensitive to solar. As expected for most combinations, the wind has a greater effect on the storage energy requirements than solar.

This makes sense, as found previously in Chapter 5, the solar capacity value is much lower, so it does not contribute much power when the load is high. After approximately 600 MW of wind penetration, solar appears to be desirable, as in these cases the high wind production is shifting the load to times when solar produces well.

The red circle indicates the point of 615 MW of wind, and 300 MW of solar, to correspond to the point at which the demonstration in section 6.2 was performed. The contour line for 500 MWh storage capacity passes through the demonstration point, indicating that it requires 500 MWh of storage capacity to achieve the 300 MW of DG reduction. This confirms the results from section 6.2. Some other interesting points are shown in the Table 10:

Table 10 Storage requirements for 300 MW DG reduction at various combinations of wind and solar

Scenario	Wind Capacity (MW)	Solar Capacity (MW)	Storage Required (MWh)
No IG	0	0	3168
Current IG	615	0	574
Max wind	1000	0	516
Max solar	0	1000	1770
Max IG	1000	1000	483

Despite solar having a much lower capacity value than wind, it is still beneficial in reducing the energy storage requirements. With no IG, NS would need 3168 MWh of storage; with 1000 MW of solar the need for storage is reduced by 44% to 1770 MWh. As expected, wind performs much better, reducing the storage required at its maximum by 84% to 516 MWh. Compared to the current capacity of 615, maximum wind only results in 10% savings in storage despite being a 63% increase wind capacity. This indicates that increasing wind beyond the current install base will have minimal effects on DG reduction.

Figure 41B shows the energy/power ratio. The reference point is close to the 2.4 hour contour line, which confirms the 2.39 hour value determined in the demonstration in section 6.2. Typically batteries are available at 2 and 4 hours, which means this would require more power than a 4 hour battery, but less than a 2 hour one. Notably the storage

time does not follow the same trend as storage capacity, the lowest time is not at the point of maximum wind and solar capacity. Some key values are shown in Table 11:

Table 11 Energy/Power ratio for 300 MW DG reduction at various combinations of wind and solar

Scenario	Wind Capacity (MW)	Solar Capacity (MW)	E/P ratio (hours)
No IG	0	0	9.82
Min E/P	390	320	2.35
Max wind	1000	0	2.57
Max solar	0	1000	5.51
Max IG	1000	1000	2.50

The lowest storage time is 320 MW of solar, and 390 MW of wind, inside the perimeter of the 2.4 hour contour line. Unlike the storage capacity in MWh, which had the lowest point at the maximum values for wind and solar, this is because as the capacities increase the power requirement decrease along with the energy. Storage power and energy requirements do not decrease evenly as generation is added. The highest energy/power ratio is at the 0 MW wind and solar point, which indicates that at this point there is much more energy required than power from the battery.

Figure 41C shows how much the storage is used, this is the total energy discharged by the energy storage divided by the capacity of the storage. The lower numbers indicate that the storage is less frequently used, because the load is met more often. The red circle indicating the demonstration point is between the 4 and 5 contour lines, indicating it is consistent with the 4.6 value found in section 6.2.

The storage usage is not proportional to the storage capacity requirement. It does not have the same shape contours as the storage graph in the top left, however the trend that the greater IG tends to have lower proportional usage than the lower levels of solar and wind remains. This is shown in more detail in Table 12:

Table 12 Discharge equivalents for 300 MW DG reduction at various combinations of wind and solar

Scenario	Wind Capacity (MW)	Solar Capacity (MW)	Discharge equivalents
No IG	0	0	13.58
Max Use	10	720	14.43
Max wind	1000	0	3.17
Max solar	0	1000	14.26
Max IG	1000	1000	2.55

At the maximum level of combined wind and solar the storage use is at its minimum. This is also the point of minimum capacity, which means not only is there less capacity, the total energy discharged has lowered faster than the capacity. The maximum usage is not at the point of no wind or solar, but with a large amount of solar and 10 MW of wind, the energy storage experiences its highest proportion of use, this is unlike the storage capacity graph which is at its maximum at no wind or solar. This is due to the increased solar reducing the energy demand of the highest-use event, but not reducing energy demand during other storage-use time periods.

Unlike solar, wind results in a decrease in storage use, with the maximum wind, being close to the minimum number of discharge equivalents. The trend of more wind resulting in lower number of discharge equivalents is true except for a brief period between 300 MW and 400 MW of installed wind generation, at which point the discharge cycle-equivalents increases before continuing to decline as the installed capacity of wind increases. This indicates that between 300 to 400 MW of wind the required capacity is dropping faster than the energy flow for a short period. This is a trend of high wind generation being misaligned with the very peak loads but helping reduce lesser peak loads. This causes the total discharge energy to be reduced, but the maximum capacity to remain the same.

Figure 41D shows additional energy curtailment. Curtailment occurred when the storage was fully charged, but there was still more IG production than load. There are two important notes regarding this: the storage controller is designed to recharge as soon as possible, rather than waiting for the IG to become excessive, so it is not optimised to prevent curtailment. Another note is that in some cases wind is already being curtailed, so

the data used has been reduced as the wind generation approaches the load, these results represent the extra curtailment required in addition to what already occurs. If the goal was to maximize the use of wind and solar then the storage could be controlled to only charge when the IG exceeded load; however that was not the objective of this model, so the curtailment often occurred whenever the IG exceeded load. Since the storage is often unused during the summer there is a substantial opportunity to reprogram it during these months to reduce curtailment.

For most of the combinations of wind and solar there is no curtailment. There begins to be large amounts of curtailment required when there are high capacities of both IG technologies. This can be seen in the Table 13 which shows the minimum threshold that curtailment is required, and the curtailment amount as wind and solar increase:

Table 13 Additional curtailment Amounts for 300 MW DG reduction at various combinations of wind and solar

Scenario	Wind Capacity (MW)	Solar Capacity (MW)	Extra Curtailment (MWh)
Max Wind	1000	0	0
No wind	0	975	>0
Min Solar	1000	330	>0
Wind = Solar I	630	630	>0
Wind = Solar II	700	700	714
Wind = Solar III	800	800	7060
Wind = Solar IV	900	900	25709
Max wind and solar	1000	1000	65511

As most of the combinations do not result in curtailment, the ">0" in Table 13 indicates the points at which it begins requiring energy curtailment with positive but near 0 MWh curtailment. Without solar, even the maximum amount of wind modelled will not result in curtailment in excess of what already occurs, there needs to be at least 330 MW of installed solar to result in curtailment. It is expected for high solar to result in more curtailment than wind, as it peaks during the summer, when the load is lower. Whereas wind was lower in the summer, and higher in the winter when load was also higher. Solar may require less curtailment if loads increase in the summer due to greater use of AC across the province.

Curtailment increases dramatically, as the IG increased, from 714 MWh at 700 MW of both, to 7060 MWh at 800 MW of both. This is because, initially, only the peak production periods result in excess generation; but as capacity increases, the peaks become greater, and the amount of time that generation is above load increases, so there is more time to be producing the excess generation. Since energy is the integral of power with respect to time, greater amounts of time, will have a multiplying effect on the power, which is also growing. For example, both IGs have 630 MW capacity there is only one five-minute period where the IG exceed load, when both have 700 MW capacity there is a cumulative 18 hours where the generation exceeds load, and when both have 800 MW capacity it is a cumulative 75 hours.

The cost of each capacity by the cost of each respective technology is determined by the capacity of each multiplied by each respective cost factor, defined in Table 9. The resulting costs for the 300 MW reduction level is shown Figure 42:

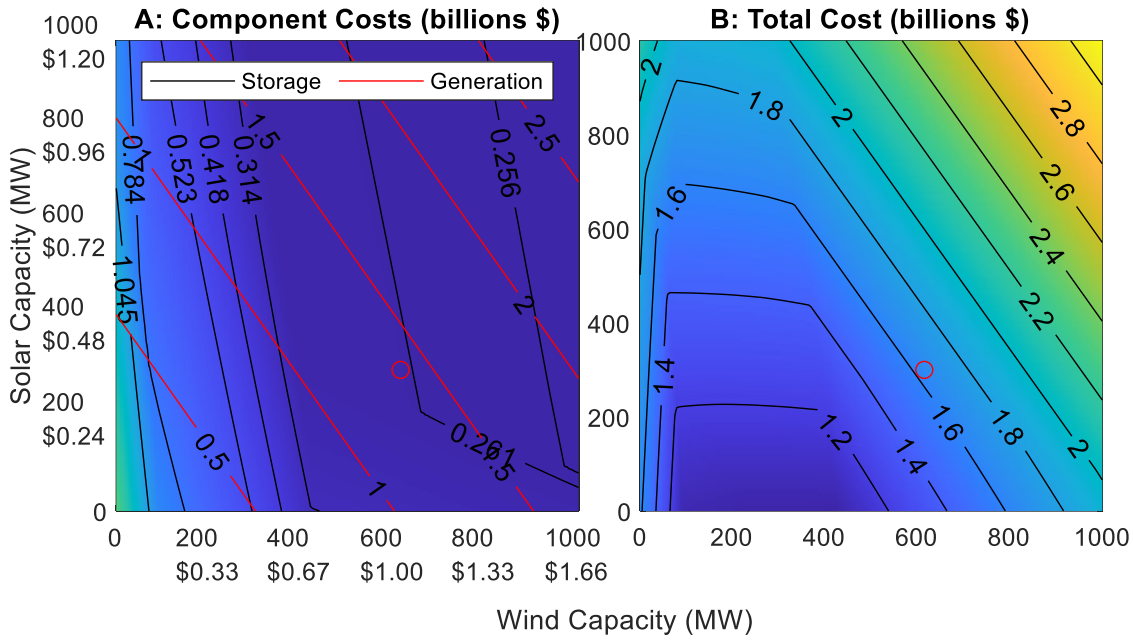

Figure 42 300 MW DG reduction component costs and total capital costs

Figure 42A shows the cost of the storage and generation separately. As described in the legend, the black contour lines represent the storage cost, the red contour line represent the cost of generation. Additionally, the changing colours on the plot represent the storage cost. The cost of each type of generation is also shown in the axis for each type.

Predictably, the storage cost contour lines have the same shape as the storage capacity, as the cost is based on capacity. The cost of generation contour lines is all parallel, as they are independent of the storage size; they are not perfectly 45° as wind installations are slightly more expensive per MW of installed capacity than solar.

When the storage cost and generation cost are combined, they equal the total capital cost, which is shown for 300 MW DG reduction in Figure 42B. At lower generation costs, the total cost follows the shape of the storage costs, while at higher generation levels the generation costs dominate. The demonstration from section 6.2 can be verified using equation 10:

$$[C]_{\text{total}} = (\$0.523/\text{MWh} \times 500\ \text{MWh} + \$1.663/\text{MW} \times 616\ \text{MW} + \$1.197/\text{MW}_{\text{ac}} \times 300\ \text{MW}_{\text{ac}}) \times 10^6$$

$$[C]_{\text{total}} = (\$261.3 + \$1022.4 + \$359.1) \times 10^6$$

$$[C]_{\text{total}} = \$1.643 \times 10^9$$

This aligns with the red circle Figure 42B. One important note is this assumes a start from 0 MW IG or storage, so the capacity of wind already installed can be negated from the cost if this were to be used. Major points are shown in Table 14:

Table 14 Costs for 300 MW DG reduction at various combinations of wind and solar

	Wind Capacity		Solar Capacity		Storage Capacity		Total Cost
Units	(MW)	(Billions $)	(MW)	(Billions $)	(MW)	(Billions $)	(Billions $)
No IG	0	0	0	0	3168	1.66	1.66
Min Cost	300	0.5	0	0	980	0.51	1.01
Max Wind	1000	1.66	0	0	517	0.27	1.93
Max Solar	0	0	1000	1.2	1770	0.93	2.12
Max IG	1000	1.66	1000	1.2	483	0.25	3.11

The highest cost of generation is when the maximum amount of solar and wind capacity are selected, which is also the point when storage capacity is at a minimum and thus has

the lowest cost. Likewise, when there is no solar or wind, the generation has no cost, but the storage requires the maximum capacity, and thus has its maximum cost.

The more interesting trends occur when looking at the combined cost for generation and storage. The lowest cost is not at either extreme, but occurs when there is 300 MW of wind, 0 MW of solar and 980 MW of storage, as shown in Table 9. At this point the cost contour lines are horizontal, indicating that the cost is most sensitive to solar, so adding any solar will increase costs faster than adding or subtracting wind. Therefore, it is uneconomic to add further solar.

7.3. Optimal Combinations

In the previous section an example was shown of the technical and economic results for retiring 300 MW of DG, the effect of closing approximately one coal plant. This section reviews the lowest cost combinations for a range of DG reduction in 50 MW increments. This optimal cost analysis can be repeated at different DG reduction levels, to graph the trend as DG gets lower and lower:

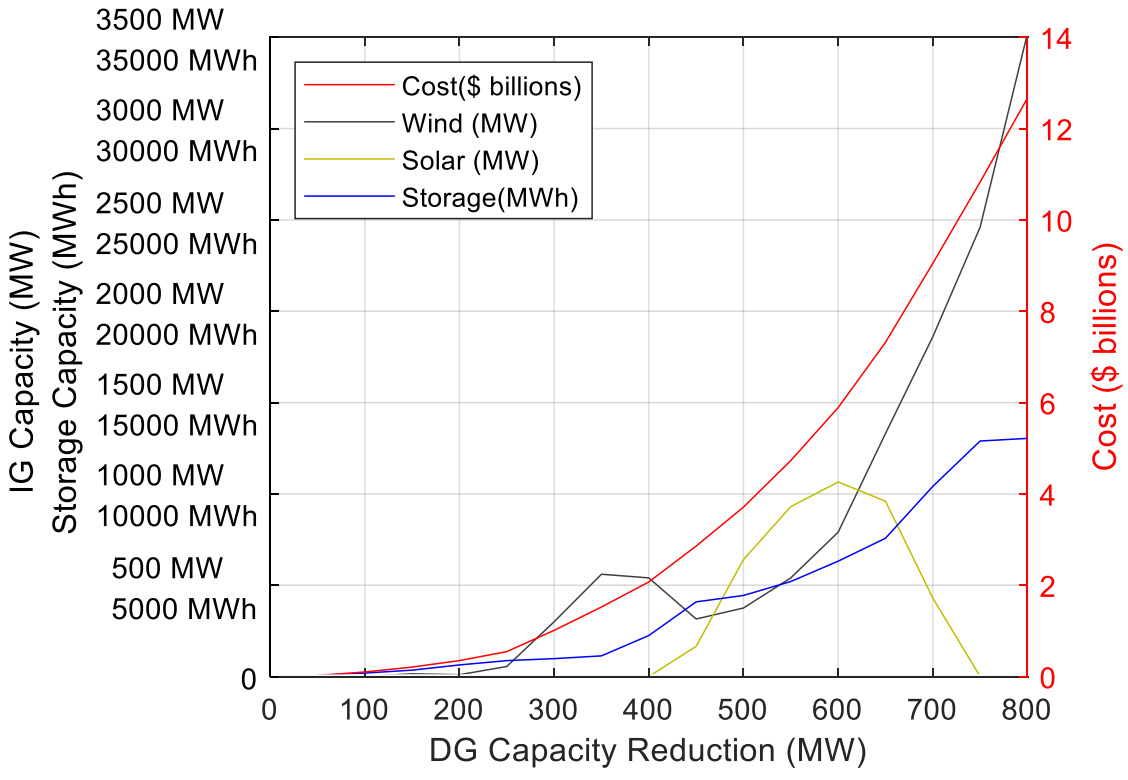

Figure 43 Wind, solar, and storage lowest cost curve

In this figure, the lowest cost combination of wind, solar and storage for each level of DG is plotted. There are three different sets of units being used, with IG capacity for wind and solar in terms of power capacity with units of MW, energy storage capacity in terms of energy with units of MWh, and cost in units of $ billions.

Storage alone is optimal until after 200 MW of DG reduction, at which point wind generation begins to contribute enough to counter its cost. The optimal amount of wind rises as dispatchable reduction increases, until after 350 MW, when it becomes more economical to increase storage. Solar becomes economical after 400 MW, which results in a reduction of wind. After the 400 MW DG reduction point the lowest cost combination begins to require solar, the demand for solar rises until after 600 MW of reduction, at which point the lowest cost combination requires less solar, until 750 MW DG reduction at which point solar is uneconomical.

7.3.1. Interplay of Wind and Solar at the 400 to 450 MW DG Reduction Level

The rises and falls of lowest cost renewable capacity as DG reduction increases are a result of the peak storage usage shifting to times with different production values of respective IG. To investigate this further, the results for the 400 MW DG reduction are shown. This is the point at which increasing solar begins being more economical than wind. To confirm the results from Figure 43, the storage capacity and cost for 400 MW DG reduction are plotted in Figure 44:

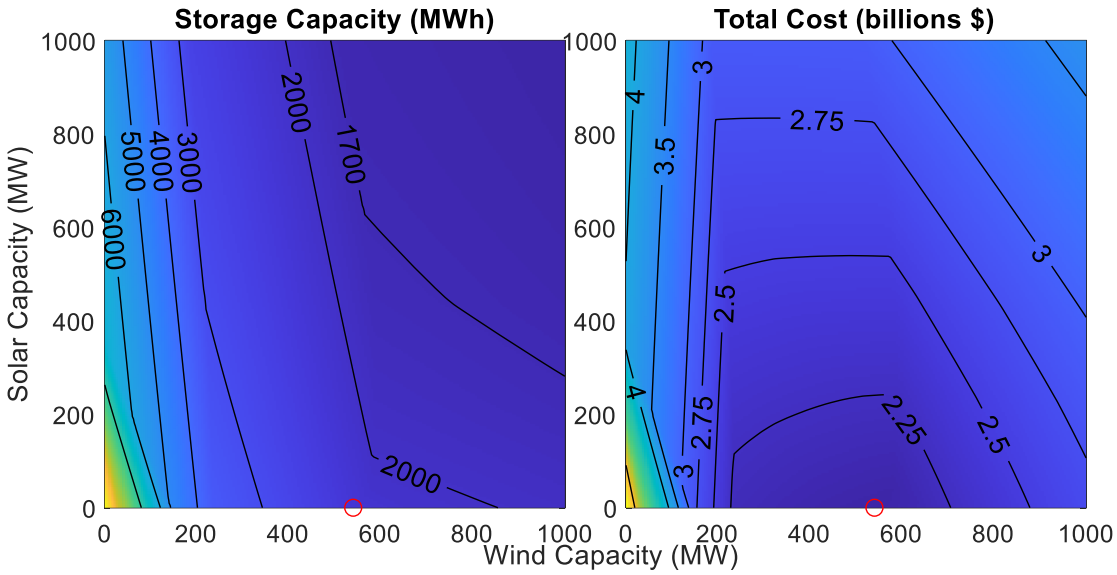

Figure 44 400 MW DG reduction storage capacity and cost

Consistent with Figure 41, the storage requirements decrease as the generation capacity increases. However, the cost is not lowest cost at lowest combination of generation, or at lowest storage, but midway through with a balance of both. The red circle is placed at the lowest cost point on the graph, which is contrasted with the 450 MW DG graph shown in Figure 45:

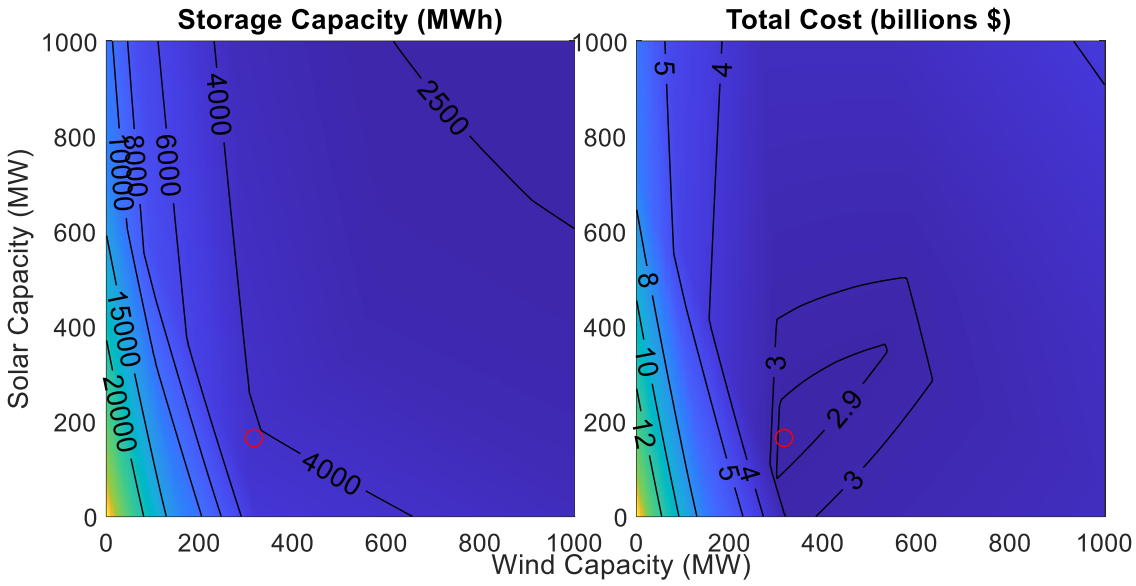

Figure 45 450 MW DG reduction storage capacity and cost

As predicted by Figure 43 the optimal wind capacity has decreased and solar increased at the 450 MW DG reduction level compared to the 400 MW DG level. The following Table 15 shows the optimal values from both Figure 44 and Figure 45:

Table 15 Optimal combination of wind, solar and storage capacities for 400 MW DG reduction vs 450 MW DG reduction

Parameter	400 MW DG reduction Optimal Value	450 MW DG reduction Optimal Value	Difference from 400 to 450 MW DG reduction
Cost	$2.07 billion	$2.86 billion	$0.79 billion
Wind	540 MW	315 MW	-225 MW
Solar	0 MW	165 MW	165 MW
Storage	2244 MWh	4086 MWh	1842 MWh

The results in Table 15 confirm the results in Figure 43. At the 400 MW point there is a clear preference for wind generation, with no solar generation being optimal at this reduction level, and comparatively lower storage capacity required. This changes at the 450 MW reduction level the desired wind capacity has fallen, and there is some solar required and much more storage capacity required.

This raises the question of what changes from the 400 MW and 450 MW reduction level that causes this drastic change in requirements? To determine this the two time series can

be plotted, the first one shown in Figure 46 shows the resulting time series with the optimal combination of wind, solar and load at 400 MW of DG reduction:

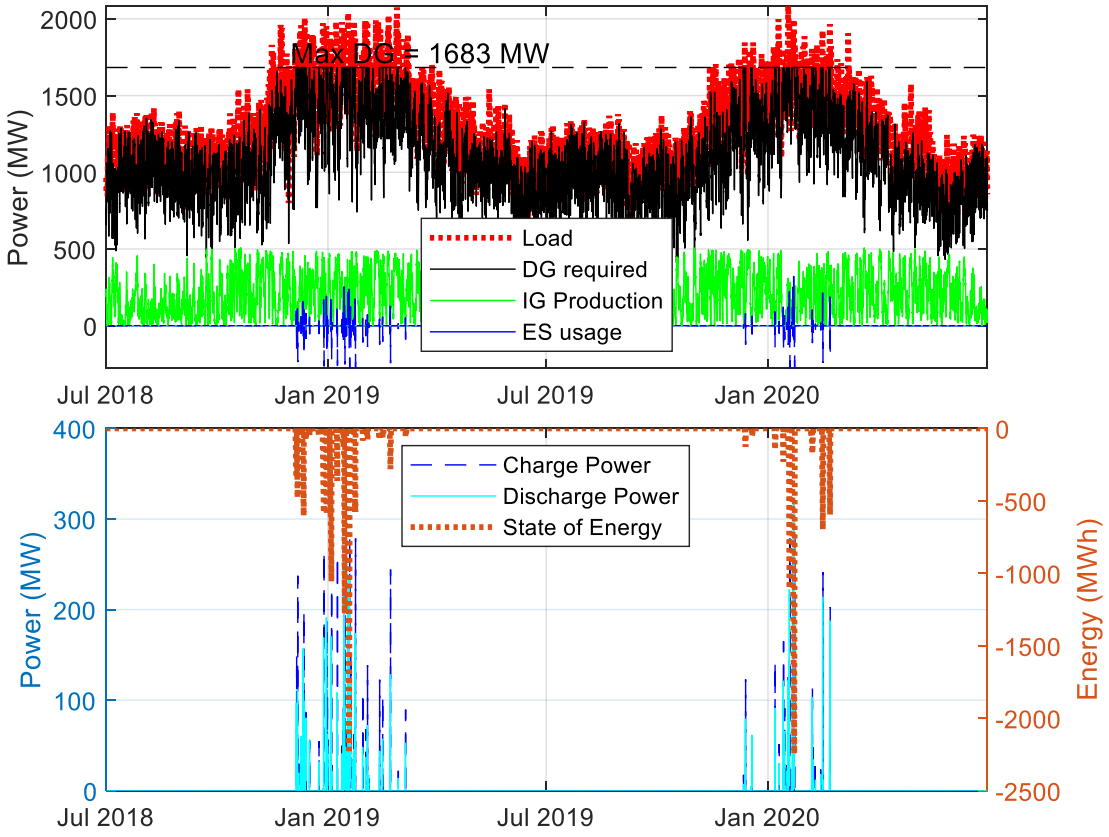

Figure 46 Power flow and energy storage time series for lowest cost 400 MW DG reduction

First the state of energy is plotted to determine which date ranges should be investigated. As before, the purpose of Figure 46 is to show a broad time series to pinpoint which dates should be focused on. The state of energy is at its lowest in January 2019, and 2020, which indicates these dates drive the demand for storage, so a closer look at these dates is warranted. These dates are shown in Figure 47:

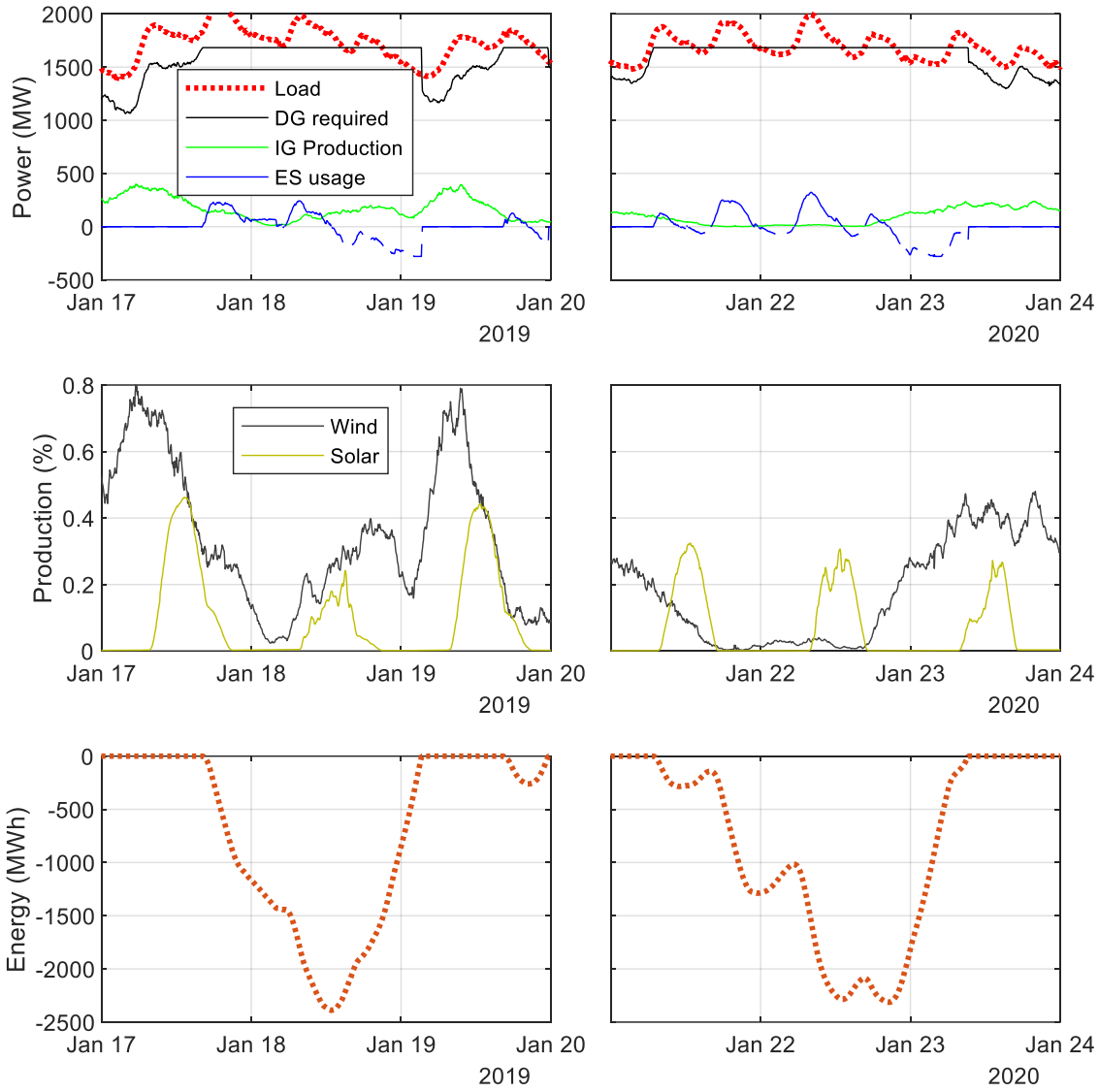

Figure 47 Winter 2019 and winter 2020 power and energy flow comparison for 400 MW DG reduction with lowest cost wind and solar capacity

Figure 47 displays the results from the peak usage days for the winters of 2018/19 and 2019/20, in each case the power flow for the system is shown in the top graph. The middle two graphs display the production for both solar and wind, to see their potential during these timeframes. The bottom graphs shows the energy deficit the battery experiences.

In both case, there is a two-day period where the battery is either charging or discharging because DG is at its maximum capacity. In both cases the IG is low in comparison to its maximum. However, in both cases, the energy in the battery begins charging as the wind

power increases. The solar has no impact because its capacity was set to 0 MW for this analysis.

There is more wind generation available during January 2019 than January 2020. This explains the limitation set on wind, even if the capacity were increased it would only reduce the net load for 2019. The net load would remain the same in the 2020 peak, causing the storage requirements to remain the same. With the same storage requirements, the excess wind capacity would cost more to build but not save costs in storage and thus would be uneconomic. This principle is why the wind demand is reduced at the 450 MW DG reduction level.

Figure 48 plots the two winters when DG is reduced by 450 MW, but the wind and solar capacity are kept the same as the optimal combination used in the 400 MW reduction:

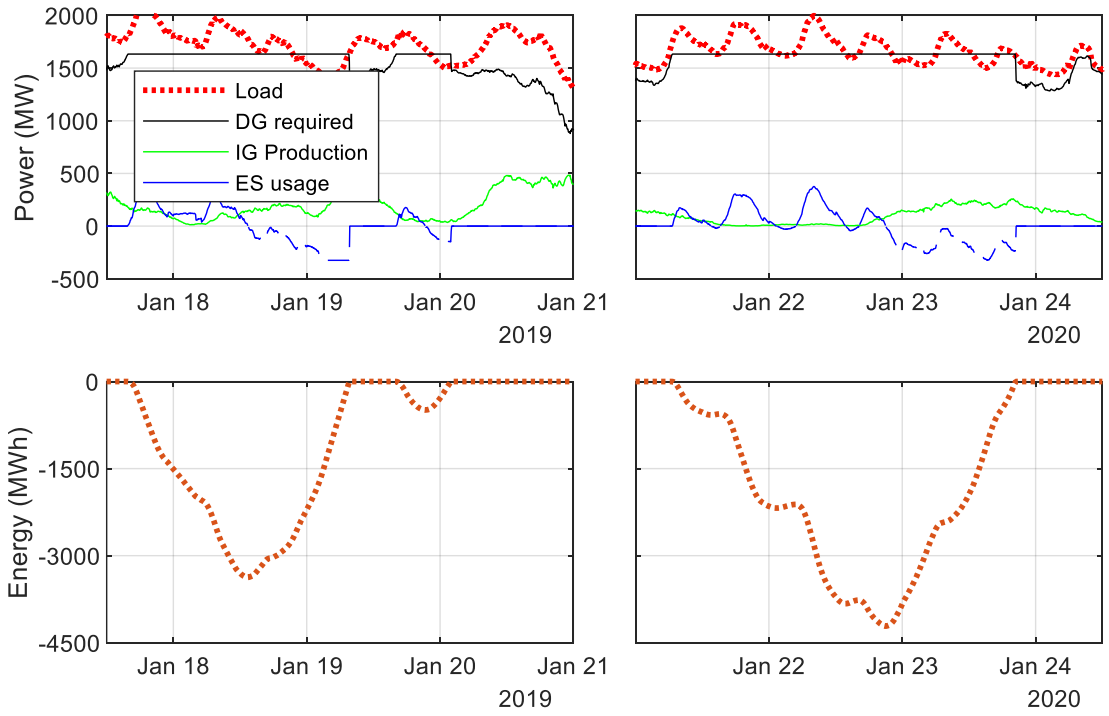

Figure 48 Winter 2018/19 and winter 2019/20 power and energy flow comparison for 450 MW DG reduction with excessive wind capacity

In the Figure 48 the same wind and solar level is simulated for the 450 MW DG reduction level. The wind and solar generation is not displayed as is identical as in Figure 47. As

expected, the storage demand is much higher, and unlike in the 400 MW DG reduction level, the 2018/19 and 2019/20 storage demands are severely imbalanced. This imbalance means that the better performance solar has in January 2020, will have a significant effect on the storage demand, which is why it is considered optimal to have 165 MW of solar, along with 315 MW of wind, and 4086 MWh of storage. To further illustrate this, the results when solar capacity is increased and wind capacity is decreased is plotted:

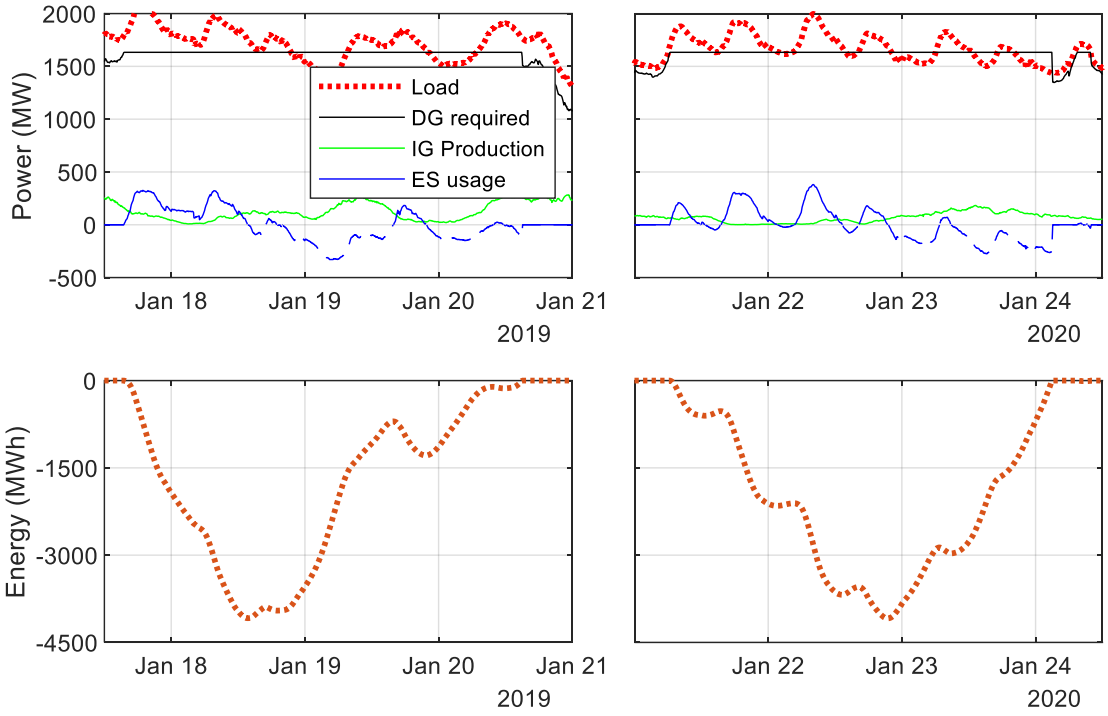

Figure 49 Winter 2018/19 and winter 2019/20 power and energy flow comparison for 450 MW DG reduction with optimal wind and solar

As expected, with lower wind, and more solar, the required energy storage increases in the January 2019 peak to balance with the January 2020 peak. The solar is enough to keep the storage requirement consistent for each year while decreasing the wind capacity. So, while the storage capacity does not increase, the generation capacity decreases. Since the cost of storage remains the same but the cost of generation decreases, the total cost decreases. This explains why there is a significant variation in optimal generation between 400 MW and 450 MW; reduced DG maximums means new peaks occur during times when there is no wind, but some solar.

7.3.2. Interplay of Wind and Solar at the 600 to 650 MW DG Reduction Level

Another point of interest is the drop in solar demand beyond the 600 MW DG reduction point. The optimal amount of solar begins to fall beginning at 600 MW reduction until it hits 0 MW solar at 750 MW. To investigate this, the 600 MW reduction and 650 MW reduction points are plotted:

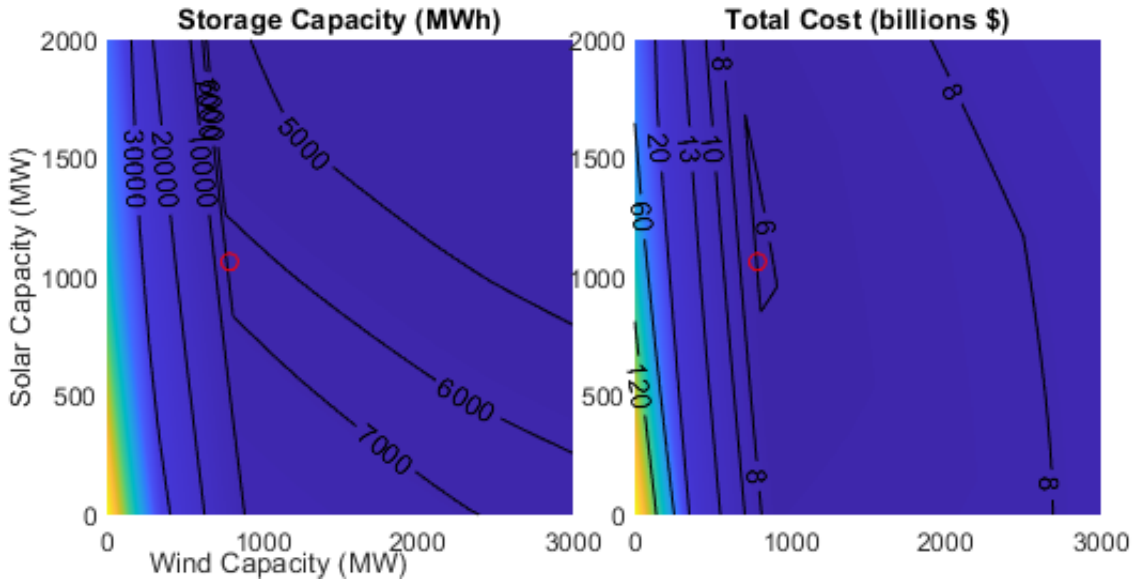

Figure 50 600 MW DG reduction storage capacity and cost

As can be seen at the 600 MW DG reduction level, the desired solar capacity is at its peak. The lowest cost combination requires a high amount of solar, wind and storage, the exact values are shown in Table 16. This is contrasted to the 650 MW DG reduction level which is shown in Figure 51:

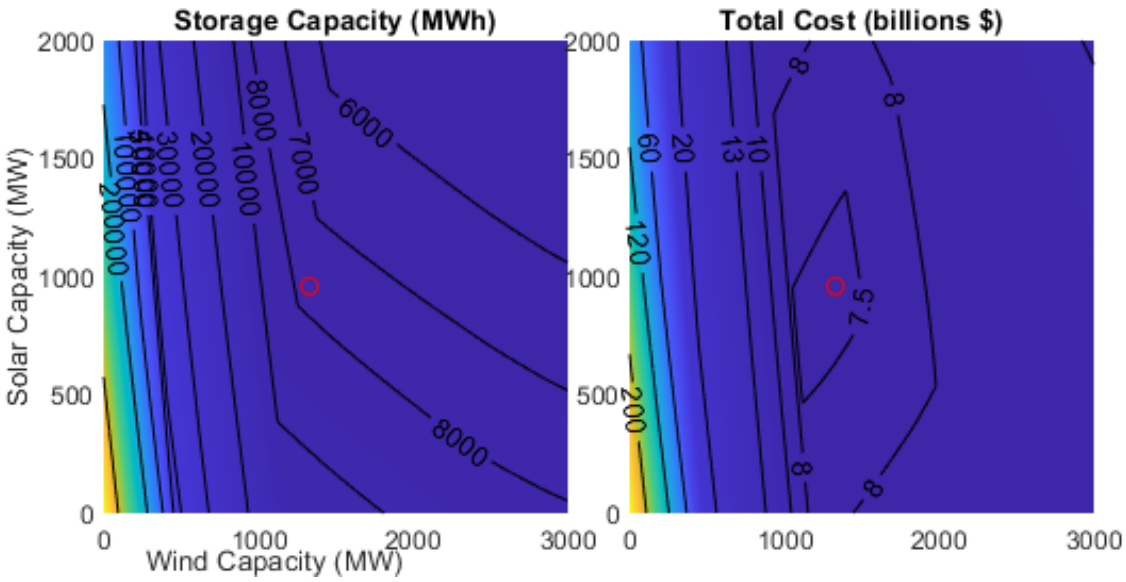

Figure 51 650 MW DG reduction storage capacity and cost

At the 650 MW DG reduction level the storage capacity and wind capacity has risen substantially, while solar has dropped from the 600 MW reduction level. The values are shown in Table 16:

Table 16 Optimal combination of wind, solar and storage capacities for 600 MW DG reduction vs 650 MW DG reduction

Parameter	600 MW DG reduction Optimal Value	650 MW DG reduction Optimal Value	Difference from 600 to 650 MW DG reduction
Cost	$5.89 billion	$7.31 billion	$1.42 billion
Wind	790 MW	1330 MW	540 MW
Solar	1065 MW	960 MW	-105 MW
Storage	6315 MWh	7568 MWh	1253 MWh

The results found Figure 50 and Figure 51 align with the results found in Figure 43. This confirms the lowest cost combination of wind, solar and load for 600 MW DG reduction and 650 MW reduction. To investigate further into why the lowest cost combination requires the reduction of solar capacity as DG capacity is reduced, the timestep series is plotted:

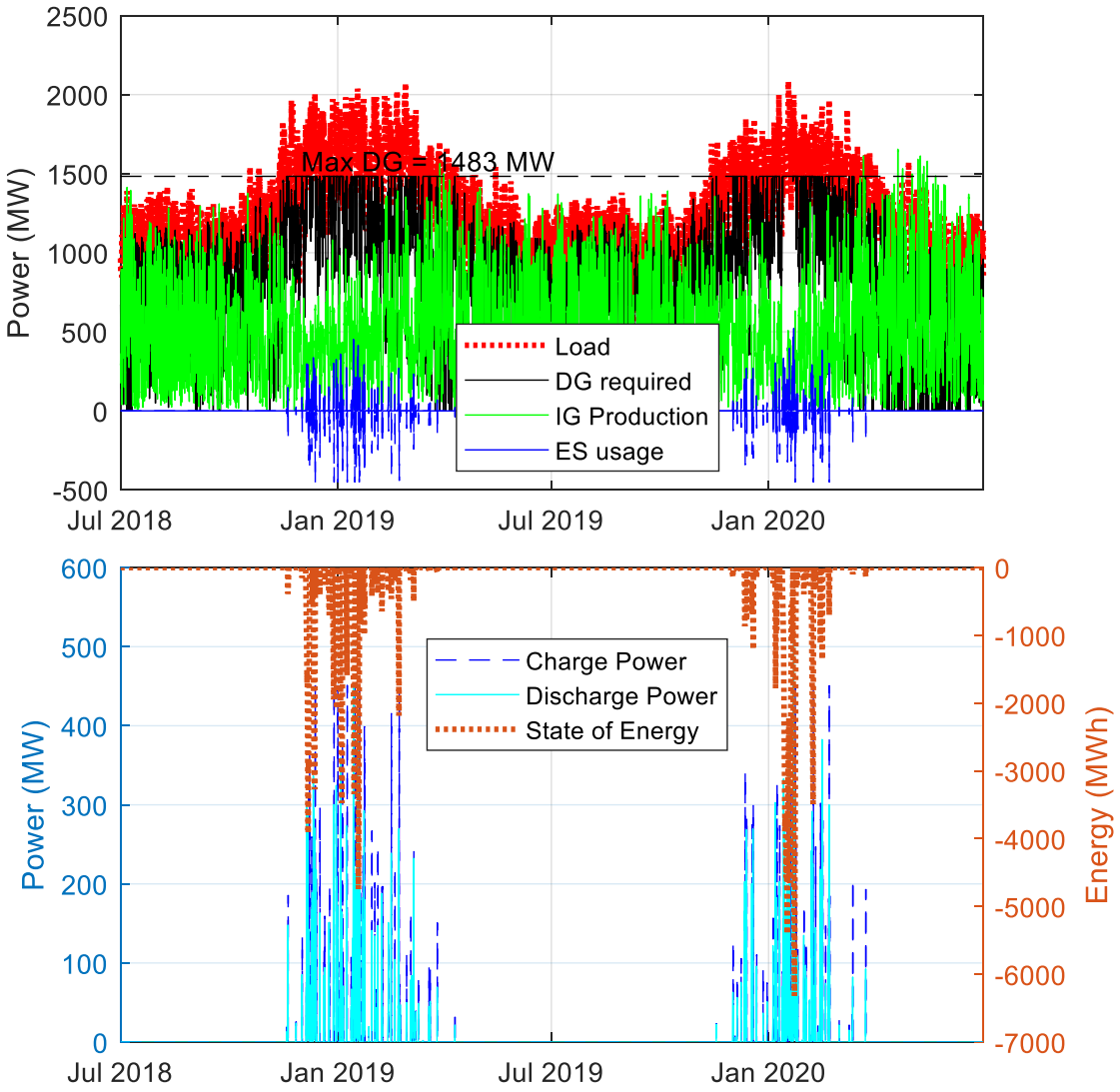

Figure 52 Energy storage time series 600 MW DG reduction

From the top graph in Figure 52 shows the amount of IG being produced at this level, the combined capacity of wind and solar is 1855 MW. As such, the required DG is substantially reduced. Despite this, there are still times with low IG which requires the storage to provide power from electricity stored earlier. Unlike in the 400 MW DG reduction analysis, the peak energy usage is solely within January 2020, there is a small peak in 2018/19, however, it is not as significant as the winter 2019/20 peak, so the focus will be made on January 2020, shown in Figure 53:

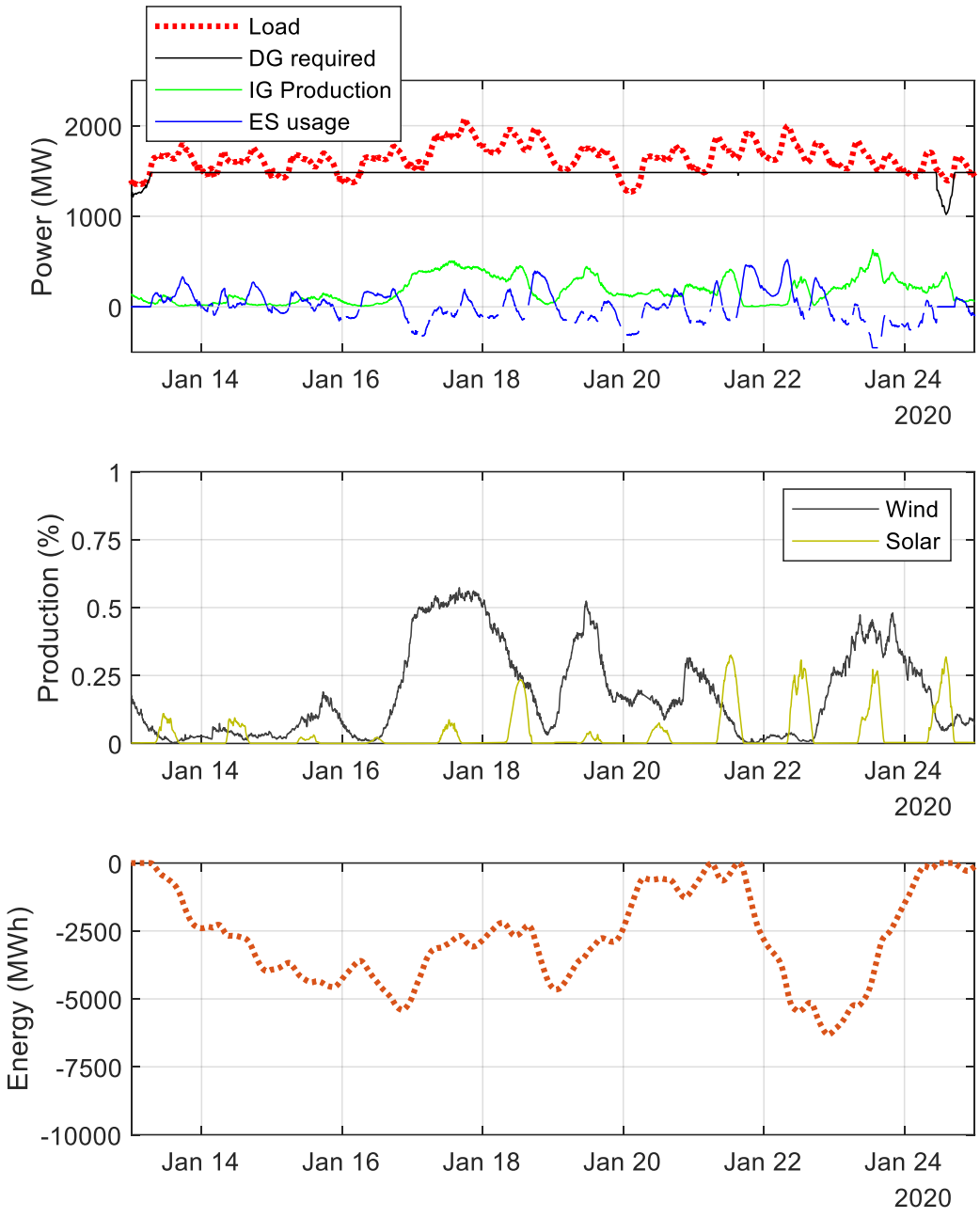

Figure 53 Winter 2020 peak power and energy flow for 600 MW DG reduction with lowest cost wind and solar capacity

The two peak energy storage usage events occur within the same ten days at the 600 MW DG level. There is a period of high load during this time, with the energy storage only fully recharging briefly between the two events when the load drops and the wind rises on January 20. The difference between the two events is shown in the relative IG amount for each, in the first even there is very little wind or solar generation, so the entire load must

be provided by the DG and the storage. This results in a drop in the stored energy, until January 17, which the wind rises, and the storage begins to recover. In the second event there is only a short period at the end of January 19 that the wind and solar generation are low, which causes the depletion of the storage to its minimum of -6315 MWh.

The expectation is that the first event will require comparitively more non-dispatchable electrical energy as the power from DG is reduced. This is because the entire load period of the second event is already above the maximum DG threshold, while the first event still has three short periods where the DG limit exceeds the load. If more time is added then it will have a amplifying effect on top of the increasing power when determining the energy demand. The first peak has the benefit of adding more time and power, whereas the second peak is only adding power, which means the energy demand from the first peak should grow more as DG is reduced.

With the first event period becoming more impactful to the storage, solar will lose the ability to reduce the dispatchable generation demand, which will result in greater storage demands. This is because solar, shown in the middle graph of Figure 53, does not produce significant electricity during until January 18. Whereas the wind generation has a small amount of production which exceeds the solar generation, with a large amount of production earlier on the 18th. This hypothesis is confirmed when the 650 MW DG time series is plotted for the two events:

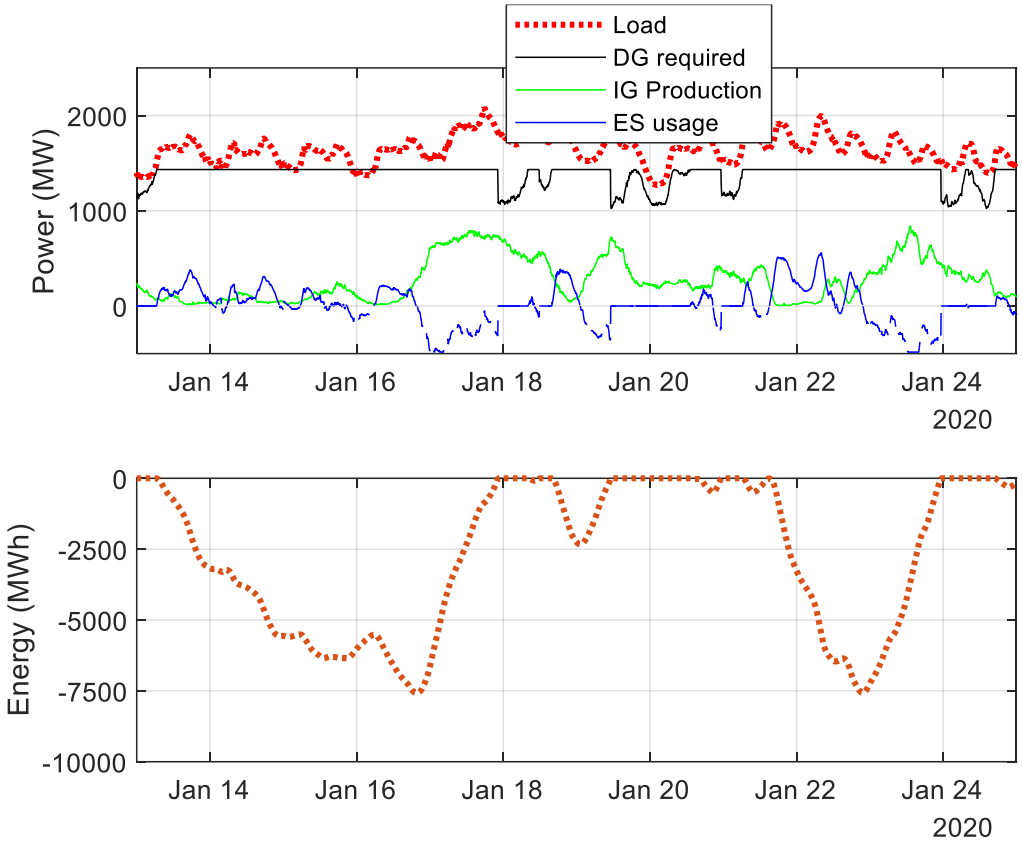

Figure 54 Winter 2020 peak power and energy flow for 650 MW DG reduction with lowest cost wind and solar capacity

As expected, the required storage increased for both peaks, with both rising to approximately 7500 MWh. The only reason that the first peak did not exceed the second, was because of the reduction of solar capacity and increase in wind capacity. Interestingly, the increase in wind capacity resulted in the period between the events becoming wider and more distinct, there is now a noticeable period where intermittent and DG can meet load with only minimal storage required.

This first event explains the need for less solar and more wind. As the timing of peak energy events changes, the makeup of the energy generation changes to match what generation source is best at that time. This same verification is accomplished by the model in minutes, by comparing all simulated combinations of wind, solar and storage at given DG amounts. The results presented in Figure 43 provide a blueprint for future renewable and storage construction for reducing the need for DG, this will help reduce the need for fossil fuel-based generation, like coal.

7.4. Summary

This chapter developed a parameter index controller with the model presented in Chapter 6 to determine the resulting storage requirements for given, wind and solar capacities, and DG reduction. Then the cost of each technology was used to determine the total cost of each combination. Using this, the least cost combination for each DG reduction level was determined. The values from 400-450 MW of DG reduction and 600-650 MW of DG reduction were investigated more closely because their lowest cost combinations in a reduction of wind and solar capacity respectively.

The lowest cost combination is typically driven by balancing two events of peak energy storage usage. These are typically the periods with high load and low IG availability. These events exclusively occur during the winter when load is higher. During the summer the energy storage is rarely used, and is available for other services,

The storage requirements increased as the dispatchable generation reduction amount increased. Wind capacity is not economical for DG reduction until 200 MW, where it steadily increases until the 350 MW DG reduction level. After 350 MW of DG reduction the lowest cost amount of wind capacity decreases until 450 MW, then increases again. Solar is not economical until 400 MW of DG reduction, then increases until 600 MW, after which point it decreases until becoming uneconomical at 750 MW.

Chapter 8. Conclusions and Recommendations

The concern with intermittent resources, is that their output is not controlled by the operator, instead it is dependent on the weather or the sun. While this phenomenon has been studied extensively, there is a gap in the literature when related to specific aspects of using these renewable generators to offset the need of dispatchable generation power capacity. Many energy storage models focused on DG energy use, not DG capacity reduction, this new model reduces the need for DG power capacity so generation facilities can be permanently retired.

The first major research contribution of this thesis is creating a model for calculating the capacity value of wind generation to continuously adjust the relevant high load region using the cumulative frequency method. This model was created and used to assess NS to determine the following conclusions:

A. Perform an initial capacity value assessment of wind generation for comparison of wind farms: which determined that adding new wind farms in new locations will improve diversity, resulting in more reliable production, and thus greater capacity value.

B. Review multiple years independently: Which determined the variation of results when only single years was assessed. This resulted in the conclusion that a single year of analysis was inaccurate and highly variable depending on which year was chosen.

C. Assess the impact of data resolution: Which found that the resolution had no significant impact as long as it was below one hour. This concluded that the resolutions from 2-minute to 1-hour timesteps had insignificant differences.

D. Determine the impact of ambient conditions: Which determined that wind generation performed better during the warmer high load hours. This confirmed that there was a negative correlation between load and temperature. This also concluded that wind capacity value was higher during warmer temperatures of high load.

E. Compare the capacity value of wind generation to solar generation, by assessing solar on an annual basis, and by comparing at high net load hours for hours of the day, and months of the year: Wind generation has a higher capacity value to solar in the winter as expected, but is similar to solar generation in the summer. As NS is a winter peaking province, wind generation has a higher capacity value overall, but in summer peaking locations solar generation has a high capacity value. Solar can still reduce the need for DG energy in the summer, even if the DG capacity is still needed in the winter.

F. New presentation of result used for both the capacity value analysis and the storage model. The capacity value is typically given as a single percentage value depending on the technology and region, since the threshold for 'high-load' varied, the graphing method displayed a varying capacity value depending on the load threshold used.

The second major research contribution of this thesis is the creation of a new control strategy and energy storage model which prioritized keeping the DG power output below a given threshold. This used normalized generation data to determine the storage requirements for given DG capacity reduction. A parameter index controller was then used to iterate this model to test multiple combinations of wind, solar, and DG limits to find the minimum storage required.

G. The results for the storage model were displayed as a series of contour plots, with wind and solar capacity chosen as the two varying coordinates. The storage capacity, energy/power ratio, discharge cycle equivalents, curtailment, and storage and generation cost can be easily read from these graphs depending on the wind, solar and DG reduction.

H. Higher loads occur during the winter than the summer, so most of the storage needs is driven by the difference between load and renewable generation during the winter. Typically, higher wind capacity results in a lower storage requirement, however, solar has some impact when there is already some wind. The

energy/power ratio has a similar trend to storage capacity, as the energy demand often rises much faster than power demand.

I. Additional curtailment typically only occurs at high levels of solar, typically when some wind generation is added. The storage is typically cycled very few times in a year, which means cycle life does not need to be prioritized, or the storage can be used for other purposes when high loads are not expected.

J. The lowest cost combinations changed as the DG capacity was reduced. The following list provides a summary of the lowest cost combinations for DG reduction:

- 0-200 MW DG reduction: Storage alone, no IG.
- 200-400 MW DG reduction: Wind and storage alone, no solar.
- 400-750 MW DG reduction: Wind, solar and storage.
- 750+ MW DG reduction: Wind and storage alone, no solar.

Solar is briefly economical before becoming less cost effective than wind and storage alone. The necessary wind capacity rises rapidly after the 450 MW DG reduction as DG reduction increases.

8.1. Recommendations

The models have several areas in which they could be improved. Points I to II indicate ways in which the capacity value analysis can be improved, IV to V are ways in which the storage model can be improved. III can be used to improve both analyses:

I. The potential impact of wind turbine icing should be investigated, as that was hypothesised to be affecting the wind turbines' capacity value at sub-zero temperatures. This could be done by comparing the performance of wind turbines with de-icing technology to wind turbines without. However, it is cautioned that the investigators normalize for factors such as geography, and local temperature.

II. The capacity value for the 2020/21 winter should be added, as this data was not available in time for this analysis, it and further years should be analysed when that data becomes available. If the results remain the same when a fourth year is added then the conclusion can be made that the multi-year analysis is effective.

III. Proper grid-scale industrial solar generation data should be used. When large scale generation data in NS exists it should be used for analysis instead of residential solar.

IV. When the 2020/21 data becomes available for wind, solar and load it should be added to the storage model. The storage demand was driven by a 1-2 events per year, so adding another year would increase the significance of the results.

V. Future analysis may focus on forecasting future demand and generation in a more sophisticated manner. This thesis shows the viability of this model but future research could use this model with a forecast load created, based on potential scenarios such as: greater AC adoption, greater EV adoption, greater electric heating, or increased population.

VI. Adding other forms of renewable energy to the model would be useful for further research. This model focused on wind and solar generation, because these are the forms of generation that both have a history of data, and are planned for further development. However, tidal and wave generation are being developed currently, so adding those are sources of generation would be relevant.

References

[1] US Energy Information Administration, “Use of electricity,” *US EIA*, 2021. https://www.eia.gov/energyexplained/electricity/use-of-electricity.php.

[2] J. A. Casey, M. Fukurai, D. Hernández, S. Balsari, and M. V. Kiang, “Power Outages and Community Health: a Narrative Review,” *Curr. Environ. Heal. Reports*, vol. 7, no. 4, pp. 371–383, 2020, doi: 10.1007/s40572-020-00295-0.

[3] H. Ritchie and M. Roser, “Fossil Fuels,” *Our World in Data*, 2021. https://ourworldindata.org/energy.

[4] J. Y. S. Leung, B. D. Russell, and S. D. Connell, “Global Warming of 1.5C Summary for Policymakers,” *IPCC*, vol. 1, no. 3, pp. 374–381, 2019, doi: 10.1016/j.oneear.2019.10.025.

[5] Environment Canada, “Canada’s Emissions Trends,” 2014. [Online]. Available: http://publications.gc.ca/pub?id=9.507466&sl=0.

[6] Canada Energy Regulator, “Canada’s Renewable Power Landscape 2017 – Energy Market Analysis,” *Electricity and Renewables*, 2020. https://www.cer-rec.gc.ca/en/data-analysis/energy-commodities/electricity/report/2017-canadian-renewable-power/canadas-renewable-power-landscape-2017-energy-market-analysis-ghg-emission.html.

[7] Government of Canada, “Coal phase-out: the Powering Past Coal Alliance,” *Canada’s international action on climate change*, 2020. https://www.canada.ca/en/services/environment/weather/climatechange/canada-international-action/coal-phase-out.html#shr-pg0.

[8] Nova Scotia Power, “How We Make Electricity,” *Electricity*, 2021. https://www.nspower.ca/about-us/electricity/producing#coal.

[9] M. Lange, “On the uncertainty of wind power predictions - Analysis of the forecast accuracy and statistical distribution of errors,” *J. Sol. Energy Eng. Trans. ASME*, vol. 127, no. 2, pp. 177–184, 2005, doi: 10.1115/1.1862266.

[10] N. Y. Krakauer and D. S. Cohan, “Interannual variability and seasonal predictability of wind and solar resources,” *Resources*, vol. 6, no. 3, pp. 1–14, 2017, doi: 10.3390/resources6030029.

[11] N. Pearre and L. Swan, “Reimagining renewable electricity grid management with dispatchable generation to stabilize energy storage,” *Energy*, vol. 203, p. 117917, 2020, doi: 10.1016/j.energy.2020.117917.

[12] N. Pearre and L. Swan, “Combining wind, solar, and in-stream tidal electricity generation with energy storage using a load-perturbation control strategy,” *Energy*, vol. 203, p. 117898, 2020, doi: 10.1016/j.energy.2020.117898.

[13] Canada Energy Regulator, “Macro Indicators,” *Canada’s Energy Future Data Appendices*, 2020. https://apps.rec-cer.gc.ca/ftrppndc/dflt.aspx.

[14] ICF International, “Market Trends for the Supply & Demand of Electricity in Nova Scotia,” 2014.

[15] Nova Scotia Power, “Time-of-day rates,” *Electric Thermal Storage*, 2021. https://www.nspower.ca/your-home/energy-products/electric-thermal-storage/benefits.

[16] B. Frisko and R. Van Horne, “Nova Scotia Power applies to get time-of-day pricing to give option for lower electricity prices,” *CTV News*, Halifax, Jul. 13, 2020.

[17] Nova Scotia Power, “2020 Integrated Resource Plan,” Halifax, 2020. [Online]. Available: https://irp.nspower.ca/.

[18] J. Hanania, K. Stenhouse, and J. Donev, “Dispatchable source of electricity,” *University of Calgary*, 2020. https://energyeducation.ca/encyclopedia/Dispatchable_source_of_electricity.

[19] S. Wang, S. Wang, and J. Liu, “Life-cycle green-house gas emissions of onshore and offshore wind turbines,” *J. Clean. Prod.*, vol. 210, pp. 804–810, 2019, doi: 10.1016/j.jclepro.2018.11.031.

[20] Canada Renewable Energy Association, “By the Numbers,” *Energy Transition*, 2020. https://renewablesassociation.ca/by-the-numbers/.

[21] Nova Scotia Power, “Wind Power,” *Clean Energy*, 2020. https://www.nspower.ca/clean-energy/renewable-energy-sources/wind-power.

[22] Nova Scotia Departement of Energy and Mines, “Hydro-electricity in Nova Scotia,” *Renewables*, 2021. https://energy.novascotia.ca/renewables/hydro-electricity.

[23] Nova Scotia Power, “Hydro & Tidal Power,” *Clean Energy*, 2020. https://www.nspower.ca/cleanandgreen/renewable-energy-sources/tidal-power.

[24] Government of Nova Scotia, “The Solar Electricity for Community Buildings Pilot Program,” *Solar*, 2021. https://novascotia.ca/solar/solar-electricity-community-buildings.asp.

[25] M. Milligan, B. Frew, E. Ibanez, J. Kiviluoma, H. Holttinen, and L. Söder, “Capacity value assessments of wind power,” *IEEE Trans. Power Syst.*, vol. 26, no. 2, pp. 564–572, 2011, doi: 10.1109/TPWRS.2010.2062543.

[26] H. Fayazi Boroujeni, M. Eghtedari, M. Abdollahi Bastaki, and E. Behzadipour, “Calculation of generation system reliability index: Loss of Load Probability,” *Life Sci. J.*, vol. 9, no. 4, pp. 3595–3599, 2012.

[27] Z. Ming, “Overview of PRM Study,” 2019. [Online]. Available: https://irp.nspower.ca/files/key-documents/presentations/20190807-02_-E3-Capacity-Study-Overview.pdf.

[28] Nova Scotia Power, “Nova Scotia Utility and Review Board: 2014 Integrated Resource Plan,” 2014, [Online]. Available: http://www.nspower.ca/site-nsp/media/nspower/2009 IRP UPDATE - FINAL REPORT COMBINED REDACTED.pdf.

[29] R. M. G. Castro and L. A. F. M. Ferreira, “A comparison between chronological and probabilistic methods to estimate wind power capacity credit,” *IEEE Trans. Power Syst.*, vol. 16, no. 4, pp. 904–909, 2001, doi: 10.1109/59.962444.

[30] Nova Scotia Department of Energy and Mines, “Current Activity,” *Energy Storage*, 2021. https://energy.novascotia.ca/renewables/energy-storage/current-activity.

[31] Nova Scotia Power, “Intelligent Feeder Project,” *Innovation*, 2021. https://www.nspower.ca/cleanandgreen/innovation/intelligent-feeder.

[32] TransAlta, “WindCharger Battery Storage,” *Plants Operation*, 2020. https://www.transalta.com/plants-operation/windcharger/ (accessed Jul. 04, 2021).

[33] J. DeLong, “Saint John Energy signs up for 2.5MWh of energy storage,” *Saint John Energy*, p. 1, 2019.

[34] T. Roszell, “Saint John Energy adding money-saving battery power to its energy grid,” *Global News*, 2020. https://globalnews.ca/news/6379160/saint-john-energy-adding-money-saving-battery-power-to-its-energy-grid/.

[35] Energie NB Power, “Shediac’s Community Solar Farm,” *Shediac Smart Energy Community Project*, 2021. https://www.nbpower.com/en/grid-modernization/smart-grid-atlantic/shediac-smart-energy-community-project/shediac-s-community-solar-farm/.

[36] IESO, “Energy Procurement and Contracts Archive,” *Energy Procurement Programs and Contracts*, 2021. https://www.ieso.ca/en/Sector-Participants/Energy-Procurement-Programs-and-Contracts/Procurement-Archive.

[37] C. K. Simoglou, P. N. Biskas, E. A. Bakirtzis, A. N. Matenli, A. I. Petridis, and A. G. Bakirtzis, “Evaluation of the capacity credit of RES: The Greek case,” *2013 IEEE Grenoble Conf. PowerTech, POWERTECH 2013*, pp. 1–6, 2013, doi: 10.1109/PTC.2013.6652340.

[38] M. Mosadeghy, R. Yan, and T. K. Saha, “Impact of PV penetration level on the capacity value of South Australian wind farms,” *Renew. Energy*, vol. 85, pp. 1135–1142, 2016, doi: 10.1016/j.renene.2015.07.072.

[39] J. P. Yáñez, A. Kunith, R. Chávez-Arroyo, A. Romo-Perea, and O. Probst, “Assessment of the capacity credit of wind power in Mexico,” *Renew. Energy*, vol. 72, pp. 62–78, 2014, doi: 10.1016/j.renene.2014.06.038.

[40] J. Jorgenson, S. Awara, G. Stephen, and T. Mai, “A systematic evaluation of wind’s capacity credit in the Western United States,” *Wind Energy*, no. December 2020, pp. 1–15, 2021, doi: 10.1002/we.2620.

[41] W. L. Schram, H. Aghaie, I. Lampropoulos, and W. G. J. H. M. va. Sark, “Insights on the capacity value of photovoltaics, community batteries and electric vehicles,” *Sustain. Energy, Grids Networks*, vol. 26, p. 100421, 2021, doi: 10.1016/j.segan.2020.100421.

[42] D. Sodano, J. DeCarolis, A. Rodrigo de Queiroz, and J. X. Johnson, “The symbiotic relationship of solar power and energy storage in providing capacity value,” *Renew. Energy*, vol. 177, pp. 823–832, 2021, doi: 10.1016/j.renene.2021.05.122.

[43] H. Johlas, S. Witherby, and J. R. Doyle, “Storage requirements for high grid penetration of wind and solar power for the MISO region of North America : A case study,” *Renew. Energy*, vol. 146, pp. 1315–1324, 2020, doi: 10.1016/j.renene.2019.07.043.

[44] C. Budischak, D. Sewell, H. Thomson, L. MacH, D. E. Veron, and W. Kempton, “Cost-minimized combinations of wind power, solar power and electrochemical storage, powering the grid up to 99.9% of the time,” *J. Power Sources*, vol. 225, pp. 60–74, 2013, doi: 10.1016/j.jpowsour.2012.09.054.

[45] S. Weitemeyer, D. Kleinhans, L. Siemer, and C. Agert, “Optimal combination of energy storages for prospective power supply systems based on Renewable Energy Sources,” *J. Energy Storage*, vol. 20, no. September 2016, pp. 581–589, 2018, doi: 10.1016/j.est.2018.10.012.

[46] M. Esteban, Q. Zhang, and A. Utama, “Estimation of the energy storage requirement of a future 100% renewable energy system in Japan,” *Energy Policy*, vol. 47, pp. 22–31, 2012, doi: 10.1016/j.enpol.2012.03.078.

[47] S. Manchester, B. Barzegar, L. Swan, and D. Groulx, “Energy storage requirements for in-stream tidal generation on a limited capacity electricity grid,” *Energy*, vol. 61, pp. 283–290, 2013, doi: 10.1016/j.energy.2013.08.036.

[48] N. S. Pearre and L. G. Swan, “Renewable electricity and energy storage to permit retirement of coal-fired generators in nova scotia,” *Sustain. Energy Technol. Assessments*, vol. 1, no. 1, pp. 44–53, 2013, doi: 10.1016/j.seta.2013.01.001.

Appendix A Permissions

Re: Image Permission Request

Lukas Swan <Lukas.Swan@Dal.Ca>
Mon 5/31/2021 11:22 AM

To: Pushkarna, Sanjeev <Sanjeev.Pushkarna@nspower.ca>
Cc: David Kiefte <David.Kiefte@dal.ca>

Thank you very much Sanjeev

On Mon, 31 May 2021 at 10:14, Pushkarna, Sanjeev <Sanjeev.Pushkarna@nspower.ca> wrote:

Permission received. As you mentioned below, please be sure to reference/credit NSP website.

Thanks and good luck with the thesis David!

Sanjeev

From: Lukas Swan <Lukas.Swan@dal.ca>
Sent: May-31-21 9:06 AM
To: David Kiefte <David.Kiefte@dal.ca>; Pushkarna, Sanjeev <Sanjeev.Pushkarna@nspower.ca>
Subject: Re: Image Permission Request

This is an external email from: Lukas.Swan@Dal.Ca - exercise caution

Hi Sanjeev

I supervise Mr. David Kiefe who is a MASc student conducting research in my laboratory.

He is writing his thesis right now, with a focus on capacity value ("reliable capacity") of wind farms throughout Nova Scotia.

To show the widespread distribution of both hydro and wind in NS, he would like to reprint the below two figures in his thesis, with proper referencing of course.

He seeks this permission. Could you please help us obtain permission from NSP to use these figures?

I believe both figures have been used extensively and appear on the NSP website, so I am hoping this is not to onerous to obtain permission.

Thanks

Lukas

Lukas Swan, PhD, PEng

Professor, Department of Mechanical Engineering

Director, Renewable Energy Storage Laboratory

Dalhousie University

Telephone: +1(902)830-0349

Email: Lukas.Swan@Dal.Ca

Twitter: https://twitter.com/DalRESL

Website: http://resl.me.dal.ca

Physical address: C302 Sexton Campus, 5269 Morris St, Halifax, Nova Scotia, B3J 0H6, Canada

Postal address: PO Box 15000, Halifax, Nova Scotia, B3H 4R2, Canada

On Fri, 28 May 2021 at 12:32, David Kiefte <David.Kiefte@dal.ca> wrote:

> Hi Lukas,
>
> Ive attached the screenshots I was hoping to use and the links to where they can be found on the NSPower website.
>
> David

> https://www.nspower.ca/cleanandgreen/renewable-energy-sources/tidal-power

https://www.nspower.ca/cleanandgreen/renewable-energy-sources/wind-power

Appendix B Wind+Solar+Storage model code

```
function [difference, SOE_MWh, Batt_Charge, Batt_Discharge, failure] = req_stg(Solar_PV,
Wind, Load, DG_cap)
% This code determines the resulting SOE, curtailment, discharge and charge
% powers required to keep the DG at or below the limit (DG_cap). Solar_PV,
% Wind and Load should all be input as the same units (typically MW). The
% Curtailment, Batt_Charge, Batt_Discharge will output in the same units of
% power discharged.

% initializing variables
failure = 0;
usemaxpwr = 1;

IG_gen = Solar_PV + Wind; % intermittent generation is sum of solar and wind
net_load = Load - IG_gen; % net load is equalt to load minus IG
difference = DG_cap - net_load; % 'difference' is stand-in for difference
% between DG peak and net load, positive difference means DG has
% excess capability, negative means net load exceeds DG capability

maxpwr = -min(difference); % limit charge rate by maximum discharge

% Set charge and discharge energy efficiency
ChargeEfficiency = 0.93;
DischargeEfficiency = 0.93;

% storage capacity initialized to 0 MWh for depletion model
stg_cap = 0;
stg_cap_MW = stg_cap.*12; % converts the storage capacity from MWh to MWx5min

% Initializes various values to be string of same length as difference
SOE = difference.*NaN; % State of Energy (MWx5min)
Batt_Discharge = difference.*0; % Discharge power (MW)
Batt_Charge = difference.*0; % Charge power (MW)

for t = 1:length(difference) % step through each time
 if t == 1
  SOE(t) = stg_cap_MW; % Assume storage initializes fully charged
 else
  SOE(t) = SOE(t-1); % SOE starts at same energy state as previous timestep
 end

 % Series of if statements to check if charging or discharging
 if difference(t) > 0 % load is lower than target load so charge
  if usemaxpwr % limits charge to maximum required for discharge
   Batt_Charge(t) = min(difference(t)*ChargeEfficiency,maxpwr*ChargeEfficiency);
   % Battery charge equation
  else % if not limiting by maximum discharge amount
   Batt_Charge(t) = difference(t)*ChargeEfficiency;
  end
```

```
   if SOE(t) + Batt_Charge(t) > stg_cap_MW % limited by overcharge
    Batt_Charge(t) = stg_cap_MW - SOE(t);
    difference(t) = Batt_Charge(t)/ChargeEfficiency;
   end

  elseif difference(t) < 0 % load is greater than target load so discharge
   Batt_Discharge(t) = difference(t)/DischargeEfficiency;
  end

  % Sets current SOE to new value depending on amount charged or
  % discharged
  SOE(t) = SOE(t) + Batt_Charge(t) + Batt_Discharge(t);


end

SOE_MWh = SOE./12;

if mode(SOE(end-round(length(SOE)/12):end)) ~= 0
  % If the simulation does not fully recharge at the end, assume that
  % there is not enough generation to sustain and output a failure
  failure = 1;
end

end
```

Appendix C Parameter Index Controller Code

```
% This code operates the parameter index controller. The file locations and
% directories required for loading data need to be added. The file should
% include normalized wind and solar data at 5-minute timesteps (code can be
% adjusted for other timesteps). The file should also include load data
% that has been synchronized with the generation data. Outputs a series of
% tables that can be used for plotting contour plots

clear all, close all, fclose all;
fprintf('Starting DG_minimization_code.m \n')

%Defining file locations and directories (removed for privacy)

create_stgtable = 1; % set to zero if not creating new table

% load data
filename = 'inputdata_5min.mat';
load([DataRoot '\' filename]); % 'DataRoot' directory must be defined


% Define start and end of simulation
startdate = datetime(2018,07,01,'TimeZone','UTC');
enddate = datetime(2020,07,01,'TimeZone','UTC');
range = timerange(startdate, enddate);

Table = Table(range,:); % limit data to simulation range

% read load data from output
Load_MW = Table.Load;

% following values used for initial test
Windlevel = 615; % Wind capacity (MW)
Solarlevel = 300; % Solar capacity (MW)
Wind = Table.WindCapFac.*Windlevel; % Wind generation array (MW)
Solar_PV = Table.SolarCapFac.*Solarlevel; % Solar generation array (MW)
DG_cap = max(Load_MW)-300; % DG limit (MW)

% initial simulation for testing:
[diff, SOE, chg, dischg, failure] = req_stg(Solar_PV, Wind, Load_MW, DG_cap);

if create_stgtable
 load([Output '\outputtable.mat']);

 % Sets initial capacity limits for wind and solar, will be expanded as
 % DG reduction increases
 windcaps = [0:5:1000]; % Wind capacity (MW)
 PVcaps = [0:5:1000]; % Solar capacity (MW)
 DG_reduct = [50:50:1000]; % DG reduction amount (MW)
```

```
for T = 1:length(DG_reduct) % begin indexing DG reduction amount
 if DG_reduct(T) >= 600 % as DG increases more IG is needed
  windcaps = [0:5:3000];
  PVcaps = [0:5:2000];
  if DG_reduct(T) >= 800
   windcaps = [0:5:4000];
   if DG_reduct(T) >= 900
    windcaps = [0:5:6000];
    if DG_reduct(T) >= 1000
     windcaps = [0:5:7000];
    end
   end
  end
 end

 % defines variable names for table being produced
 rownames = table(PVcaps');
 % initial array of correct dimensions
 blank = NaN(length(PVcaps),length(windcaps));

 % create tables of correct dimensions
 STGreqTable = array2table(blank); % Required storage capacity (MWh)
 % set variable names on tables.
 STGreqTable.Properties.VariableNames = cellstr(num2str(windcaps(:)));
 STGreqTable.Properties.RowNames = cellstr(num2str(PVcaps(:)));

 % initialize other tables with same dimensions and variable names
 PWRreqTable = STGreqTable; % Required storage power (MW)
 CRTLMTTable = STGreqTable; % Curtailment (MWh)
 BATuseTable = STGreqTable; % Energy used from battery (MWh)
 IGProdTable = STGreqTable; % total IG production (MWh)

 % Set DG limit based on reduction desired
 DG_maxcap = max(Load_MW) - DG_reduct(T);

 tic % start timer for troubleshooting

 for W = 1:length(windcaps) % begin indexing wind capacity

  Wind = Table.WindCapFac.*windcaps(W); % Wind generation (MW)

  for PV = 1:length(PVcaps) % begin indexing solar capacity
   Solar_PV = Table.SolarCapFac.*PVcaps(PV); % solar generation (MW)
   % run storage model:
   [diff, SOE, chg, dischg, failure] = req_stg(Solar_PV, Wind, Load_MW, DG_maxcap,
wintertimes);

   if ~failure % if no failure
    % required storage is absolute value of lowest state of energy
    stg_cap = abs(min(SOE)); % Required storage capacity (MWh)
```

```
        DG_load = net_load + diff; % required dispatchable generation (MW)
        IG_Production = (nansum(Solar_PV) + nansum(Wind))./12; % IG production (MWh)
        Curtailed = abs(nansum(DG_load(DG_load<0)./12)); % Curtailed IG (MWh)
        dischg_cap = -min(dischg); % Discharge limit % MW
        Batt_use = abs(nansum(dischg./12)); % Energy used from battery (MWh)
        pwr_cap = dischg_cap; % Required storage power (MW)
      else
        stg_cap = NaN;
        pwr_cap = NaN;
        Batt_use = NaN;
        Curtailed = NaN;
        IG_Production = NaN;
      end
      % put values into respective places in tables
      STGreqTable(PV,W) = array2table(stg_cap); % Required storage capacity (MWh)
      PWRreqTable(PV,W) = array2table(pwr_cap); % Required storage power (MW)
      BATuseTable(PV,W) = array2table(Batt_use); % Energy used from battery (MWh)
      CRTLMTTable(PV,W) = array2table(Curtailed); % Curtailed IG (MWh)
      IGProdTable(PV,W) = array2table(IG_Production); % IG production (MWh)
    end
    if W == round(length(windcaps)/2)
      % provides heads-up when halfway done to verify program is running
      fprintf('Halfway\n')
      toc
      tic
    end



  end
  % Provides heads-up when done and moving on to next DG reduction level
  fprintf('Second half of %d MW reduction\n', DG_reduct(T))
  toc
  stackeddata(T).STGTable = STGreqTable;
  stackeddata(T).PWRTable = PWRreqTable;
  stackeddata(T).BATTable = BATuseTable;
  stackeddata(T).CRTLMTTable = CRTLMTTable;
  stackeddata.IGPTable = IGProdTable;

 end

 % Save data to matlab file. 'Output' must be defined
 save([Output '\outputtable.mat'],'stackeddata','PVcaps','windcaps','DG_reduct');

end
```